Atmos. Chem. Phys., 25, 8289–8328, 2025
https://doi.org/10.5194/acp-25-8289-2025

Atmospheric Chemistry and Physics
Open Access
EGU

Opinion: The role of AerChemMIP in advancing climate and air quality research

Paul T. Griffiths[1,2,★], Laura J. Wilcox[3,★], Robert J. Allen[4,★], Vaishali Naik[5], Fiona M. O'Connor[6,7], Michael Prather[8], Alex Archibald[1], Florence Brown[9], Makoto Deushi[10], William Collins[11], Stephanie Fiedler[12], Naga Oshima[10], Lee T. Murray[13], Bjørn H. Samset[14], Chris Smith[15,16], Steven Turnock[5,17], Duncan Watson-Parris[18,19], and Paul J. Young[20,21]

[1]National Centre for Atmospheric Science, Cambridge University, Cambridge, UK
[2]School of Chemistry, Bristol University, Bristol, UK
[3]National Centre for Atmospheric Science, Department of Meteorology, University of Reading, Reading, UK
[4]Department of Earth and Planetary Sciences, UC Riverside, Riverside, CA, USA
[5]NOAA Geophysical Fluid Dynamics Laboratory, Princeton, NJ, USA
[6]Met Office Hadley Centre, Exeter, UK
[7]Department of Mathematics & Statistics, Global Systems Institute, University of Exeter, Exeter, UK
[8]Department of Earth System Science University of California, Irvine, CA, USA
[9]Institute for Atmospheric and Climate Science, ETH Zurich, Zurich, Switzerland
[10]Department of Atmosphere, Ocean, and Earth System Modeling Research, Meteorological Research Institute, Tsukuba, Japan
[11]Department of Meteorology, University of Reading, Reading, UK
[12]GEOMAR Helmholtz Centre for Ocean Research Kiel & Faculty of Mathematics and Natural Sciences, Christian-Albrechts-University of Kiel, Kiel, Germany
[13]Department of Earth and Environmental Sciences, University of Rochester, Rochester, NY, USA
[14]CICERO Center for International Climate Research, Oslo, Norway
[15]School of Earth and Environment, University of Leeds, Leeds, UK
[16]Integrated Assessment and Climate Change Research Group, International Institute for Applied Systems Analysis, Laxenburg, Austria
[17]University of Leeds Met Office Strategic (LUMOS) Research Group, University of Leeds, Leeds, UK
[18]Scripps Institution of Oceanography, UC San Diego, San Diego, CA, USA
[19]Halıcıoğlu Data Science Institute, UC San Diego, San Diego, CA, USA
[20]JBA Risk Management Ltd, Skipton, UK
[21]School of Engineering, Newcastle University, Newcastle, UK
★These authors contributed equally to this work.

Correspondence: Paul T. Griffiths (paul.griffiths@ncas.ac.uk)

Received: 9 August 2024 – Discussion started: 5 September 2024
Revised: 29 April 2025 – Accepted: 14 May 2025 – Published: 31 July 2025

Abstract. The Aerosol Chemistry Model Intercomparison Project (AerChemMIP) was endorsed by the Coupled Model Intercomparison Project 6 (CMIP6) and was designed to quantify the climate and air quality impacts of aerosols and chemically reactive gases. AerChemMIP provided the first consistent calculation of effective radiative forcing (ERF) for a wide range of forcing agents, which was a vital contribution to the Sixth Assessment Report (AR6) of the Intergovernmental Panel on Climate Change. It supported the quantification of composition–climate feedback parameters and the climate response to short-lived climate forcers (SLCFs), as well as enabled the future impacts of air pollution mitigation to be identified, and the study of interactions between climate and air quality in a transient simulations. Here we review AerChemMIP in detail and assess the project against its

stated objectives, its contribution to the CMIP6 project, and the wider scientific efforts designed to understand the role of aerosols and chemistry in the Earth system. We assess the successes of the project and the remaining challenges and gaps. We conclude with some recommendations that we hope will provide input to planning for future MIPs in this area. In particular, we highlight the necessity of sufficient ensemble size for the attribution of regional climate responses and the need for coordination across projects to ensure key science questions are addressed. Summary data for CMIP6 and AerChemMIP models such as model components, model configurations, and emergent quantities are included.

1 Introduction

The goal of the Coupled Model Intercomparison Projects (CMIPs), used to inform successive generations of Intergovernmental Panel on Climate Change (IPCC) assessments, is to provide attribution and understanding of climate changes in the past, for the present day, and in future projections. Here we use "climate" as writ large, encompassing the Earth system, particularly the atmospheric composition of greenhouse gases (GHGs), chemically active trace gases, and aerosols. Model assessment in a multi-model context, core to the CMIPs, is a necessary part of this process, establishing both the accuracy of models in matching observations and their consistency in projecting change, thus enabling confidence in climate actions. An essential element of CMIPs is not just presenting the model spread, but also in providing critical diagnostics so that we can understand the cause of model differences and identify better modelling approaches.

The IPCC released the Sixth Assessment Report (AR6) over the period 2021–2023 based on and informed by the 6th Phase of CMIP (CMIP6). CMIP6 defined a series of common experiments, including the DECK (Diagnostic, Evaluation and Characterization of Klima; Eyring et al., 2016) and historical experiments, standardized input datasets to drive model experiments (input4MIPs), sponsored infrastructure activities, such as input4MIPs and the Earth System Grid Federation (ESGF), and endorsed a host of sub-MIPs focused on specific science questions. The design of the DECK provided experiments for assessing internal model variability (*piControl*), calculating climate sensitivity (*abrupt-4xCO2* and *1pctCO2*), and providing data for comparison with observations (AMIP). Alongside the coupled transient *historical* experiment, these simulations represented the "entry card" for CMIP6 (Eyring et al., 2016).

In this paper, we review the Aerosol and Chemistry MIP (AerChemMIP; Collins et al., 2017), one of the endorsed MIPs of CMIP6, examining its requested experiments, model participation, and the overall contribution to our understanding of the role of short-lived climate forcers (SLCFs) in climate change, including chemistry–aerosol–climate couplings and feedbacks. The criteria for the endorsed MIPs were set by CMIP6 (Meehl et al., 2014; Eyring et al., 2016; Stouffer et al., 2017) such that they needed to address one or more of three broad scientific questions. (Q1) How does the Earth system respond to forcing? (Q2) What are the origins and consequences of systematic model biases? (Q3) How can we assess future climate changes given climate variability, predictability, and uncertainties in scenarios? AerChemMIP addressed all of these questions, to varying degrees.

2 AerChemMIP – objectives and protocol design

A primary objective for AerChemMIP was to diagnose and document forcings and climate responses to changes in aerosols and GHGs, such as ozone and methane, in the CMIP6 models (Collins et al., 2017). The AerChemMIP experiments enabled the assessment of the role of SLCFs, i.e. aerosols and chemically reactive gases, in historical and future climate change, as well as a more robust quantification of climate sensitivities to chemistry and aerosol changes based on the current generation of comprehensive Earth system models (ESMs) (Thornhill et al., 2021a). The focus of AerChemMIP on SLCFs was due to the findings of the IPCC Fifth Assessment Report (AR5) that SLCFs were the main source of uncertainty in estimates of the effective radiative forcing (ERF). SLCF contributions to anthropogenic forcing include changes in aerosols and their precursors; methane; tropospheric ozone, formed from sunlight, nitrogen oxides (NO_x), carbon monoxide, volatile organic compounds, and methane; and stratosphere ozone levels, which are affected by ozone-depleting substances (ODSs). These have contributed significantly to past climate change, with a combined pre-industrial (PI) to present-day (PD) GHG forcing from short-lived GHGs such as methane and tropospheric ozone, estimated in AR5 to be comparable to that of carbon dioxide, and cooling from the direct and indirect effects of aerosol of a similar magnitude.

Taken together, anthropogenic aerosols act to cool the climate and have offset around a third of GHG-driven warming since 1850 (Szopa et al., 2021a). They have also accounted for the largest component of uncertainty in anthropogenic radiative forcing through successive IPCC assessment reports, reflecting, amongst other issues, diverse approaches to modelling aerosol processes and their interaction with the climate system, as well as difficulties in using observations to constrain aerosol forcing (Boucher et al., 2013; Bellouin et al., 2020; Forster et al., 2021). CMIP5 brought a significant advance in the representation of aerosol–climate interac-

tions, with two-thirds of models including a representation of aerosol–cloud interactions and more models including interactive aerosol schemes (Wilcox et al., 2013; Ekman, 2014). In CMIP6, a new generation of ESMs came online with structural changes such as two-moment aerosol schemes; online interactive biogenic volatile organic compound (BVOC) emissions, which serve as ozone and aerosol precursors; and ocean biogeochemistry describing e.g. sulfur-containing aerosol precursor species, such as dimethyl sulfide (DMS), with implications for the natural background aerosol state. This change in the background state has the potential to have a large impact on the calculation of PI-to-PD radiative forcing from anthropogenic sulfate aerosol (Carslaw et al., 2013).

Of the reactive gases, methane and ozone were of primary interest for AerChemMIP. Methane is an important GHG, and atmospheric concentrations have increased by a factor of $\sim$2.5 since PI times (e.g. Skeie et al., 2023). It serves as a precursor to tropospheric ozone and stratospheric water vapour and as a sink for the hydroxyl radical, with a significant impact on tropospheric oxidizing capacity and therefore the lifetimes of several climate forcers (e.g. halocarbons and methane itself). Accurate simulation of atmospheric methane trends from emissions remains a challenge, as there exist a variety of anthropogenic and natural sources such as wetlands which are capable of responding to climate change, and for this reason, as in CMIP5, many of the CMIP6 models used prescribed model lower boundary conditions for historical and future simulations, produced from integrated assessment models.

Tropospheric ozone is an important SLCF. It is a GHG that has its largest radiative impact in the upper troposphere–lower stratosphere (UT/LS). High surface levels of ozone are associated with adverse effects on human health and vegetation (e.g. Anenberg et al., 2009; Emberson, 2020). It is therefore important to attribute the causes of increases since PI times and understand its evolution in the future with changing climate and precursor emissions. CMIP6 was the first CMIP in which a significant number of modelling centres included interactive tropospheric and stratospheric ozone in their flagship models, with whole-atmosphere chemical schemes allowing the effect of stratospheric changes on tropospheric chemistry to be attributed (Stevenson et al., 2020; Zeng et al., 2022). BVOCs serve as ozone precursors, and their emissions are dependent on climate state. All models bar one (MRI-ESM2-0) used in the CMIP6 assessment for tropospheric ozone had some form of online isoprene emissions, with some including more detailed treatments (monoterpene emissions, the effect of carbon dioxide (CO_2) inhibition, and/or a larger suite of online BVOC emissions) (Griffiths et al., 2021).

2.1 AerChemMIP objectives

The AerChemMIP science questions, as set out in Collins et al. (2017) using the nomenclature of near-term climate forcers (NTCFs), subsequently renamed in AR6 to SLCFs, were as follows.

- A1. How have anthropogenic emissions contributed to global radiative forcing and affected regional climate over the historical period?
- A2. How might future policies (on climate, air quality, and land use) affect the abundances of NTCFs and their climate impacts?
- A3. How do uncertainties in historical NTCF emissions affect radiative forcing estimates?
- A4. How important are climate feedbacks to natural NTCF emissions, atmospheric composition, and radiative effects?

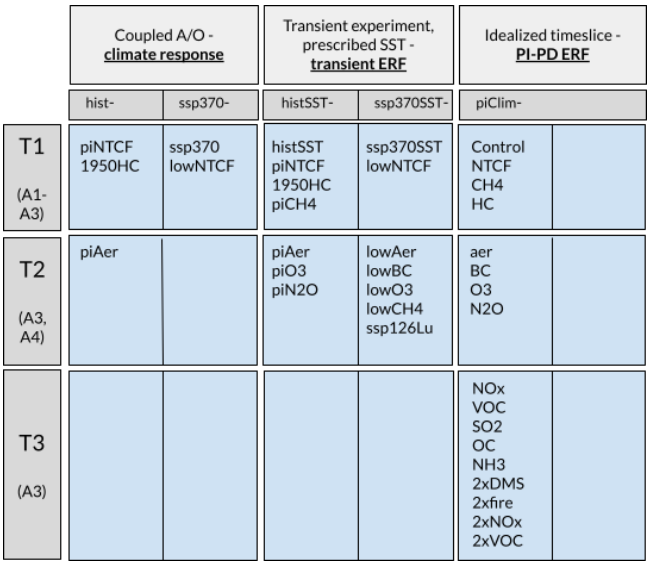

Figure 1. Schematic of AerChemMIP protocol experiments, showing tiers (T), AerChemMIP objectives (A), and species involved.

As a CMIP6-endorsed MIP, AerChemMIP was designed to build on the DECK and historical experiments, particularly the historical coupled atmosphere–ocean and the atmosphere-only AMIP experiments, and to interface with future scenario simulations coordinated by ScenarioMIP (O'Neill et al., 2016). AerChemMIP experiments were sorted into tiers according to priority, with the tiers loosely tied to the science questions: Tier 1 experiments aimed to answer questions A1 and A2, and Tier 2 experiments addressed A4 with Tiers 1–3 aiming to answer A3. The AerChemMIP requested additional diagnostics to complement analyses of CMIP and ScenarioMIP experiments. Figure 1 shows the AerChemMIP experimental tiers.

In support of its objectives, the AerChemMIP protocol defined historical and future experiments, as well as transient experiments, which are based on the parent CMIP *historical*

and ScenarioMIP *SS3P3-7.0* experiments, and idealized, so-called "timeslice" experiments which were forced with sea surface temperatures (SSTs) and sea ice from the corresponding coupled Atmosphere–Ocean General Circulation Model (AOGCM) and with other boundary conditions appropriate to a single year used for calculating ERFs.

The calculation of ERFs, addressing A1, was an important focus of AerChemMIP. When the concept of ERF was introduced in AR5 Working Group 1 (WG1), ERFs for historical GHGs, natural forcings, aerosols, and ozone were inferred from coupled transient simulations by removing the effect of the surface temperature response (Forster et al., 2013). ERF contributions from ozone and aerosols were diagnosed in offline calculations (Shindell et al., 2013), based on changes in composition derived in the Atmospheric Chemistry and Climate MIP (ACCMIP; Lamarque et al., 2013). The model configurations participating in ACCMIP were in many cases different from those in CMIP5 in terms of both resolution and complexity of chemistry and aerosols, which resulted in ACCMIP not being able to fully describe the forcings in the coupled models. The systematic approach for calculating ERFs due to individual SLCF species in AerChemMIP represents a significant advance for CMIP6 over the CMIP5 approach.

2.2 AerChemMIP timeslice experiments

The AerChemMIP protocol described the simulations needed to calculate PI-to-PD and transient historical ERFs for individual species, such as methane (CH_4) and sulfur dioxide (SO_2). The *piClim-X* experiments in AerChemMIP consisted of a control experiment (*piClim-control*) that had all well-mixed GHG (WMGHG) concentrations and SLCF emissions at PI levels and individual experiments where one species (or group of species) was changed to PD levels. These simulations were run as "timeslice" experiments in which an atmosphere-only GCM is forced with SSTs from a corresponding coupled atmosphere–ocean GCM and other boundary conditions appropriate to a single year. The internal model variability (mainly clouds) generates considerable interannual variability in ERFs, and the perpetually repeating boundary conditions allow for repeated realizations of the atmospheric state that both incorporate this internal variability and allow for improved statistics for the estimation of small changes in e.g. top-of-atmosphere (TOA) radiative forcing. Moreover, these shorter, 30-year timeslice simulations were able to be performed for more forcing agents, with more models, compared to analogous 165-year transient historical simulations. The AOGCM timeslice experiments allow the ERFs to be diagnosed directly, in the absence of slow climate responses and feedbacks, rather than being inferred. It should be noted that some groups found it necessary to extend the *piClim-X* experiments to 45 years to allow stratospheric concentrations of WMGHGs sufficient time to spin up (O'Connor et al., 2021).

AerChemMIP timeslice experiments for natural 2× experiments are analogous to the above, but here the specified PI natural emission flux is doubled by scaling either the parameterizations in an interactive scheme or the input data files for specified emissions (Collins et al., 2017). For most of these experiments, the emission flux to be doubled is intuitive (e.g. dust emissions are doubled for *piClim-2xdust*). For *piClim-2xfire*, fire-related emissions for several species are doubled, e.g. NO_x, black carbon (BC), organic carbon (OC), CO, and VOCs.

2.3 AerChemMIP historical transient experiments

AerChemMIP coupled transient-attribution experiments, addressing the role of historical or future emissions changes, were grouped into species categories (*hist-piNTCF*, *-piO3*, *-1950HC*) to keep down computational cost, while the less expensive prescribed SST experiments were performed over a wider range of forcings to quantify pre-industrial (PI) to present-day (PD) and historical transient ERFs due to changes in the individual forcing agents. This "everything but" (i.e. every forcing follows the historical trajectory except for a single named forcing held at PI levels) approach meant that any non-linearities arising due to a warming climate were captured in the AerChemMIP experiments, making them a useful counterpoint to the DAMIP (Detection and Attribution MIP) single-forcing experiments. These were designed to be used in optimal fingerprinting approaches for detection and attribution, involving a linear regression of historical climate observations onto corresponding models. The DAMIP approach assumed that the climate responses to single forcings can be combined linearly, an assumption that often breaks down at regional scales and can be tested by a comparison between AerChemMIP and DAMIP experiments.

2.4 AerChemMIP *ssp370* experiments

Future climate and air pollution was targeted using the Shared Socioeconomic Pathway 3-7.0 (SSP3-7.0; Rao et al., 2017; Riahi et al., 2017) – a "regional rivalry" scenario without climate policy and weak air pollution mitigation policies. ScenarioMIP contributed the coupled AOGCM *ssp370* experiments (40 models, 379 experiments) as a baseline for understanding the role of aerosols and chemistry in a future climate (O'Neill et al., 2016). AerChemMIP provided complementary *ssp370SST* experiments for transient ERF calculations and a coupled AOGCM *ssp370-lowNTCF* experiment to attribute the role of aerosols and gaseous emissions, excluding methane, on climate and composition (Allen et al., 2020). For most short-lived precursor species for air quality and aerosol climate forcing, including NO_x, CO, CH_4, non-methane VOCs, SO_2, BC, and OC, the emissions or surface boundary conditions in the *SSP3-7.0* scenario were substantially higher than those in the most extreme warming sce-

nario considered by CMIP6 (*SSP5-8.5*). For the purposes of attributing the impact of emissions changes, this scenario offered the strongest signal and therefore the greatest potential for attribution. For the purposes of policy development, simulations were required until 2055 with most models extending to 2100. Land-use changes were separately assessed via the Land Use MIP (LUMIP; Lawrence et al., 2016) experiment, *ssp370-ssp126Lu*.

To isolate the effects of air pollution mitigation policies, the *SSP3-7.0-lowNTCF* scenario uses the same socioeconomic scenario and the same emissions drivers as *SSP3-7.0* but with "strong" air pollution mitigation policies. In the case of air pollutant species (e.g. SO_2, BC, OC, NO_x, NH_3, and anthropogenic VOCs), the emissions factors used in the sustainability pathway SSP1 were adopted (Gidden et al., 2019). *SSP3-7.0-lowNTCF* was designed so that the reduced NTCF emissions relative to *SSP3-7.0* came only from changes in air quality policy, neglecting changes coming from simultaneous changes in climate policy. The decrease in air pollutant species emissions is due to swift ramping up of end-of-pipe measures for air pollution control, not from the reduction in co-emissions accompanying the CO_2 emissions also seen in *SSP1*. The result was that, under *SSP3-7.0-lowNTCF*, global emissions of all aerosols and gaseous precursors decrease, particularly by mid-century by $\sim 30\,\%$–$50\,\%$: reductions comparable to those seen in *SSP2-4.5*, e.g. Fig. 1 of Wilcox et al. (2023). In contrast, the corresponding emissions under *SSP3-7.0* generally increase (weakly) by mid-century by $\sim 10\,\%$ (Allen et al., 2021).

Subsequent to the publication of Collins et al. (2017), further experiments were developed to attribute the role of individual SLCFs, such as the coupled AOGCM experiment *ssp370-lowNTCFCH4*, addressing the additional role of methane mitigation (Allen et al., 2021), and *ssp370pdSST*, employing future emissions but prescribing a PD climatology of SSTs and sea ice to characterize the effect of future climate change on composition (Zanis et al., 2022). For completeness, these experiments are included in Table 1 despite not being assigned a tier in Collins et al. (2017), using their designation on ES-DOC (https://search.es-doc.org/, last access: 4 January 2025, mirrored at https://errata.ipsl.fr, last access: 30 July 2025). These experiments were critical for drawing two conclusions relating to SLCFs in the IPCC AR6: (1) changes in future air pollution are more likely to be driven by changes in anthropogenic emissions than climate change and (2) controls on SLCF emissions, particularly methane, are important for meeting climate goals with simultaneous air quality benefits.

2.5 AerChemMIP and other CMIP6 MIPs

AerChemMIP aimed to draw on the skills and interests of the atmospheric chemistry, aerosol, and radiative forcing communities to address research questions of mutual interest. The community coalesced around semiannual "TriMIP" meetings (reviewed in Fiedler et al., 2024), involving meetings of the Precipitation Driver and Response Model Intercomparison Project (PDRMIP; Myhre et al., 2017), the Radiative Forcing Model Intercomparison Project (RFMIP; Pincus et al., 2016), and AerChemMIP. These three MIPs shared many interests and scientific goals but with different foci and approaches (Fiedler et al., 2024).

AerChemMIP was designed to advance the understanding of the role of SLCFs in transient climate change and the magnitude of the climate response to realistic forcings.

PDRMIP investigated the role of various drivers of climate change for mean and extreme precipitation changes. It included a range of present-day equilibrium experiments with large, idealized perturbations in either emissions or concentrations of well-mixed GHGs (WMGHGs), SLCFs, or natural forcings. The application of such large forcings resulted in clear signals that advanced our physical understanding of the climate response to these forcings. However, information from such idealized experiments can be difficult to apply to the real world, and PDRMIP was complemented by AerChemMIP in this regard, which focused on well-defined pathways describing historical and future forcings.

RFMIP aimed to provide both a foundational understanding of the Earth system response to forcing and described a range of experiments for the quantification of the ERF of individual or groups of forcing agents. Quantifying ERF was a common goal between AerChemMIP and RFMIP, with complementary protocols: firstly, AerChemMIP and RFMIP both included experiments designed to calculate the 2014 vs. 1850 ERF due to SLCFs. There were common control simulations of *piClim-control* and *piClim-aerO3* in RFMIP and *piClim-control* and *piClim-NTCF* in AerChemMIP. These ERF calculations were based on common definitions of the present day (PD) vs. pre-industrial (PI, 1850) for individual species (concentrations or emissions) and a common protocol of 30-year (perpetually repeating) timeslice experiments driven by fixed monthly climatological (1850) SSTs and sea ice, as recommended by Forster et al. (2016). Secondly, both RFMIP and AerChemMIP protocols defined experiments to diagnose the transient ERF for the historical period (*piClim-histaerO3* for RFMIP and *histSST* and *histSST-piNTCF* for AerChemMIP). However, while the timeslice experiments for the 2014 vs. 1850 ERF due to SLCFs were identical in RFMIP and AerChemMIP, the experimental designs were different for these transient experiments. For transient experiments, pre-industrial SSTs and sea-ice concentrations were prescribed for RFMIP compared to SSTs and sea-ice concentrations from the historical experiment for AerChemMIP. AerChemMIP also used the "everything but" design, while RFMIP used the single-forcing approach taken by the Detection and Attribution MIP (DAMIP; Gillett et al., 2016).

AerChemMIP also aligned with Detection and Attribution MIP (DAMIP; Gillett et al., 2016), which used single-forcing experiments in multiple generations of CMIP to quantify the proportion of an observed trend likely to be driven by a par-

https://doi.org/10.5194/acp-25-8289-2025

Table 1. Information on AerChemMIP simulations, including (horizontally displayed) experiment abbreviations (EXPT ID) and (vertically displayed) experiment tier (TIER, i.e. priority), number of models that performed a given experiment (MODELS), and the total number of ensemble members (MEMBERS; i.e. independent realizations).

EXPT ID	hist-1950HC	hist-piNTCF	histSST	histSST-1950HC	histSST-piCH4	histSST-piNTCF	piClim-CH4	piClim-HC	piClim-NTCF	piClim-control
TIER	1	1	1	1	1	1	1	1	1	1
MODELS	6	11	12	6	8	11	9	6	11	22
MEMBERS	19	27	13	6	8	12	10	6	12	32
EXPT ID	hist-piAer	histSST-piAer	histSST-piN2O	histSST-piO3	piClim-2xdust	piClim-2xSS	piClim-BC	piClim-N2O	piClim-O3	piClim-aer
TIER	2	2	2	2	2	2	2	2	2	2
MODELS	10	8	4	4	9	9	11	6	6	19
MEMBERS	24	9	4	4	10	10	12	7	6	25
EXPT ID	piClim-2xDMS	piClim-2xNOx	piClim-2xVOC	piClim-2xfire	piClim-NH3	piClim-NOx	piClim-OC	piClim-SO2	piClim-VOC	
TIER	3	3	3	3	3	3	3	3	3	
MODELS	6	4	6	6	2	6	10	11	6	
MEMBERS	7	4	7	6	2	6	12	13	6	
EXPT ID	ssp370-lowNTCF	ssp370SST	ssp370SST-lowNTCF	ssp370SST-lowAer	ssp370SST-BC	ssp370SST-lowO3	ssp370SST-lowCH4	ssp370-ssp126Lu	ssp370SST-lowNTCFCH4	
TIER	1	1	1	2	2	2	2	2	2	
MODELS	13	11	8	6	6	3	4	5	6	
MEMBERS	40	11	8	6	6	3	4	5	6	
EXPT ID		ssp370pdSST		ssp370-lowNTCFCH4						
TIER		2+		1+						
MODELS		7		6						
MEMBERS		7		12						

ticular forcer. However, the DAMIP approach rests on the assumption that the climate response to individual forcers, or groups of forcers, can be combined linearly to reproduce the total climate response. This assumption does not always hold, especially for regional climate (Steptoe et al., 2016; Deng et al., 2020; Aizawa et al., 2022), and even the forcings themselves do not combine linearly (O'Connor et al., 2021). AerChemMIP experiments therefore provide additional experiments to enable the assessment of DAMIP analyses.

3 Contributions and successes

At the time of writing, there are 12 published articles in the special issue of *Atmospheric Chemistry and Physics* (Shonk et al., 2020; Stevenson et al., 2020; Zanis et al., 2020; Wilcox et al., 2020; Turnock et al., 2020; Allen et al., 2020; Mortier et al., 2020; Griffiths et al., 2021; Gliß et al., 2021; Thornhill et al., 2021a; O'Connor et al., 2021; Zhang et al., 2021a), with some early synthesis reports also contributed (Forster et al., 2016). While it is difficult to completely separate AerChemMIP from the wider CMIP6 publications, a further 22 articles mention AerChemMIP (Web of Science, 26 July 2024). Articles highlighted the role of oxidants (Karset et al., 2018; O'Connor et al., 2021; Griffiths et al., 2021), aerosol processes (Zhang et al., 2021a), and methane (Stevenson et al., 2020; O'Connor et al., 2022).

The number of experiments (37) and the number of simulated model and ensemble years (1265 for Tier 1, 1369 for Tier 2, and 270 for Tier 3) made AerChemMIP the largest of the CMIP6-endorsed MIPs. Despite this, there was good uptake by modelling centres, with up to 19 models performing at least one of the AerChemMIP experiments. Table 1 shows details of the data available via the ESGF archive in August 2024. Over the historical period, the coupled Atmosphere–Ocean General Circulation Model (AOGCM) experiments are well represented with more than 10 models performing *hist-piNTCF* and *hist-piAer*. In general, experiments targeting historical aerosol emissions received the most effort (Fig. 2). The average number of models per experiment was seven, and for coupled hist-AOGCM experiments, there was an average of three ensembles per experiment. The AerChemMIP research questions were at the cutting edge of the capability of the current generation of climate models, and participation reflected model capability; e.g. models using offline chemistry were necessarily excluded from experiments, such as *hist-piO3*, limiting the number of models running this experiment to five. These five ESMs (UKESM1-0-LL, MRI-ESM2-0, GISS-E2.1-G, CESM2-WACCM, and GFDL-ESM4) with interactive chemistry in fact ran the majority of the experiments of which they were capable, contributing to all AerChemMIP tiers. The experiment with the lowest number of participating models was *piClim-NH3*, run only by IPSL-CM6A-LR-INCA and GISS-E2.1-G, which are two of only a small number of CMIP6 models to feature online ammonia emissions and to treat explicitly the formation of ammonium-containing aerosol. While the absolute number of participating models is a useful metric, the statistics do inevitably reflect the number of models *capable* of running a given experiment. In this sense, AerChemMIP enjoyed very pleasing success with community members contributing data to nearly every experiment that their models were capable of running.

AerChemMIP within CMIP6 provided several key points of analysis to inform AR6. These included quantitative understanding of the role of anthropogenic drivers in historical oxidizing capacity; an assessment of emissions-based effective radiative forcings for SLCFs, cumulatively and individually; an improved estimate of forcing by ozone-depleting substances using an observational constraint; assessment of climate and air quality impacts due to mitigation of SLCFs (in particular the role of methane); a more robust quantification of non-CO_2 biogeochemical climate feedbacks; and several evaluations including tropospheric ozone, stratospheric ozone and water vapour, and air quality. The work informed quantification and improved understanding of model biases (e.g. UKESM1 response to ozone-depleting substances (Morgenstern et al., 2020); surface ozone biases (Liu et al., 2022); historical temperature biases (Zhang et al., 2021a)) and the development of emulators (Smith et al., 2024). It continued the use of fixed SST and coupled simulations for quantifying responses on different timescales pioneered in PDRMIP, demonstrated the value of a consistent set of aerosol and gas-phase experiments for attribution, and improved links to other projects such as the Chemistry Climate Model Initiative (CCMI) which used the CMIP6 scenarios for its projections of ozone recovery.

3.1 AerChemMIP *piClim* experiments

As shown in Table 1, the *-CH4* and halocarbon (*-HC*) chemistry experiments have received the most effort. For experiments requiring online chemistry, participating centres were more likely to perform *piClim-X* experiments than the analogous *histSST-piX* experiments.

The ERFs from the *piClim-X* experiments were analysed by Thornhill et al. (2021b) and more recently by Kalisoras et al. (2024) from the online radiation diagnostics. The ERFs were further broken down into instantaneous radiative forcings (IRFs) and adjustment terms due to temperature (tropospheric and stratospheric), water vapour, surface albedo, and clouds using offline radiative kernels. Using this approach, the separation of the ERF due to aerosols into aerosol–radiation interactions (ARIs) and aerosol–cloud interactions (ACIs) showed reasonable agreement with the double-call radiation diagnostics for aerosol and cloud forcing based on the methodology of Ghan (2013). Oshima et al. (2020) estimated the present-day ERFs from individual anthropogenic agents comprehensively and suggested the importance of the interactions of aerosols with ice clouds over

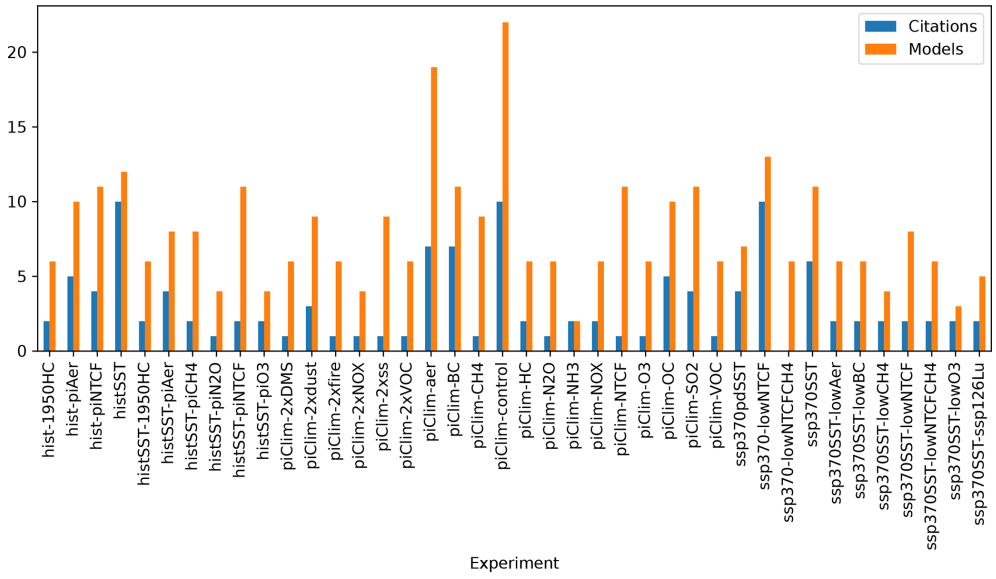

Figure 2. The AerChemMIP experiments and the number of models used to perform them (orange bars), based on the availability of data in the ESGF archive in August 2024. Blue bars show the number of publications using each experiment to date, according to the Web of Science.

the tropics and possible important role of black carbon (BC) in Arctic surface warming. A notable result of the analysis of the adjustment terms was that for some models (UKESM1 in particular) there was a significant contribution to the ERFs for ozone precursors (such as CH_4 and anthropogenic NO_x) from changes in cloud radiative effects due to changes in the atmospheric oxidizing capacity. O'Connor et al. (2021, 2022) concluded that much of the cloud radiative effect originated through changes in levels of OH and O_3 and associated changes in the gas-phase (rather than aqueous-phase) oxidation of SO_2 and aerosol size distribution. Further interactions between NO_x and ERF would be expected through changes in nitrate aerosol. Nitrate aerosols are treated in GFDL-ESM4, for instance, but not in UKESM1. The role of nitrate aerosol in aerosol–cloud interactions remains largely unexplored in CMIP6 models, and future generations of AerChemMIP may need additional experiments to understand the coupling between NO_x emissions, nitrate aerosol, and aerosol–cloud interactions.

AerChemMIP found that NO_x emissions made the largest contribution to the PI-to-PD tropospheric ozone forcing (Thornhill et al., 2021b), whereas ACCMIP had found that the largest contribution was from methane (Stevenson et al., 2013), although part of this difference in the attribution of the ozone forcing may be related to the difference in NO_x emissions between CMIP5 and CMIP6.

The NO_x emissions used in CMIP6 from the Community Emission Data System (CEDS; Hoesly et al., 2018) are smaller than the CMIP5 estimates until the mid-20th century. This is largely because of the explicit representation of the lower NO_x emissions from biomass fuels in early periods, which combust at lower temperatures compared to coal. In 1970, CEDS NO_x emissions began to diverge from CMIP5 estimates, generally becoming larger due to waste, transportation, and energy sectors. CEDS emissions remain about 10 % larger than those of CMIP5 in 1980 and 1990. Both global estimates increase and start to flatten around 1990. However, CEDS values flatten until 2000 and then increase again, while CMIP5 values decrease from 1990 to 2000. IPCC also noted that differences in modelling protocol may have an effect.

In terms of ozone, many more models included a representation of chemistry in the stratosphere, and these whole-atmosphere schemes enabled the calculation of ERFs from stratospheric ODSs such as halocarbons and nitrous oxide (N_2O), as well as a more complete calculation of the ERFs from tropospheric ozone precursors, from which the production of ozone often extends into the lower stratosphere. AerChemMIP was not able to isolate an ERF due solely to ozone changes as the diagnosed ERFs included changes in WMGHGs (CH_4, N_2O, ODSs) and impacts on aerosols. In future MIPs, prescribed ozone experiments or methods for isolating ozone radiative effects might be needed (Collins et al., 2024).

The halocarbon ERFs diagnosed in AerChemMIP showed significant reductions compared to that expected from the direct greenhouse effect with a range of -0.18 to $0.32\,W\,m^{-2}$ (Thornhill et al., 2021b). This strong reduction in ERF compared to RF is partly attributed by Morgenstern et al. (2020) to negative cloud responses in the Southern Hemisphere. Moreover, AerChemMIP models span a wide range of simulated ozone depletion. Morgenstern et al. (2020) found that

there was a strong correlation between the modelled historical total ozone column (TOC) change and the halocarbon ERF. The observed TOC trend was used to generate an emergent constraint on the halocarbon ERF of −0.05 to 0.13 W m^{-2}, a much narrower range than from Thornhill et al. (2021b) but still with a chance of a negative ERF. Despite the uncertainty, largely the result of a large underestimate in a single model's ozone field, the claim that the Montreal Protocol had a positive climate benefit still holds.

As well as radiative diagnostics, the *piClim-X* experiments provide information on how the SLCFs influence atmospheric composition. These include impacts on ozone concentrations and the oxidants that destroy methane and thereby control its lifetime. The effect of N_2O on the methane lifetime (through depletion of tropical upper-stratospheric ozone) is larger in the AerChemMIP models than had previously been estimated. This AerChemMIP result led to a slight reduction in the global warming potential (GWP) of N_2O as assessed in IPCC AR6 (Forster et al., 2021) although partially compensated by a positive ozone forcing through the contribution of N_2O to tropospheric and lower-stratospheric ozone production.

AerChemMIP also analysed the radiative effects of other emissions relevant to the Earth system: dust, sea salt, DMS, BVOCs, lightning NO_x, and fires. Since emissions of these species are generally prognostic within climate models rather than prescribed, emissions were doubled compared to the *piClim-control* instead of prescribing 2014 emissions, as was done for anthropogenic emissions. For dust emissions, there was little agreement even on the sign of the ERF (Thornhill et al., 2021a), reflecting the diverse dust emission rates across models, which are largely due to differences in the near-surface wind (Zhao et al., 2022), and diversity in simulated dust properties (Kok et al., 2021). For BVOC emissions, the models agreed that the negative ERF from increased organic aerosols dominated over the positive contribution from increased ozone production. These experiments were used to derive radiative efficiencies (per mass emitted) for the natural species and, in combination with the DECK *abrupt-4xCO2* experiment, to calculate climate feedback parameters (W m^{-2} K^{-1}) due to biogeochemical processes (Thornhill et al., 2021a). The dominant aerosol and chemistry feedbacks were found to be negative.

The quantification of ERFs by species is essential information in attributing climate change to the emissions of different pollutants that can be used by policymakers to target the mitigation of specific emissions. The results from AerChemMIP were used to derive the contributions of emissions of different species to the PI-to-PD forcing (Fig. 6.12 in Szopa et al., 2021a) and global surface temperature (Fig. SPM2c in IPCC, 2021) for IPCC AR6. This work also forms the basis for updates to climate change indicators (Forster et al., 2023).

Figure 3 shows the application of AerChemMIP *piClim-X* experiments in the attribution of drivers of historical climate change. AerChemMIP provided experiments and underpinning data for each species apart from the CO_2 forcing from CO_2 emissions, as indicated by the hatching. These data contribute to Fig. SPM.2 of IPCC (2021).

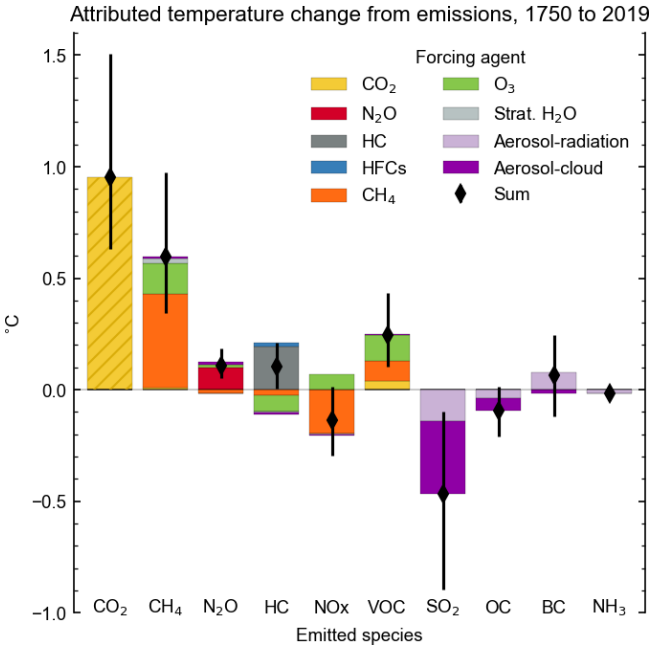

Figure 3. Attributed change in near-surface temperature for 1750–2019 from emitted species. Data are replotted from Fig. 6.12 of IPCC AR6 Working Group 1 (Szopa et al., 2021b; Blichner and Berntsen, 2023). Assessments that were derived directly or indirectly from AerChemMIP experiments are shown unhatched.

Using *piClim-X* experiments, studies looked at the so-called "fast" circulation responses to aerosols, i.e. the responses that are independent of SST changes (e.g. Amiri-Farahani et al., 2020; Zanis et al., 2020). As expected, the fast PI-to-PD response to all aerosols included continental cooling, especially in the Northern Hemisphere, with the largest cooling over East Asia and India. Interestingly, however, multi-model mean Arctic winter warming occurred (albeit with large inter-model variability), consistent with warm air advection associated with intensification of the Icelandic Low and an anticyclonic anomaly over southeastern Europe (Zanis et al., 2020). The corresponding fast precipitation responses were largest in the tropics and generally associated with a precipitation decrease over continental regions, consistent with weakening of the monsoons of east Asia, Africa, and the Americas (Zanis et al., 2020). Amiri-Farahani et al. (2020) used *piClim-2xfire* simulations to investigate the fast atmospheric circulation response to fire emissions, including anomalous ascent and upper-level divergence over the African continent. Previous analyses of idealized PDRMIP (Myhre et al., 2017) simulations have shown the utility of decomposing the climate responses into fast and slow components, particularly for precipitation. For example, the global mean fast precipitation response scales with the change in

atmospheric absorption (e.g. due to black carbon) and the slow response scales with the change in surface temperature (Samset et al., 2016; Liu et al., 2018). A similar decomposition has also been used to understand precipitation responses to methane shortwave absorption under both idealized and realistic methane perturbations (Allen et al., 2023, 2024b).

3.2 AerChemMIP *histSST* experiments

The transient historical prescribed SST (*histSST*) experiments were designed principally to calculate transient ERFs. They were used to attribute historical changes in ERF to individual forcing agents and in calculations of changes to the Earth's energy budget and integrated radiative forcing. Transient ERFs reveal more detail about historical changes in SLCFs. The magnitude and pattern of forcing can differ markedly from the ERFs calculated from piClim experiments, depending on the time period they are calculated for. An example of this is the aerosol radiative forcing, which peaks over North America and Europe in the mid-1980s and over Asia at the end of the simulation in 2014 (e.g. Kalisoras et al., 2024). This means that ERFs calculated from piClim experiments have a spatial pattern that is more strongly influenced by Asia than most of the historical period, potentially causing issues for attribution if applied to periods before 1980. The *histSST* experiments also found wider application, with experiments such as *histSST-1950HC* and *histSST-piCH4* allowing attribution of the effect of historical emissions and/or concentrations on atmospheric composition. Stevenson et al. (2020) used these experiments to identify the drivers of hydroxyl (OH) change over the historical period, examining the effect of changing ODSs and ozone precursor emissions on methane levels via changes to the methane sink and the strength of methane chemical feedbacks. An analysis of the linearity of the total change in methane over the historical period vs. that in the individual attribution experiments indicated the potential role of climate change, higher global temperatures, and the increase in OH derived from increased humidity, but their analysis suggests the utility of a separate experiment to identify the climate-driven, rather than emissions-driven, changes in composition. Subsequently, Zeng et al. (2022) used the *histSST* experiments to determine the role of emissions changes on both stratospheric and tropospheric composition, focusing on the ozone response. In this case, *histSST-piN2O* was crucial, despite being available in a smaller number of models, for assessing the role of long-lived GHGs and changes to stratospheric temperatures on ozone levels. The climate (i.e. CO_2)-driven change in ozone was calculated similar to Stevenson et al. (2020) as the residual between *histSST* and the sum of relevant *histSST* single- or multi-forcing attribution experiments. The analysis by Zeng et al. (2022) contributed to the World Meteorological Organization (WMO) assessment of the recovery of stratospheric ozone (2023). In CMIP6, O'Connor et al. (2021) identified the need for separate *histSST-piVOC* and *histSST-piNOx* to disentangle the drivers of e.g. tropospheric ozone change, similar to *piClim-VOC* and *piClim-NOx* (O'Connor et al., 2021). Experiments such as these are useful in transient experiments where the timing of emissions changes can be used to identify drivers of e.g. ozone production efficiency against a changing set of emissions.

Figure 4 shows the analysis of the ozone burdens in various AerChemMIP experiments (Griffiths et al., 2023) for four of the models employing online chemistry. Here the AerChemMIP experiments isolate the response to a consistent perturbation to the anthropogenic emissions of e.g. ozone precursors applied to each model. Data availability prevents a full comparison across each experiment, but there are data available for *histSST-piNTCF*, *histSST-1950HC*, and *histSST* experiments for all four models, while three also feature *histSST-piO3* and *histSST-piCH4*. It can be seen that GFDL-ESM4 and MRI-ESM2-0 show similar responses to historical changes in concentrations of methane and halocarbon species and that most models except UKESM1 show an increase in ozone due to historical emissions (via the NTCF experiment). While further work is required to understand the origin of these differences, the figure highlights the usefulness of the idealized *histSST-piX* for understanding the origin of model diversity.

3.3 AerChemMIP *hist* experiments

Fully coupled transient simulations enable the impacts of SLCFs, aerosols, and halocarbons (*hist-piNTCF*, *-piAer*, and *-1950HC*) on surface temperature, the hydrological cycle, and atmospheric and oceanic circulation to be assessed. Although these experiments were Tiers 1 and 2, six models performed the simulations in time to be used for the IPCC AR6 report. Ultimately, the modelling centres' contributions increased to 10 models for *hist-piAer* and 11 for *hist-piNTCF*, but the ensemble size from participating models remains small, with a majority of centres only providing a single member for these experiments. Unfortunately, this is not sufficient for use in attribution studies of regional climate change or of changes in the atmospheric or oceanic circulation. Compared to global/hemispheric scales, detecting and attributing a regional climate response is generally more difficult due to a smaller signal-to-noise (i.e. internal climate variability) ratio, and community uptake of the AerChemMIP simulations has been limited as a result. More ensemble members are available for some of the similar DAMIP experiments, such as *hist-aer*. However, the AerChemMIP experiments have been used to attribute global- and hemispheric-scale climate trends to SLCFs. Zhang et al. (2021a) showed that the common bias of CMIP6 ESMs overestimating the magnitude of mid-20th century cooling was primarily due to the higher aerosol burden in these models compared to their physical model counterparts. Using the difference between the historical and *hist-piAer* experiments, Zhang et al.

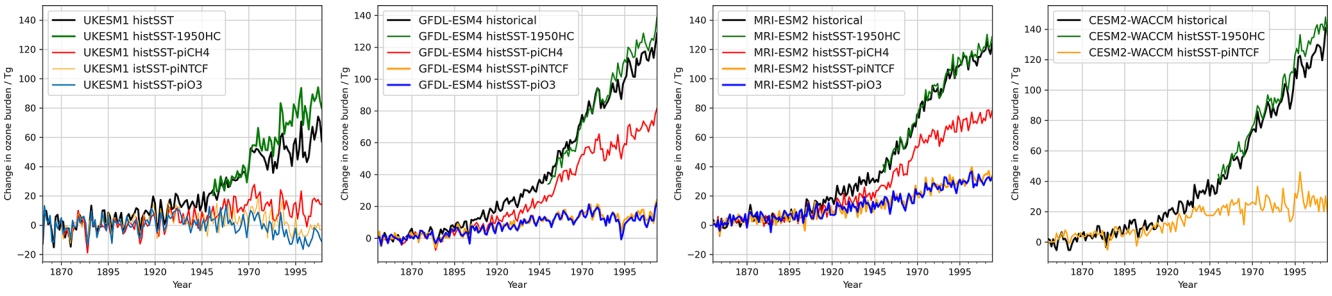

Figure 4. Ozone burdens in AerChemMIP *histSST-X* experiments taken from models using online chemistry. Burdens were calculated using the online tropopause as in Griffiths et al. (2021).

(2021a) confirmed that the bias was driven by high aerosol burdens rather than high sensitivities to aerosol forcing, as had previously been speculated. In a separate publication, Zhang et al. (2021b) used the same experiments to show that the dominant influence of anthropogenic aerosols on the terrestrial carbon sink is due to the increase in diffuse radiation from an increase in aerosol emissions leading to an increase in photosynthesis rather than due to the aerosol influence on temperature, precipitation, or the amount of incident shortwave radiation at the surface.

The *hist-piAer* experiments have been used to confirm the main processes behind features of PD climate. Diamond et al. (2022) discuss the current asymmetry between Northern Hemisphere (NH) and Southern Hemisphere (SH) albedo, which they find to be a transient feature of global climate. The NH is more reflective in clear skies, but the SH is more cloudy. However, the difference in continental coverage between the hemispheres is offset by the larger extent of Antarctic ice compared to the Arctic, so PD asymmetry in clear-sky albedo is dominated by aerosol (confirmed by a comparison between the *historical* and *hist-piAer* experiments). The *hist-piNTCF* experiments have also been useful for investigating where emissions or processes do not play a major role in climate change. DeRepentigny et al. (2020) used the experiments to indicate that SLCFs are not important for the timing of the occurrence of an ice-free Arctic (in CESM2) or the deceleration of the rate of PD ice loss in their model. The initial occurrence of an ice-free Arctic in the near future is instead primarily controlled by internal variability, while the rate of sea-ice decline on longer timescales is determined by CO_2 concentrations. Zeng et al. (2022) use a comparison between the *histSST-piX* experiments and *hist-piNTCF* to confirm that coupling to an interactive ocean has little impact on simulated ozone trends, confirming the utility of fixed SST experiments for studying atmospheric composition. Similarity in methane lifetimes between the *historical* and *histSST* experiments was noted by Stevenson et al. (2020).

The ability to use the difference between the *historical* and *hist-piX* experiments to isolate the role of a set of forcers in climate trends is also useful for model evaluation. Moseid et al. (2020) evaluated global and regional trends in downwelling shortwave radiation at the surface between 1961 and 2014, comparing model output from the *historical* simulation to surface observations. CMIP6 models generally performed well compared to observations over Europe but poorly over China. Using *hist-piAer*, Moseid et al. (2020) demonstrated that this was due to incorrect SO_2 emission trends over China.

3.4 AerChemMIP *ssp370* experiments

Allen et al. (2021) used the AOGCM *ssp370* and *ssp370-lowNTCF* experiments, together with the additional *ssp370-lowNTCFCH4* experiment, to investigate air quality benefits and climate impacts from SLCF mitigation. Coupled AOGCM experiments allowed the effect of SLCF on surface temperature and precipitation to be derived, finding significant perturbations in the hydrological cycle and highlighting the beneficial role of methane concentration reductions in counteracting the warming and wetting effects from aerosol reductions. Similar work by Shim et al. (2021) focuses on air quality in Asia, as does that by Li et al. (2023), which focuses on both air quality and climate in Asia. Zanis et al. (2022) used the *ssp370SST* and *ssp370pdSST* experiments to derive the change in surface ozone with increasing temperature, the "ozone–climate penalty," showing an overall negative relationship between surface ozone and global temperature change, the result of large rates of ozone destruction over marine areas, with increases in ozone over the polluted regions of South Asia and East Asia. Recently, the *ssp370* and related experiments have been used in studies examining the future burden of disease due to changing air quality (Akritidis et al., 2024; Turnock et al., 2023). The *o3ste* diagnostic output, a stratospheric ozone tracer intended to map stratosphere-to-troposphere exchange, was shown to be useful for identifying the role of circulation changes, particularly increased stratosphere-to-troposphere transport of ozone as the level of ODSs decrease in the future, on future ozone levels. Brown et al. (2022) used *ssp370SST* and *ssp370pdSST* to identify the emissions and chemistry drivers of the ozone–climate penalty in Africa and South America,

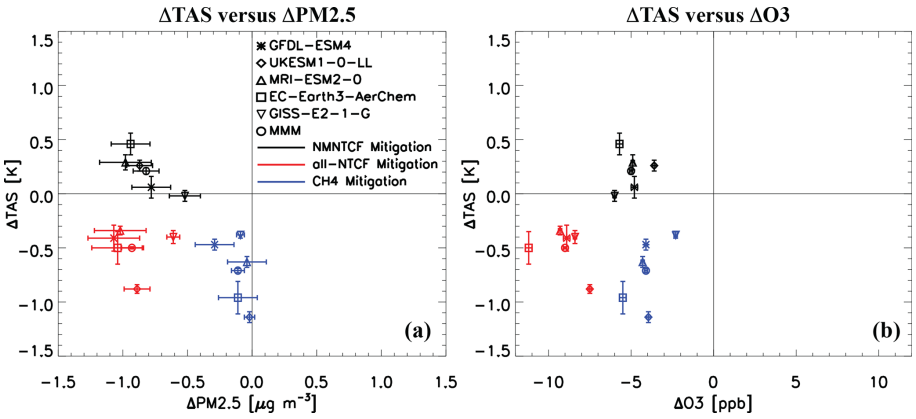

Figure 5. Global annual mean 2090–2099 relative to 2014–2005 mitigation response scatterplots, based on analysis in the work of Allen et al. (2021). Surface temperature [K] vs. surface **(a)** $PM_{2.5}$ [$\mu g\ m^{-3}$] and **(b)** ozone [ppb] for five AerChemMIP models (as designated in the legend by symbols) and the corresponding multi-model mean (MMM) under non-methane near-term climate forcer mitigation (NMTNCF; black), all-NTCF mitigation (red), and methane-only mitigation (CH4; blue). Error bars represent the 95 % confidence interval, estimated as twice the standard error. In the case of multiple realizations (UKESM1-0-LL, MRI-ESM2-0, and GISS-E2-G each performed 3 realizations per simulation), the symbol represents the model mean.

including lightning NO_x changes, changes in the formation of NO_x reservoirs such as isoprene nitrate and peroxyacetyl nitrate (PAN), and temperature-driven changes in the emissions of BVOCs such as isoprene. A difference in the sign of the ozone–climate penalty was noted, depending on background NO_x levels and highlighting the need for detailed chemical diagnostics when considering air quality and climate change interactions. The coupled AOGCM experiments were also used to investigate the effects of SLCF mitigation on the Atlantic meridional overturning circulation (AMOC), showing that future reductions in aerosol and ozone precursors alone induce end-of-century weakening of the AMOC, but this weakening is offset if methane reductions are applied (Hassan et al., 2022).

Figure 5 shows an illustration of how AerChemMIP data may be used for combined air quality and climate co-benefit studies. The figure shows that non-methane NTCF (NMNTCF) mitigation (aerosols and precursor gases only) improves air quality (both particulate matter with a diameter of less than 2.5 µm ($PM_{2.5}$) and ozone) but at the expense of climate warming. Methane mitigation yields global cooling (a climate benefit) as well as improved ozone-related air quality with minor changes in $PM_{2.5}$. All-NTCF mitigation (methane as well as aerosols and precursor gases) yields both a climate benefit (cooling but less than that under methane mitigation) and an air quality benefit in terms of both $PM_{2.5}$ and ozone.

As mentioned above, AerChemMIP contributed to the development of the WGI IPCC AR6, being referenced in the "Summary for Policymakers", Chaps. 4, 6, and 7, and the atlas, as well as contributing important assessment/evaluation papers that underpin the report. Furthermore, the AerChemMIP experiments allowed the attribution of historical surface temperature changes to composition changes by comparing the CMIP historical experiment to the AerChemMIP *histpiAer* experiment and the attribution of radiative forcing to individual components using 6 models (ESGF now shows near-surface temperature (tas) from 10 models).

The AerChemMIP data contributed to the development of emulators. The contributions to PD ozone forcing from CH_4, NO_x, N_2O, halocarbons, CO, VOCs, and climate are derived from AerChemMIP *piClim-X* single-forced experiments (Thornhill et al., 2021b, a) and the coupled CMIP6 *historical* experiment (Skeie et al., 2020). This relationship was used in AR6 Working Group 1 Chap. 7 to derive the historical ozone forcing time series. AerChemMIP also allowed an evaluation of the sensitivity of methane's chemical lifetime to reactive gases and climate (Thornhill et al., 2021a, b). The *histSST-piAer* experiment, along with RFMIP's *piClim-histaer*, allowed the diagnosis of historical aerosol forcing from emissions of SO_2, BC, and OC, which was used to construct time series of historical aerosol forcing (both ARI and ACI components) for AR6 (Smith et al., 2021). All of these emission- and burden-derived relationships are now incorporated into the FaIR reduced-complexity climate model (Smith et al., 2018; Leach et al., 2021). Furthermore, methane's contribution to ozone forcing and the methane lifetime self-feedback factor were used in the computation of emissions metrics for methane in AR6 such as GWP (Forster et al., 2021). The *ssp370-lowNTCF* simulations were also used to supplement ScenarioMIP and DAMIP simulations in the training of machine-learning-based emulators participating in the ClimateBench benchmark dataset (Watson-Parris et al., 2022).

In Tables 2 and 3 we provide summaries of model components, grids, relevant physics options, and emergent prop-

https://doi.org/10.5194/acp-25-8289-2025

Table 2. Model atmospheric, aerosol, chemistry, ocean, sea-ice, and land-use components of CMIP6 models, with the models contributing multiple coupled transient experiments to AerChemMIP highlighted in bold. A full description of the representation of aerosol–radiation interactions, aerosol–cloud interactions, atmospheric chemistry, dust emissions, and biomass burning emissions in the AerChemMIP models can be found in Wilcox (2024). This description uses text extracted from model documentation papers and entries in ES-DOC.

		Model components						ES-DOC		References	
Model	Centre	Atmosphere	Aerosol	Chemistry	Ocean	Sea ice	Land	Aerosol	Chem	Data	Documentation
ACCESS-CM2	CSIRO-ARCCSS	MetUM-HadGEM3-GA7.1	UKCA-GLOMAP-mode		ACCESS-OM2 (GFDL-MOM5)	CICE5.1.2	CABLE2.5	N		Dix et al. (2019)	Bi et al. (2020)
ACCESS-ESM1-5	CSIRO	HadGAM2	CLASSIC (v1.0)		ACCESS-OM2	CICE4.1	CABLE2.4	Y		Ziehn et al. (2019)	Ziehn et al. (2020)
AWI-ESM-1-1-LR	AWI	ECHAM6.3.04p1	MACv2-SP		FESOM 1.4	FESOM 1.4	JSBACH 3.20 with dynamic vegetation	N		Danek et al. (2020)	Sidorenko et al. (2015)
BCC-CSM2-MR	BCC	BCC_AGCM3_MR	MACv2-SP		MOM4	SIS2	BCC_AVIM2	N		Wu et al. (2018)	Wu et al. (2019)
BCC-ESM1	**BCC**	**BCC_AGCM3_LR**		**BCC-AGCM3-Chem**	**MOM4**	**SIS2**	**BCC_AVIM2**	N	N	Zhang et al. (2018)	Wu et al. (2020)
CAMS-CSM1-0	CAMS	ECHAM5_CAMS			MOM4	SIS 1.0	CoLM 1.0	N	N	Rong (2019)	Chen et al. (2019), Rong et al. (2018)
CanESM5	CCCma	CanAM5	Interactive	Specified oxidants	NEMO3.4.1	LIM2	CLASS3.6-CTEM1.2	Y		Swart et al. (2019a)	Swart et al. (2019b)
CAS-ESM2-0	CAS	IAP AGCM 5.0	IAP AACM	IAP AACM	LICOM2.0	CICE4	CoLM	N	N	Chen et al. (2019)	Zhang et al. (2020)
CESM2-FV2	NCAR	CAM6	MAM4	MAM4	POP2	CICE5.1	CLM5	N	N	Danabasoglu (2019a)	Danabasoglu et al. (2020)
CESM2	NCAR	CAM6	MAM4	MAM4	POP2	CICE5.1	CLM5	Y	Y	Danabasoglu (2019d)	Danabasoglu et al. (2020)
CESM2-WACCM-FV2	NCAR	WACCM6	MAM4	MAM4	POP2	CICE5.1	CLM5	N	N	Danabasoglu (2019b)	Danabasoglu et al. (2020)
CESM2-WACCM	**NCAR**	**WACCM6**	**MAM4**	**MAM4**	**POP2**	**CICE5.1**	**CLM5**	N	N	Danabasoglu (2019c)	Danabasoglu et al. (2020)
CIESM	THU	CIESM-AM	MAM4	trop_mam4	CIESM-OM	CICE4	CIESM-LM	N	N	Huang (2019)	Lin et al. (2020)
CMCC-CM2-HR4	CMCC	CAM4	MACv2-SP		NEMO3.6	CICE4.0	CLM4.5	N		Scoccimarro et al. (2020)	Cherchi et al. (2019)
CMCC-CM2-SR5	CMCC	CAM5.3	MAM3		NEMO3.6	CICE4.0	CLM4.5	Y		Lovato and Peano (2020)	Cherchi et al. (2019)

https://doi.org/10.5194/acp-25-8289-2025

Table 2. Continued.

		Model components						ES-DOC		References	
Model	Centre	Atmosphere	Aerosol	Chemistry	Ocean	Sea ice	Land	Aerosol	Chem	Data	Documentation
CNRM-CM6-1	CNRM-CERFACS	Arpege 6.3	Prescribed monthly fields computed by TACTIC_v2	OZL_v2	NEMO3.6	Gelato 6.1	Surfex 8.0c	N	N	Voldoire (2018)	Voldoire et al. (2019)
CNRM-ESM2-1	**CNRM-CERFACS**	**Arpege 6.3**	**TACTIC_v2**	**REPROBUS-C_v2**	**NEMO3.6**	**Gelato 6.1**	**Surfex 8.0c**	Y	Y	Seferian (2018)	Séférian et al. (2019)
E3SM-1-0	E3SM-Project	EAM v1.0	MAM4	Troposphere specified oxidants for aerosols. Stratosphere linearized interactive ozone (LINOZ v2)	MPAS-Ocean v6.0	MPAS-Seaice v6.0	ELM v1.0	N	N	Bader et al. (2019a)	Golaz et al. (2019)
E3SM-1-1	E3SM-Project	EAM v1.1	MAM4	Troposphere specified oxidants for aerosols. Stratosphere linearized interactive ozone (LINOZ v2)	MPAS-Ocean v6.0	MPAS-Seaice v6.0	ELM v1.1	N	N	Bader et al. (2019b)	Burrows et al. (2020)
EC-Earth3-AerChem	**EC-Earth-Consortium**	**IFS cy36r4**	**TM5**	**TM5**	**NEMO3.6**	**LIM3**	**HTESSEL**	Y	Y	EC-Earth (2020)	van Noije et al. (2021)
EC-Earth3	EC-Earth-Consortium	IFS cy36r4	MACv2-SP	TM5	NEMO3.6	LIM3	HTESSEL	N	N	EC-Earth (2019b)	Döscher et al. (2022)
EC-Earth3-Veg	EC-Earth-Consortium	IFS cy36r4	MACv2-SP	TM5	NEMO3.6	LIM3	LPJ-GUESS v4	N	N	EC-Earth (2019a)	Döscher et al. (2022)
FGOALS-f3-L	CAS	FAMIL2.2	MACv2-SP		LICOM3.0	CICE4.0	CLM4.0	N		Yu (2019)	He et al. (2020)
FGOALS-g3	CAS	GAMIL3	MACv2-SP		LICOM3.0	CICE4.0	CAS-LSM	N		Li (2019)	Li et al. (2020)
FIO-ESM-2-0	FIO-QLNM	CAM4	Prescribed monthly fields		POP2-W (POP2 coupled with MASNUM surface wave model)	CICE4.0	CLM4.0	N		Song et al. (2019)	Bao et al. (2020)
GFDL-CM4	NOAA-GFDL	GFDL-AM4.0.1	Interactive	Fast chemistry, aerosol only	GFDL-OM4p25 (GFDL-MOM6)	GFDL-SIM4p25 (GFDL-SIS2.0)	GFDL-LM4.0.1	Y	N	Guo et al. (2018)	Held et al. (2019)

Table 2. Continued.

Model	Centre	Model components						ES-DOC		References	
		Atmosphere	Aerosol	Chemistry	Ocean	Sea ice	Land	Aerosol	Chem	Data	Documentation
GFDL-ESM4	**NOAA-GFDL**	**GFDL-AM4.1**	**Interactive**	**GFDL-ATMCHEM4.1**	**GFDL-OM4p5**	**GFDL-SIM4p5**	**GFDL-LM4.1**	Y	Y	Krasting et al. (2018)	Dunne et al. (2020)
GISS-E2-1-G-CC	NASA-GISS	GISS-E2.1	Varies with physics version	Varies with physics version	GISS Ocean	GISS SI	GISS LSM	N	N	NASA/GISS (2019a)	Kelley et al. (2020), Miller et al. (2021)
GISS-E2-1-G (p1)	NASA-GISS	GISS-E2.1	"None"	Non-interactive	GISS Ocean	GISS SI	GISS LSM	N		NASA/GISS (2018)	Kelley et al. (2020), Miller et al. (2021)
GISS-E2-1-H (p1)	NASA-GISS	GISS-E2.1	"None"	Non-interactive	HYCOM Ocean	GISS SI	GISS LSM	N		NASA/GISS (2019b)	Kelley et al. (2020), Miller et al. (2021)
GISS-E2-1-G (p3)	**NASA-GISS**	**GISS-E2.1**	**OMA**	**GPUCCINI**	**GISS Ocean**	**GIS SI**	**GISS LSM**	N	N	NASA/GISS (2018)	Kelley et al. (2020), Miller et al. (2021)
GISS-E2-1-H (p3)	NASA-GISS	GISS-E2.1	OMA	GPUCCINI	HYCOM Ocean	GISS SI	GISS LSM	N	N	NASA/GISS (2019b)	Kelley et al. (2020), Miller et al. (2021)
GISS-E2-1-G (p5)	NASA-GISS	GISS-E2.1	MATRIX	GPUCCINI	GISS Ocean	GISS SI	GISS LSM	N	N	NASA/GISS (2018)	Kelley et al. (2020), Miller et al. (2021)
GISS-E2-1-H (p5)	NASA-GISS	GISS-E2.1	MATRIX	GPUCCINI	HYCOM Ocean	GISS SI	GISS LSM	N	N	NASA/GISS (2019b)	Kelley et al. (2020), Miller et al. (2021)
HadGEM3-GC31-LL	MOHC	MetUM-HadGEM3-GA7.1	UKCA-GLOMAP-mode		NEMO-HadGEM3-GO6.0	CICE-HadGEM3-GSI8	JULES-HadGEM3-GL7.1	N	N	Ridley et al. (2019a)	Andrews et al. (2020), Kuhlbrodt et al. (2018)
HadGEM3-GC31-MM	MOHC	MetUM-HadGEM3-GA7.1	UKCA-GLOMAP-mode		NEMO-HadGEM3-GO6.0	CICE-HadGEM3-GSI8	JULES-HadGEM3-GL7.1	N	N	Ridley et al. (2019b)	Andrews et al. (2020)
INM-CM4-8	INM	INM-AM4-8	INM-AER1		INM-OM5	INM-ICE1	INM-LND1	N		Volodin et al. (2019a)	Volodin et al. (2010)
INM-CM5-0	INM	INM-AM5-0	INM-AER1		INM-OM5	INM-ICE1	INM-LND1	N		Volodin et al. (2019b)	Volodin et al. (2017), Volodin and Kostrykin (2016)
IPSL-CM6A-LR	IPSL	LMDZ	INCA v6 AER		NEMO-OPA	NEMO-LIM3	ORCHIDEE (v2.0)	N		Boucher et al. (2021)	Boucher et al. (2020)

https://doi.org/10.5194/acp-25-8289-2025

Table 2. Continued.

Model	Centre	Model components						ES-DOC		References	
		Atmosphere	Aerosol	Chemistry	Ocean	Sea ice	Land	Aerosol	Chem	Data	Documentation
KACE-1-0-G	NIMS-KMA	MetUM-HadGEM3-GA7.1	UKCA-GLOMAP-mode		MOM4p1	CICE-HadGEM3-GSI8	JULES-HadGEM3-GL7.1	N		Byun et al. (2019)	Lee et al. (2020a)
KIOST-ESM	KIOST	GFDL-AM2.0	MACv2-SP	Simple carbon aerosol model (emission type)	MOM5.0	SIS	CLM4	N	N	Kim et al. (2019)	Pak et al. (2021)
MIROC6	**MIROC**	**CCSR AGCM**	**SPRINTARS6.0**		**COCO4.9**	**COCO4.9**	**MATSIRO6.0**	Y		Tatebe and Watanabe (2018)	Tatebe et al. (2019)
MIROC-ES2L	MIROC	CCSR AGCM	SPRINTARS6.0		COCO4.9	COCO4.9	MATSIRO6.0 + VISIT-e ver.1.0	N		Hajima et al. (2019)	Hajima et al. (2020)
MPI-ESM-1-2-HAM	**HAMMOZ-Consortium**	**ECHAM6.3**	**HAM2.3**	**Sulfur chemistry**	**MPIOM1.63**	**Thermodynamic (Semtner zero-layer) dynamic (Hibler 79) sea-ice model**	**JSBACH 3.20**	Y		Neubauer et al. (2019)	Mauritsen et al. (2019)
MPI-ESM1-2-HR	MPI-M	ECHAM6.2	MACv2-SP		MPIOM1.63	Thermodynamic (Semtner zero-layer) dynamic (Hibler 79) sea-ice model	JSBACH3.20	N		Jungclaus et al. (2019)	Mauritsen et al. (2019), Stevens et al. (2013)
MPI-ESM1-2-LR	MPI-M	ECHAM6.3	MACv2-SP		MPIOM1.63	Thermodynamic (Semtner zero-layer) dynamic (Hibler 79) sea-ice model	JSBACH3.20	N		Wieners et al. (2019)	Wieners et al. (2019), Stevens et al. (2013)
MRI-ESM2-0	MRI	MRI-AGCM3.5	MASINGAR mk2r4	MRI-CCM2.1	MRI.COM4.4	MRI.COM4.4	HAL 1.0	Y	Y	Yukimoto et al. (2019b)	Yukimoto et al. (2019a)
NESM3	NUIST	ECHAM v6.3	MACv2-SP		NEMO v3.4	CICE4.1	JSBACH v3.1	N		Cao and Wang (2019)	Cao et al. (2018)
NorCPM1	NCC	CAM-OSLO4.1	OsloAero4.1	OsloChemSimp4.1	MICOM1.1	CICE4	CLM4	Y	Y	Bethke et al. (2019)	Bethke et al. (2021)
NorESM2-LM	**NCC**	**CAM-OSLO**	**OsloAero**	**OsloChemSimp**	**MICOM**	**CICE**	**CLM**	Y	Y	Seland et al. (2019)	Seland et al. (2020)

Table 2. Continued.

Model	Centre	Model components					ES-DOC		References	
		Atmosphere	Aerosol	Chemistry	Ocean	Sea ice	Land	Aerosol	Chem	Data	Documentation
NorESM2-MM	NCC	CAM-OSLO	OsloAero	OsloChemSimp	MICOM	CICE	CLM	Y	Y	Bentsen et al. (2019)	Seland et al. (2020)
SAM0-UNICON	SNU	CAM5.3 with UNICON	MAM3		POP2	CICE4.0	CLM4.0	Y		Park and Shin (2019)	Park et al. (2019)
TaiESM1	**AS-RCEC**	**TaiAM1**	**SNAP**	**SNAP**	**POP2**	**CICE4**	**CLM4.0**	N	N	Lee and Liang (2020)	Lee et al. (2020b)
UKESM1-0-LL	**MOHC**	**MetUM-HadGEM3-GA7.1**	**UKCA-GLOMAP-mode**	**UKCA-StratTrop**	**NEMO-HadGEM3-GO6.0**	**CICE-HadGEM3-GSI8**	**JULES-ES-1.0**	N	N	Tang et al. (2019)s	Sellar et al. (2019)

erties for models contributing to CMIP6. In these tables we highlight those models contributing multiple coupled transient experiments to AerChemMIP. The table includes equilibrium climate sensitivity data from Schlund et al. (2023), as well as ERF due to anthropogenic aerosol and the hemispheric contrast in absorbed solar radiation (as a proxy for ERF when the necessary experiments were not available to calculate ERF).

In summary, AerChemMIP provided significant advances, notably coupled transient experiments and the attribution of the role of SLCFs in radiative forcing and climate changes, and enabled keystone analyses of air quality and the identification of the interactions of climate and air quality.

4 AerChemMIP – challenges and gaps

4.1 Timelines

The design of CMIP6, with no hard deadlines for data release, meant that modelling centres were free to deliver data as they became available. However, the IPCC assessment report timeline process was again very tight, making preparation for CMIP6 challenging. This was constrained further by the late release of the forcing datasets needed to perform simulations and the cost of data processing to Climate Model Output Rewriter (CMOR) standards. Data came on-stream over the period 2019–2021, and, across AerChemMIP, only a quarter of the models eventually delivering data had done so by the end of June 2019, with three-quarters delivering by the December 2019 submission deadline for papers to be included in AR6. With hindsight, it may have been better for key experiments to have been identified early and for the data to address assessment-relevant scientific questions to be available sooner.

Although the availability of model documentation and description was improved for CMIP6 relative to CMIP5 with the advent of ES-DOC, data for many models were published ahead of model documentation. This meant that it was difficult to use these models in process studies as modelling centres needed to be contacted directly to obtain information, e.g. which parameterization schemes had been used for aerosol microphysics.

4.2 Coordination across MIPs

In its preparation, AerChemMIP assumed extensive collaboration with DECK, the CMIP historical experiments, RFMIP, and ScenarioMIP. The *piControl*, *historical*, and *ssp370* experiments provided baselines for the AerChemMIP experiments and provided SST and sea-ice fields for experiments where these were prescribed, while complementary experiments for calculating ERFs for WMGHGs, land use, and natural forcing came from RFMIP.

DAMIP and AerChemMIP proposed similar coupled historical experiments, and closer integration with DAMIP's

https://doi.org/10.5194/acp-25-8289-2025

Table 3. Model atmospheric, aerosol, and chemistry components of CMIP6 models; their atmospheric grids; and emergent properties, with the models contributing multiple coupled transient experiments to AerChemMIP highlighted in **bold**. Equilibrium climate sensitivity (ECS) is taken from Schlund et al. (2020). Effective radiative forcing due to anthropogenic aerosol (ERF_AA) was calculated by the authors for the period 2014 vs. 1850 using RFMIP *piClim-aer* and *piClim* simulations. The difference in absorbed solar radiation between the Southern Hemisphere and Northern Hemisphere (ASR_HD) is used as a proxy for aerosol radiative forcing, which can be calculated from historical simulations. Here, the change in this index over the period from 1850 to 1985, when it is most closely related to aerosol forcing, is shown and is taken from Menary et al. (2020).

		Model components			Model grid				Emergent properties			
Model	Centre	Atmosphere	Aerosol	Chemistry	nx	ny	nz	Model top	ECS	ERF_AA	ASR_HD	Reference
ACCESS-CM2	CSIRO-ARCCSS	MetUM-HadGEM3-GA7.1	UKCA-GLOMAP-mode		192	144	85	85 km	4.72	−1.09	2.19	Bi et al. (2020)
ACCESS-ESM1-5	CSIRO	HadGAM2	CLASSIC (v1.0)		192	145	38	39 km	3.87	−1.15	1.90	Ziehn et al. (2020)
AWI-ESM-1-1-LR	AWI	ECHAM6.3.04p1	MACv2-SP		192	96	47	80 km	3.16			Sidorenko et al. (2015)
BCC-CSM2-MR	BCC	BCC_AGCM3_MR	MACv2-SP		320	160	46	1.46 hPa	3.04		0.60	Wu et al. (2019)
BCC-ESM1	**BCC**	**BCC_AGCM3_LR**		**BCC-AGCM3-Chem**	128	64	26	2.19 hPa	3.26		2.04	Wu et al. (2020)
CAMS-CSM1-0	CAMS	ECHAM5_CAMS			320	160	31	10 hPa	2.29		−0.01	Chen et al. (2019), Rong et al. (2018)
CanESM5	CCCma	CanAM5	Interactive	Specified oxidants	128	64	49	1 hPa	5.62	−0.85	1.61	Swart et al. (2019b)
CAS-ESM2-0	CAS	IAP AGCM 5.0	IAP AACM	IAP AACM	256	128	35	2.2 hPa	3.51		2.51	Zhang et al. (2020)
CESM2-FV2	NCAR	CAM6	MAM4	MAM4	144	96	32	2.25 hPa	5.14		2.95	Danabasoglu et al. (2020)
CESM2	NCAR	CAM6	MAM4	MAM4	288	192	32	2.25 hPa	5.16	−1.37	2.55	Danabasoglu et al. (2020)
CESM2-WACCM-FV2	NCAR	WACCM6	MAM4	MAM4	144	96	70	4.5E-6 hPa	4.79		2.82	Danabasoglu et al. (2020)
CESM2-WACCM	**NCAR**	**WACCM6**	**MAM4**	**MAM4**	288	192	70	4.5E-6 hPa	4.75		2.74	Danabasoglu et al. (2020)
CIESM	THU	CIESM-AM	MAM4	trop_mam4	288	192	30	2.255 hPa	5.67		0.45	Lin et al. (2020)
CMCC-CM2-HR4	CMCC	CAM4	MACv2-SP		288	192	26	2 hPa			0.58	Cherchi et al. (2019)
CMCC-CM2-SR5	CMCC	CAM5.3	MAM3		288	192	30	2.2 hPa	3.52		0.48	Cherchi et al. (2019)
CNRM-CM6-1	CNRM-CERFACS	Arpege 6.3	Prescribed monthly fields computed by TACTIC_v2	OZL_v2		128	91	78.4 km	4.83	−1.15	1.05	Voldoire et al. (2019)
CNRM-ESM2-1	**CNRM-CERFACS**	**Arpege 6.3**	**TACTIC_v2**	**REPROBUS-C_v2**	256	128	91	78.4 km	4.76	−0.74	1.21	Séférian et al. (2019)

Table 3. Continued.

Model	Centre	Model components			Model grid				Emergent properties			Reference
		Atmosphere	Aerosol	Chemistry	nx	ny	nz	Model top	ECS	ERF_AA	ASR_HD	
E3SM-1-0	E3SM-Project	EAM v1.0	MAM4	Troposphere specified oxidants for aerosols. Stratosphere linearized interactive ozone (LINOZ v2)			72	0.1 hPa	5.32	−1.65	3.37	Golaz et al. (2019)
E3SM-1-1	E3SM-Project	EAM v1.1	MAM4	Troposphere specified oxidants for aerosols. Stratosphere linearized interactive ozone (LINOZ v2)			72	0.1 hPa			4.04	Burrows et al. (2020)
EC-Earth3-AerChem	EC-Earth-Consortium	IFS cy36r4	TM5	TM5	512	256	91	0.01 hPa	3.90	−0.70	3.95	van Noije et al. (2021)
EC-Earth3	EC-Earth-Consortium	IFS cy36r4	MACv2-SP	TM5	512	256	91	0.01 hPa		−0.91	2.43	Döscher et al. (2022)
EC-Earth3-Veg	EC-Earth-Consortium	IFS cy36r4	MACv2-SP	TM5	512	256	91	0.01 hPa	4.31		−0.37	Döscher et al. (2022)
FGOALS-f3-L	CAS	FAMIL2.2	MACv2-SP		360	180	32	2.16 hPa	3		1.43	He et al. (2020)
FGOALS-g3	CAS	GAMIL3	MACv2-SP		360	180	26	2.19 hPa	2.88		0.10	Li et al. (2020)
FIO-ESM-2-0	FIO-QLNM	CAM4	Prescribed monthly fields		192	288	26	2 hPa			0.46	Bao et al. (2020)
GFDL-CM4	NOAA-GFDL	GFDL-AM4.0.1	Interactive	Fast chemistry, aerosol only	360	180	33	1 hPa	5	−0.73	1.81	Held et al. (2019)
GFDL-ESM4	**NOAA-GFDL**	**GFDL-AM4.1**	**Interactive**	**GFDL-ATMCHEM4.1**	360	180	49	1 hPa			1.43	Dunne et al. (2020)
SAM0-UNICON	NASA-GISS	GISS-E2.1	Varies with physics version	Varies with physics version	144	90	40	0.1 hPa			1.84	Kelley et al. (2020), Miller et al. (2021)
GISS-E2-1-G (p1)	NASA-GISS	GISS-E2.1	"None"	Non-interactive	144	90	40	0.1 hPa	2.72	−1.32	1.76	Kelley et al. (2020), Miller et al. (2021)
GISS-E2-1-H (p1)	NASA-GISS	GISS-E2.1	"None"	Non-interactive	144	90	40	0.1 hPa	3.11		1.68	Kelley et al. (2020), Miller et al. (2021)
GISS-E2-1-G (p3)	**NASA-GISS**	**GISS-E2.1**	**OMA**	**GPUCCINI**	144	90	40	0.1 hPa	2.60	−1.85		Kelley et al. (2020), Miller et al. (2021)
GISS-E2-1-H (p3)	NASA-GISS	GISS-E2.1	OMA	GPUCCINI	144	90	40	0.1 hPa	3.10			Kelley et al. (2020), Miller et al. (2021)
GISS-E2-1-G (p5)	NASA-GISS	GISS-E2.1	MATRIX	GPUCCINI	144	90	40	0.1 hPa	2.80	−1.36		Kelley et al. (2020), Miller et al. (2021)
GISS-E2-1-H (p5)	NASA-GISS	GISS-E2.1	MATRIX	GPUCCINI	144	90	40	0.1 hPa				Kelley et al. (2020), Miller et al. (2021)

https://doi.org/10.5194/acp-25-8289-2025

Table 3. Continued.

Model	Centre	Model components			Model grid				Emergent properties			Reference
		Atmosphere	Aerosol	Chemistry	nx	ny	nz	Model top	ECS	ERF_AA	ASR_HD	
HadGEM3-GC31-LL	MOHC	MetUM-HadGEM3-GA7.1	UKCA-GLOMAP-mode		192	144	85	85 km	5.55	−1.10	2.47	Andrews et al. (2020), Kuhlbrodt et al. (2018)
HadGEM3-GC31-MM	MOHC	MetUM-HadGEM3-GA7.1	UKCA-GLOMAP-mode		423	324	85	85 km	5.42		2.65	Andrews et al. (2020)
INM-CM4-8	INM	INM-AM4-8	INM-AER1		180	120	21	0.01 sigma	1.83			Volodin et al. (2010)
INM-CM5-0	INM	INM-AM5-0	INM-AER1		180	120	73	002 sigma	1.92		0.18	Volodin et al. (2017), Volodin and Kostrykin (2016)
IPSL-CM6A-LR	**IPSL**	**LMDZ**	**INCA v6 AER**		144	143	79	80 km	4.56	−0.59	0.35	Boucher et al. (2020)
KACE-1-0-G	NIMS-KMA	MetUM-HadGEM3-GA7.1	UKCA-GLOMAP-mode		192	144	85	85 km	4.48		1.76	Lee et al. (2020a)
KIOST-ESM	KIOST	GFDL-AM2.0	MACv2-SP	Simple carbon aerosol model (emission type)	192	96	32	2 hPa	3.36		0.02	Pak et al. (2021)
MIROC6	**MIROC**	**CCSR AGCM**	**SPRINTARS6.0**		256	128	81	04 hPa	2.61	−1.06	0.81	Tatebe et al. (2019)
MIROC-ES2L	MIROC	CCSR AGCM	SPRINTARS6.0		128	64	40	3 hPa	2.68		0.94	Hajima et al. (2020)
MPI-ESM-1-2-HAM	**HAMMOZ-Consortium**	**ECHAM6.3**	**HAM2.3**	**Sulfur chemistry**	192	96	47	0.01 hPa	2.96		2.23	Mauritsen et al. (2019)
MPI-ESM1-2-HR	MPI-M	ECHAM6.2	MACv2-SP		384	192	95	0.01 hPa	3		0.11	Mauritsen et al. (2019), Stevens et al. (2013)
MPI-ESM1-2-LR	MPI-M	ECHAM6.3	MACv2-SP		192	96	47	0.01 hPa	3		0.24	Mauritsen et al. (2019), Stevens et al. (2013)
MRI-ESM2-0	**MRI**	**MRI-AGCM3.5**	**MASINGAR mk2r4**	**MRI-CCM2.1**	320	160	80	0.01 hPa	3.15	−1.19	2.35	Yukimoto et al. (2019a)
NESM3	NUIST	ECHAM v6.3	MACv2-SP		192	96	47	1 hPa	4.72		1.45	Cao et al. (2018)
NorCPM1	NCC	CAM-OSLO4.1	OsloAero4.1	OsloChemSimp4.1	144	96	26	2 hPa	3.05		2.41	Bethke et al. (2021)
NorESM2-LM	**NCC**	**CAM-OSLO**	**OsloAero**	**OsloChemSimp**	144	96	32	3 MB	2.54	−1.21	2.24	Seland et al. (2020)
NorESM2-MM	NCC	CAM-OSLO	OsloAero	OsloChemSimp	288	192	32	3 MB	2.50	−1.26	2.13	Seland et al. (2020)
SAM0-UNICON	SNU	CAM5.3 with UNICON	MAM3		288	192	30	2 hPa	3.72	−1.23	1.68	Park et al. (2019)
TaiESM1	**AS-RCEC**	**TaiAM1**	**SNAP**	**SNAP**	288	192	20	2 hPa	4.31		2.79	Lee et al. (2020b)
UKESM1-0-LL	**MOHC**	**MetUM-HadGEM3-GA7.1**	**UKCA-GLOMAP-mode**	**UKCA-StratTrop**	192	144	85	85 km	5.34	−1.11	2.84	Sellar et al. (2019)

complementary *hist-X* experiment would have been beneficial. At the time of writing, six models have contributed data from both DAMIP *hist-Aer* and AerChemMIP *hist-piAer*. Given the demands on modelling centres, it was perhaps prohibitively costly to ask for both variants (*hist-X* and *hist-piX*) for an attribution experiment, but it would certainly have been preferable to have both variants available. The *hist-piX* experiment design avoids the assumption of linearity that underpins the analysis of *hist-X* experiments. For many of the species considered by AerChemMIP, a degree of non-linearity is expected in the climate response as the world warms, related to changing reaction rates or changes in cloud distribution and properties. However, for the quantification of the effect of such non-linearities, these "everything but" style experiments need to be paired with single-forcing simulations, requiring better overlap between model participation in DAMIP and AerChemMIP. Diamond et al. (2022) used the AerChemMIP *hist-piAer* as a substitute for missing DAMIP *hist-GHG* experiments in order to include UKESM1 and MPI-ESM-1-2-HAM in their investigation of delayed eastern equatorial Pacific warming, but without further analysis of the linearity of the response to changing aerosol emissions in a warming world it is difficult to know how sound this assumption is, especially as the degree of linearity is likely to be model-dependent (Simpson et al., 2023).

4.3 Coordinated variable request

There was a lack of consistent diagnostics across participating models in CMIP6, even for standard Tier 1 variables. This raised some challenges for analysis of the AerChemMIP data, effectively making a small (6–7 model) ensemble even smaller and limiting the utility of the experiments. Consistent output variables over all models and all scenarios would have allowed larger ensembles to be used in analysis: models were sometimes rejected from studies for not including (Tier 1) variables of interest (Griffiths et al., 2021).

SSP3-7.0, a pathway involving weak air quality control measures, was chosen as a future baseline by AerChemMIP. From a policy perspective, it is clear that diagnostic data from other SSPs with stronger air quality measures, such as SSP2-4.5 (middle of the road) and SSP1-1.9 (sustainability), would have been useful. AerChemMIP specified priority variables and their domain and frequency for the *historical* and *ssp370* experiments, and it was envisaged that a similar level of detail would be provided by other centres for other ScenarioMIP experiments. Given the pressure on data processing and data archival, some centres omitted the AerChemMIP diagnostics from other ScenarioMIP experiments, prohibiting comparative analysis of e.g. chemical and aerosol processes. In particular, the inclusion of air quality diagnostics in the *ssp245* experiment would have allowed a more direct comparison between CMIP6 studies and those based around the ECLIPSE (Evaluating the Climate and Air Quality Impacts of Short-Lived Pollutants) (Stohl et al., 2015) experiments, which use an RCP4.5 baseline. Improved availability of air quality diagnostics over a wide range of future emission pathways would have enabled better understanding of the future interactions of climate change and air quality, and these diagnostics merit inclusion in a wider variety of scenarios by all centres in future MIP eras. At present, the attribution of the drivers of air quality changes in future scenarios other than SSP3-7.0 in a multi-model sense is still lacking due in part to the lack of data to perform such analyses, although Turnock et al. (2020) were able to perform analyses across the various SSPs for surface ozone and $PM_{2.5}$.

4.4 Experiment design

AerChemMIP encouraged participating models to include interactive aerosol and online tropospheric and stratospheric chemistry schemes, which meant that it was only possible for a small subset of CMIP6 models to perform all AerChemMIP experiments (Table 1). The bulk of AerChemMIP data comes from 11 models: BCC-ESM1, CESM2-WACCM, CNRM-ESM (interactive stratosphere only), EC-Earth3-AerChem, GFDL-ESM4, GISS-E2, MIROC6-SPRINTARS, MPI-ESM1.2, MRI-ESM2, NorEMS2, and UKESM1, of which MPI-ESM1.2 and NorESM2 use offline chemistry. Although similar to the number (seven) of models participating in the chemistry model intercomparison projects of Hemispheric Transport of Air Pollution (HTAP) Phase 2 and the Air Quality Model Evaluation International Initiative (AQMEII), this represents approximately 15 % of the 70 models and model variants contributing to CMIP6. Within this small subset, there is large variance between model results, and it becomes difficult to construct, and have faith in, reliable multi-model means. In this situation, identifying outliers also becomes challenging.

In addition to expanding the range of scenarios with AerChemMIP diagnostics, it is useful in each scenario to specify additional complementary experiments, similar to the *ssp370-pdSST* which was used as a complement to *ssp370SST* (Turnock et al., 2022), so as to be able to determine ozone–climate penalties and to assess the linearity of the climate response. This is similar to the RFMIP *piClim-histaerO3* (historical) experiment but for the future. Additional experiments to address the role of methane in future climate and air quality are needed to more completely address the role of SLCFs in climate change.

4.5 Ensemble size

A single member of a coupled transient simulation is insufficient to identify where differences between models are due to differences in the response to forcing, as opposed to internal variability or other structural differences between the models. AerChemMIP requested at least three ensemble members per coupled experiment. However, these were not always performed, with some centres submitting only

one member per experiment. Unfortunately, this makes it impossible to identify forced responses in transient experiments with realistic forcing, and it meant that while these simulations could be used for the AerChemMIP model ensemble as a whole, they could not be used to understand inter-model differences. Small ensemble sizes more generally present difficulties for the analysis of regional climate responses, which are key for AerChemMIP-related issues, such as air quality, and also for climate extremes. Recent work by Fiore et al. (2022) used a 15-member initial condition ensemble to examine the role of ensemble size in simulating atmospheric composition trends and separating forced trends from internal variability, demonstrating that on multi-decadal timescales, the two are comparably important in some regions. Monerie et al. (2021) examined the role of ensemble size in identifying regional precipitation trends and concluded that 10 members represent a good balance between regional information and computational expense.

4.6 Diagnostics

There is a need for all MIPs to carefully review requested diagnostics for future MIPs to ensure that they are well-designed to address science goals and that diagnostics are delivered in a standard format. For AerChemMIP, diagnostics relating to the ozone budget and tropopause (e.g. dynamical tropopause) were needed and there was a shortage of output for aerosol optical properties (Fiedler et al., 2024).

In the case of tropospheric ozone, ozone production and destruction rates, *o3prod* and *o3loss*, were specified in CMIP6 to cover only a portion of the ozone budget. They are, by definition, insufficient to infer stratospheric ozone input to the troposphere, as the budget closure cannot be guaranteed, making the quantitative equivalence of a residual budget term with stratospheric input impossible. This is especially true as models include additional chemistry, such as tropospheric halogen chemistry, that will strongly influence our interpretation of which reactions should be included in *o3prod* and *o3loss*. Furthermore, subsetting some reactions was in practice prone to human error in implementation. The CCMI diagnostic *do3chm*, the tendency due to chemistry, is strongly encouraged for future MIPs. Whereas isolated production (P) and loss (L) terms are preferable, operator tendencies (i.e. net $P - L$) are much more straightforward to code as a diagnostic and are therefore less prone to implementation errors while still containing valuable information. The increasing adoption of whole-atmosphere online chemistry models, which allows a consistent treatment of ozone chemistry and removes the need for boundary conditions or prescribed ozone fields, is a significant advantage.

New diagnostic output of WMO thermal tropopause height and pressure was available in CMIP6, which allowed the separate evaluation of tropospheric and stratospheric ozone. The tropopause introduces strong variations in stratospheric ozone column between models which are less pronounced when an ozonopause is used (as in CMIP5). For the diagnosis of stratosphere–troposphere transport, a diagnostic tropopause is probably more useful, e.g. a potential-vorticity-based or blended tropical–extra-tropical tropopause definition. Tracer–tracer correlations are also useful here to understand downward transport, and synthetic tracers would add significant value, e.g. *e90* (Abalos et al., 2017; Prather et al., 2011). It may be advantageous to perform whole-atmosphere evaluations and assessments in the future.

Given the difficulty in consistently defining the tropopause, it may be wise to consider the assessment of model performance against e.g. total column ozone and Earth observation (EO) products that target the UT/LS region where the radiative forcing of ozone is largest. Tropospheric ozone burden and column should be treated as less reliable quantities for intercomparison and assessment until such time as reliable diagnostic output is available and their derivation from EO products is less problematic (Gaudel et al., 2018). It was regrettable that some centres did not provide tropopause output, preventing calculations of burdens and other useful diagnostics.

4.7 Emulators and impact assessments

The consideration of the experimental design for the development of flexible and comprehensive emulators, whether a physical reduced-complexity model (Smith et al., 2018) or machine-learning-based model (Watson-Parris et al., 2021), requires many similar considerations to answer the fundamental questions addressed above but also presents other challenges. For example, the use of idealized, single-forcing experiments to isolate individual contributions to radiative forcing and composition can be very valuable in this setting for either training or validation. In order to ensure that the emulator is interpolating between simulations rather than extrapolating beyond them (in emissions, concentration or forcing), it is valuable to have data points at the extrema of the relevant space. In this regard, very high-emissions scenarios (such as SSP5-8.5), very ambitious scenarios (such as SSP1-1.9), and other corner cases (such as SSP3-7.0-lowNTCF) are extremely useful, regardless of their realism, as is participation in single-forcing experiments by a variety of models. However, while such scenarios have very different global mean emissions, they do not explore very different spatial distributions of emissions, which are so important for aerosol and other short-lived chemical species. Sampling this space is the focus of the Regional Aerosol MIP (RAMIP; Wilcox et al., 2023), which, with the aid of large ensembles, will ensure robust signals.

While AerChemMIP has shone a light on model diversity in e.g. aerosol forcing, sampling the process uncertainty explicitly within each model would provide valuable insights into the contribution to this spread from structural vs. parametric uncertainty (Lee et al., 2011). Sampling full parametric uncertainty requires hundreds of simulations, but simple

scalings of the aerosol indirect effect, for example, would allow the useful determination of the role of such processes in inter-model diversity and persistent discrepancies with observations. Such ensembles can also be incorporated into the emulators described above to more fully capture model uncertainties and potentially constrain them with energy budget considerations.

5 Planning and designing future aerosol and chemistry MIPs

So far we have considered the success of AerChemMIP's objectives and its support of wider CMIP goals, as well as identifying some remaining areas for future study. In this section, we present some reflections by the AerChemMIP community on future CMIP and AerChemMIP activities, addressing this from the perspective of the CMIP, sub-MIP, and modelling centre level.

5.1 Coordination across MIPs

CMIP is comprised of various specialist sub-MIPs such as AerChemMIP. It is to be expected that new sub-MIPs will arise and evolve over time and may eventually be folded into the standard DECK or core experiments. The recent proposal of a "fast track" for CMIP7, incorporating experiments previously in AerChemMIP and RFMIP exemplifies this. The CMIP project brings essential early-stage planning and coordination for the community, provides crucial oversight, and enables cross-cutting activities such as fast track and task teams for supporting CMIP activities, such as forcing updates, defining standard data requests, and designing simulations. From our perspective, an important role for CMIP remains in providing oversight of and coordination between the individual participating MIPs. This coordination across MIPs is vital as each sub-MIP forms a part of the CMIP landscape, and CMIP needs to ensure its underpinning goals and science questions are being addressed. It is also important to ensure that each sub-MIP integrates well with other MIPs, avoiding duplication of effort and enabling the best possible exploitation of modelling efforts.

Coordination is needed in several areas: firstly, by working with the community to define key science questions; secondly, by working with sub-MIPs to define key experiments and required analyses; thirdly, by identifying priority variables, such as the IPCC priority variable list, which is also useful for prioritizing data processing and availability; lastly, by coordinating experiments, protocols, and diagnostic output across modelling centres to standardize data delivery. CMIP can also coordinate the community review that is critical to ensure experiments meet community needs, address open-science questions, and achieve buy-in from modelling centres, e.g. CovidMIP, where specific science questions motivated quick turnaround.

The task of model evaluation, which aims to build and improve confidence in climate model projections, is an important part of CMIP activities. While AR6 did not in this cycle feature a chapter devoted to the evaluation of climate models, instead moving this work within the individual chapters as required, the importance of assessing and evaluating the components of individual climate models and the overall performance of ESMs remains clear. Future versions of CMIP are expected to continue to assess model performance and to quantify the causes of the diversity in model projections. The preceding phases of CMIP show that the progressive evolution of climate models and model capability necessarily changes what evaluation is possible and how this assessment should be done and modifies the evaluation and assessment requirements and metrics. Effective model evaluation requires the supporting MIPs to be mindful of the progress of the state of the field, and it should be expected that the evaluation activities may change further over time. As ESMs become increasingly complex, understanding sources of inter-model diversity requires more effort as there are more processes included and the coupling between them is likely stronger. Additionally, as ESMs evolve, the structural differences between models may play an increasing role in driving inter-model differences. As model complexity and the treatment of feedbacks increase, understanding and attributing differences become more challenging and more important.

In addition to model evaluation, an important goal of CMIP is to understand the evolution of ESMs. This requires some consistency in experimental design and diagnostic data across the various phases of CMIP. The use of digital object identifiers associated with climate model datasets through CMIP6 is a welcome step forward. In CMIP6, the adoption of CF-compliant formats and the use of CMOR functions to reprocess model output allowed the archiving of consistent output between models and a better interface to evaluate code such as ESMValTool (Schlund et al., 2023). ESMValTool and other model evaluation frameworks such as PCMDI (Lee et al., 2024) provide an important piece of infrastructure for model evaluation, and it would be helpful for the community to standardize further around these tools, as it enables the distribution of model evaluation methods, multi-model comparison, and traceability of model performance across MIP eras. In this regard, researchers may wish to port their evaluation scripts from the CMIP6 GitHub repository to ESMValTool and other standardized evaluation platforms. The use of ESMValTool or similar models during model development would provide a traceable picture of model evolution between release versions.

It is essential for model evaluation, intercomparison, and process studies that a single and, above all, comprehensive source of information on MIPs, models, and simulations is available. The ES-DOC service provided by CMIP (https://search.es-doc.org/, mirrored at https://errata.ipsl.fr) has proved to be very valuable. The ES-DOC format was

initiated in the fifth phase of CMIP as a metadata repository to provide such information (Guilyardi et al., 2013) and was then extended for use in CMIP6 (Balaji et al., 2018; Pascoe et al., 2020). ES-DOC improves our understanding of model data, increases the value of data for use in the future, and, by making earlier work more findable, potentially minimizes the need to re-run models. In AerChemMIP, ES-DOC was used to successfully document new model simulations (e.g. *ssp370-lowNTCFCH4*; Allen et al., 2021) that were proposed after the publication of the AerChemMIP protocol paper (Collins et al., 2017). The Errata system (https://errata.es-doc.org/static/index.html, last access: 4 January 2025, mirrored at https://errata.ipsl.fr) also worked well for reporting errors in the simulations. For example, when UKESM1 atmosphere-only simulations were found to have a bug, an issue notice was raised to document these data and the relevant experiments were withdrawn from the ESGF and replaced. While ES-DOC also aimed to provide standard information on models, this was less successful. In some cases, model information provided by modelling centres did not appear on ES-DOC. In other cases, the information available was not sufficiently detailed from an AerChemMIP perspective, was available but difficult to find, or was incorrect. It would be beneficial, for example, to have standard and more consistent information on the chemistry/aerosol schemes used and to connect better to the individual model description and evaluation papers. In general, high-quality, useful, and perhaps even overly explicit model description papers are required. Although there were improvements over CMIP5, it was still unfortunately common in AR6 for model description papers to appear after the data had been uploaded to ESGF, leaving a gap in information when preparing multi-model assessments, identifying outliers, and generating high-confidence projections. Where model components were common across several generations of a model, even basic details about this component tended to be omitted from the description paper of the CMIP6 model version. While including such information would make a description paper cumbersome and cause problems with plagiarism checks by journals, such details are important for process studies and for weighting multi-model ensembles to avoid dominance by a particular model family and closely related models and would be a valuable addition to ES-DOC.

Improving the search facility (e.g. by component or by process), making the questionnaire provided to modelling centres less opaque, making the repository straightforward and accessible to correct or update, and better communication with modelling centres and MIPs would all be beneficial. ES-DOC is being re-visited for CMIP7, and the new CMIP International Project Office (IPO) will help to provide a forum for improved communication. Together, these improvements should facilitate multi-model assessments and decrease the burden on centres responding to the questionnaire or to clarifying questions by scientists involved in model evaluation. However, sufficient resources will be required to overcome the technical challenges identified and to fully meet user needs.

To align with the principles of findability, accessibility, interoperability, and reusability (FAIR), it may ultimately be necessary for ESGF or similar repositories to consider archiving source code. It may be helpful if model description papers could feature a minimum, standardized set of information, and it may be necessary to make model descriptions machine-readable or to expand the ES-DOC requirements. Trawling the model literature for intercomparison/process papers is difficult and time-consuming and leads to large amounts of duplicated effort.

5.2 The AerChemMIP project

In preparing for the next phase of an aerosols and chemistry MIP, it is expected that the underpinning science questions will be reviewed along with the criteria for participating models, the experiment designs, and the diagnostic data request. It is however envisaged that the next phase of CMIP will feature a second phase of AerChemMIP, with the focus remaining on the role of aerosols and chemistry in the Earth system and climate change.

It will be necessary for ScenarioMIP, AerChemMIP, and CMIP to coordinate in defining future scenarios and to define trajectories for SLCFs in support of the CMIP science questions. For AerChemMIP, SSP3-7.0 was chosen as the future baseline and provided high signal to noise in counterfactual experiments involving strong air quality interventions. Recent work has highlighted that focussing on a single scenario may limit the usefulness of climate change projections in impact assessments. This is particularly relevant in the context of SLCFs, as future aerosol/precursor emissions scenarios span a large range, including minimal changes through the entire 21st century (e.g. SSP3-7.0) to rapid reductions over the next three decades (e.g. SSP1-1.9) that are comparable to the growth of emissions over the entire industrial era (e.g. Persad et al., 2023). In addition to these global emissions differences, we also note the importance of large diversity in regional SLCF emissions.

In light of the CMIP7 commitment to halve its carbon emissions relative to CMIP6, the ensemble size and the volume of output diagnostics need to be considered alongside other sources of experimental cost such as model resolution and the model complexity (Fiedler et al., 2024). In this light, for future MIPs it may be fruitful to revisit the goals of experiments and intended analyses and energy/storage requirements.

For diagnosing ERFs, *piClim-X* timeslice experiments are required, and for understanding climate responses, coupled atmosphere–ocean *hist-piX* experiments should be retained. Transient ERFs can be calculated from the *histSST-piX* experiments. Combined experiments targeting SLCFs are clearly beneficial, although additional single-forcing experiments are useful for understanding drivers. Clearly some

tradeoff and accommodations need to be made in a MIP addressing both reactive gases and aerosols – *piNTCF*, *piAer*, *piNOx*, and *piVOC* experiments have all been useful, but any expansion in experiment number should be considered in light of the stated aim to keep the CMIP computational expense to a minimum. A diagnosis of model sensitivities and response to forcings, performed in AerChemMIP with single-forcing experiments, may be possible with an expanded set of diagnostics rather than these dedicated attribution experiments. This should be considered.

It may be necessary to consider experiment design and the participating models in tandem. As noted above, the number of ESMs participating in AerChemMIP using online chemistry may be a concern in the future in light of the decreased participation in CMIP6. In terms of representation of aerosol, there was a wide range of complexity in the treatment of aerosol and aerosol–cloud interactions in CMIP6, but the representation of aerosol processes was generally not a barrier to participation in AerChemMIP. However, only a small number of ESMs featured online chemistry: ACCMIP, for CMIP5, featured 15 atmospheric chemistry models in its assessment of tropospheric ozone, while only 5 models were able to be used in CMIP6 ozone assessments. The low number of online chemistry models introduced challenges in evaluation and robustly identifying outliers. Future CMIP experiments aiming to address the role of aerosols and reactive trace gases such as AerChemMIP should aim to achieve greater participation, perhaps beyond ESMs, across the modelling community and to reverse the declining trend in participation. For the purposes of AerChemMIP, it may be beneficial to consider if models not meeting the DECK entry card could be included as they are a valuable additional resource for understanding the origins of inter-model diversity. In ACCMIP, chemical transport models (CTMs) were included using timeslice approaches and/or offline meteorology. A future chemistry-focused MIP remains an attractive prospect and has been the subject of recent discussions (Archibald et al., 2022). This should focus on both PI and PD conditions, with the objective of understanding the sources of model spread in both periods and in quantifying model skill. In evaluating model skill, observations are essential, making the AMIP DECK period of 1979–2015, designed to cover the post-satellite era, the most valuable.

Models of intermediate complexity could be useful for longer transient experiments and idealized forcings. As we discuss above, there is a need to include more processes, both to assess the role of processes missing from ESMs and to understand how structural differences impact future predictions. For this purpose, experiments over limited periods of the historical or future periods may be useful, particularly if coupled with higher-quality (process-level or time resolution) diagnostics. The value from these experiments would be amplified if all centres/models chose the same period, e.g. the 2050s. This also reduces additional storage and processing overheads and makes it easier to re-run models.

CMIP6 showed that the evaluation and assessment of coupled ESMs is an increasing challenge, particularly for atmospheric composition. In planning for future phases of AerChemMIP, the presence of ESMs featuring online atmospheric chemistry and the increasing use of online components for natural or biogenic sources of ozone and aerosol precursors are to be expected and encouraged, as they provide more realistic treatment of Earth system feedbacks. Certainly, in CMIP6, interactive descriptions of ocean biogeochemistry, land surface feedbacks, and emissions of biogenic species were increasingly common. Moreover, CMIP6 showed that the inter-model range of natural/biogenic sources of ozone and aerosol precursors is now large and is a key driver of inter-model diversity, particularly in the PI period, in both ozone and sinks for methane such as OH, and, as BVOCs can also oxidize to form secondary organic aerosol (SOA), the large range in BVOC emissions also contributes to inter-model diversity in SOA. Future projections of atmospheric composition using ESMs will depend sensitively on the response of these natural emissions, and other processes, to climate. The AerChemMIP *piClim-2x* experiments which target natural sources of SLCFs will be useful here and should be expanded as required, for instance if online methane or fire-related emissions become standard. Expanding these types of simulations to coupled transient experiments would be useful and would allow insight into the climate impacts associated with dust, fires, sea salt, etc. in a multi-model context. It will also be essential to perform intercomparison and evaluation of these natural emissions, and the response to climate change of emissions such as NO_x from natural sources such as lightning (Finney et al., 2016; Murray et al., 2013) or wetland methane emissions will need further investigation and may merit separate intermodel comparison exercises, such as that done for wetland CH_4 emissions (WETCHIMP; Melton et al., 2013).

AerChemMIP provided three tiers of experiments and various sets of experiments across the period 1850–2100. Practically, it was found that not all experiments required the same effort to set up and process, with variants of experiments, e.g. *piClim-SO2* and *piClim-NOx*, requiring relatively less effort to set up than e.g. *ssp370pdSST* and *ssp370-lowNTCF*, with the longer transient experiments requiring significantly more supervision during execution compared to the timeslice experiments. Within centres, experiments motivated by new and targeted science questions clearly received significant additional effort. Incorporating these "bottom-up" designs of experiments and making clear how proposed experiments have the ability to address and respond to current and emerging science questions will be beneficial to future MIPs.

It may also be more fruitful to produce mid-sized to large ensembles for a smaller number of experiments than a large number of experiments with a small (< 5 member) number of ensembles. As mentioned above, it would be advantageous to develop new MIP experiments in tandem with the design for their diagnostic output required for their analy-

sis and also to provide criteria for verification of required output. This is a critical point to avoid missing diagnostics or experiments, potentially limiting the usefulness of experiments and reducing the value of potentially costly experiments. As an example, the attribution of dynamical responses in AerChemMIP coupled transient experiments is often a challenge due to small ensemble size – as the number of ensemble members increases, it becomes easier to distinguish weak signals and the effects of structural uncertainty from internal model variability. The viable ensemble size for analysis needs to be considered when both designing and performing experiments. AerChemMIP requested three ensembles for each of the coupled transient *hist-piX* experiments, but these were not delivered by all participating models. It is now clear that a larger ensemble size is required to characterize regional climate responses, especially regional precipitation changes (Monerie et al., 2021). With this in mind, MIPs focussed on attribution typically request larger ensembles: DAMIP requested 5 members per experiment for CMIP6, and the RAMIP requested 10. However, if the focus is on composition and/or forcing, fewer experiments are required, although timeslice experiments longer than 30 years are required for many species.

Given the size of the ensemble in the historical and SSP simulations used as the AerChemMIP baselines, there is an opportunity to expand the AerChemMIP ensemble member size so that the experiments provide clearer climate information at spatial and temporal scales where internal variability is large and so that more robust conclusions about the role of model structural uncertainty can be drawn.

To verify the presence of required output, an AerChemMIP variable request, i.e. a list of required diagnostics, may be useful. This should additionally list the analyses that they underpin. For instance, it may be necessary to document a consistent method for the generation of $PM_{2.5}$ concentrations or to specify which species are necessary to be output at high time resolution, such as planetary boundary layer height and dry deposition fluxes, for as full an understanding as possible of future air pollution and its drivers. One option may be to ensure better coordination between ScenarioMIP and AerChemMIP to ensure that the AerChemMIP diagnostic data request is present in all ScenarioMIP experiments for at least five ensemble members but ideally more.

5.3 Modelling centres

In understanding model evolution, traceability is essential. Finally, we encourage modelling centres to use their model description papers to document the differences/changes with respect to an existing model or model description paper. Understanding how models have changed also requires the availability of codebases to interested researchers.

It is also necessary for modelling centres to document as clearly as possible the origin of variant data. A standard approach for identifying model variants needs to be adopted for CMIP7. This was inconsistent in CMIP6, resulting in model variants being used incorrectly by authors. CMIP naming conventions support the identification of model variants through use of a physics code in ensemble member names: the "p1" in "r1i1p1f1", for example. For CMIP6, there was a burden on the user to establish what these codes meant and how the data should be treated to take this into account, as conventions differed between centres. For example, p1 and p2 variants of CanESM5 included stochastic perturbations and could be combined into a single CanESM5 ensemble. However, for GISS-E2, the p codes indicate the use of different aerosol and chemistry schemes, and these variants should be treated as different models. When model variants are using different modules, this would be better reflected in the use of different model names rather than different physics versions, which was the widely adopted approach to indicating different model resolution, for example, in CMIP6 (e.g. NorESM2-LM vs. NorESM2-MM).

6 Conclusions

The AerChemMIP project, endorsed by CMIP6, has led to significant progress in our understanding of the role of aerosols and reactive gases in the climate system, both from a historical perspective and extending out into the future, and has worked well alongside PDRMIP and RFMIP.

The design of AerChemMIP focused on the effect of composition changes. Radiative forcing was calculated using a comparison between perturbation and control atmosphere-only timeslice experiments, a protocol common with RFMIP. The role of historical emissions changes was examined in "all-but-one" transient atmosphere-only attribution experiments allowing radiative forcing to be calculated and the role of the drivers of composition changes to be deduced. Counterfactual coupled transient atmosphere–ocean experiments produced important data on the climate response to historical emissions. Transient experiments investigating the future SSP3-7.0 pathway allowed insight into the role of SLCFs in future climate and air quality.

The resulting literature based on AerChemMIP compares very well against questions A1 ("How have anthropogenic emissions contributed to global radiative forcing and affected regional climate over the historical period?" and A2 ("How might future policies (on climate, air quality, and land use) affect the abundances of SLCFs and their climate impacts?") with the *piClim-X* in particular being targeted at A1 and *ssp370* and *ssp370-lowNTCF* experiments targeting A2. The effect on global climate (A1/A2) was well-characterized (e.g. Allen et al., 2020; Thornhill et al., 2021a, b; Allen et al., 2021), but, as we note above, the coupled transient experiments were generally only performed with small ensemble sizes, which limited their scope.

AerChemMIP performed perhaps less well against A3 ("How do uncertainties in historical SLCF emissions affect

radiative forcing estimates?"), at least in time for AR6. The original aim in Collins et al. (2017) was to scale the ERFs from all the piClim experiments with the emission uncertainty to quantify the contribution from emission uncertainty to the NTCF forcing uncertainty. This task is still feasible and could be identified as a remaining task for future MIPs. Some effort was made to bound the effect of emissions changes through the *ssp370-lowNTCF*. In future MIPs, uncertainties in anthropogenic emissions estimates, which were not provided for CMIP6, would be a welcome addition for this task, although the size of such a task is certainly daunting, particularly in coupled experiments. However, there is work being done to look into the sensitivity of models to uncertainties in emissions (e.g. Booth et al., 2018; Fyfe et al., 2021; Ahsan et al., 2023; Holland et al., 2024).

AerChemMIP performed well against the objectives of question A4 ("How important are climate feedbacks to natural NTCF emissions, atmospheric composition, and radiative effects?") via the *piClim-2x* experiments. However, the use of the DECK *abrupt-4xCO2* and *piControl* simulations to quantify how these natural emissions change with climate needs to be improved. In particular, there is a need to separate the radiative effects of CO_2 from the biophysical effects of CO_2 in any new experiments in a consistent way due to the impact of future CO_2 on biogeochemical feedbacks (e.g. Arora et al., 2020; Allen et al., 2024a).

The AerChemMIP contributions to AR6 were mainly through Chap. 6 ("Short-lived Climate Forcers"; Szopa et al., 2021b) and Chap. 7 ("The Earth's Energy Budget, Climate Feedbacks and Climate Sensitivity"; Forster et al., 2021). For example, the *piClim-X* experiments were instrumental in being able to construct the emission-based forcing bar chart (Figs. 6.12 in Szopa et al., 2021a, and TS15(a)) and from these to drive attributions of the historical temperature rise (Figs. TS15(b) and SPM.2 of IPCC, 2021). Such contributions came both through the AerChemMIP-specific experiments and through the AerChemMIP-specific diagnostics. For instance, the historical ozone RF was diagnosed from the historical simulations using the ozone mixing ratio on model levels: a diagnostic requested by AerChemMIP.

AerChemMIP contributed not just to AR6 but to ongoing research efforts. The database of experiments is rich, in terms of experiments, participating models, and the sophistication of the treatment of chemistry and aerosols and their role in the climate system. These data form a part of the climate data landscape and are enabling new analyses to be performed. We hope that this legacy of AerChemMIP also enables future work on the role of aerosols and short-lived reactive gases in the climate system.

Data availability. All data from the Earth system models used in this paper are available on the Earth System Grid Federation website and can be downloaded from https://esgf-node.llnl.gov/search/cmip6/ (CMIP6, 2025). The data for Tables 2 and 3 are available at https://doi.org/10.17605/OSF.IO/8FWJ3 (Wilcox, 2024).

Author contributions. PTG, LJW, and RJA led the writing of this paper. All authors contributed to the writing and discussion of this paper.

Competing interests. At least one of the (co-)authors is a member of the editorial board of *Atmospheric Chemistry and Physics*. The peer-review process was guided by an independent editor, and the authors also have no other competing interests to declare.

Disclaimer. Publisher's note: Copernicus Publications remains neutral with regard to jurisdictional claims made in the text, published maps, institutional affiliations, or any other geographical representation in this paper. While Copernicus Publications makes every effort to include appropriate place names, the final responsibility lies with the authors.

Acknowledgements. Paul T. Griffiths and Laura J. Wilcox are supported by the Natural Environment Research Council (NERC; grant NE/W004895/1, TerraFIRMA). Alex Archibald, Paul T. Griffiths, and Laura J. Wilcox are additionally supported by the National Centre for Atmospheric Science. Robert J. Allen acknowledges support from NSF grant AGS-2153486. Robert J. Allen, Bjørn H. Samset, and Laura J. Wilcox acknowledge funding by the Research Council of Norway through grant no. 324128 (CATHY). Paul T. Griffiths acknowledges support from the Environmental Geochemical Cycle Research Group, Earth Surface System Research Center, Japan Agency for Marine Science and Technology, Yokohama, for visiting scientist support. Makoto Deushi and Naga Oshima were supported by the Environment Research and Technology Development Fund (JPMEERF20202003, JPMEERF20205001, and JPMEERF20232001) of the Environmental Restoration and Conservation Agency Provided by the Ministry of Environment of Japan, the Arctic Challenge for Sustainability II (ArCS II), program grant number JPMXD1420318865, and a grant for the Global Environmental Research Coordination System from the Ministry of the Environment of Japan (MLIT2253). Chris Smith was supported by a NERC/IIASA Collaborative Research Fellowship (NE/T009381/1). Steven Turnock was funded by the Met Office Climate Science for Service Partnership (CSSP) China project under the International Science Partnerships Fund (ISPF). Fiona M. O'Connor was supported by the European Union's Horizon 2020 project ESM2025 (under grant agreement no. 101003536) and the Met Office Hadley Centre Climate Programme funded by DSIT, UK. Stephanie Fiedler is supported by the German Science Foundation (DFG) with the Collaborative Research Center DETECT (SFB1502, grant no. DFG 450058266) and by HORIZON Europe with the project EXPECT (grant no. 101137656).

Financial support. This research has been supported by the Natural Environment Research Council, National Centre for Atmospheric Science (grant nos. NE/W004895/1 and NE/T009381/1),

the International Science Partnerships Fund (ISPF), the US NSF (grant no. AGS-2153486), Environment Research and Technology Development Fund of the Environmental Restoration and Conservation Agency provided by the Ministry of Environment of Japan (grant nos. JPMEERF20202003, JPMEERF20205001, and JPMEERF20232001), the Arctic Challenge for Sustainability II (grant no. JPMXD1420318865), Japan Global Environmental Research Coordination System (grant no. MLIT2253), the Norges Forskningsråd (grant no. 324128), the EU Horizon 2020 (grant nos. 101003536 and 101137656), and the Deutsche Forschungsgemeinschaft (grant no. 450058266).

Review statement. This paper was edited by Xiaohong Liu and Rolf Müller and reviewed by two anonymous referees.

References

Abalos, M., Randel, W. J., Kinnison, D. E., and Garcia, R. R.: Using the Artificial Tracer e90 to Examine Present and Future UTLS Tracer Transport in WACCM, J. Atmos. Sci., 74, 3383–3403, https://doi.org/10.1175/JAS-D-17-0135.1, 2017.

Ahsan, H., Wang, H., Wu, J., Wu, M., Smith, S. J., Bauer, S., Suchyta, H., Olivié, D., Myhre, G., Matsui, H., Bian, H., Lamarque, J.-F., Carslaw, K., Horowitz, L., Regayre, L., Chin, M., Schulz, M., Skeie, R. B., Takemura, T., and Naik, V.: The Emissions Model Intercomparison Project (Emissions-MIP): quantifying model sensitivity to emission characteristics, Atmos. Chem. Phys., 23, 14779–14799, https://doi.org/10.5194/acp-23-14779-2023, 2023.

Aizawa, T., Oshima, N., and Yukimoto, S.: Contributions of Anthropogenic Aerosol Forcing and Multidecadal Internal Variability to Mid-20th Century Arctic Cooling—CMIP6/DAMIP Multimodel Analysis, Geophys. Res. Lett., 49, e2021GL097093, https://doi.org/10.1029/2021GL097093, 2022.

Akritidis, D., Bacer, S., Zanis, P., Georgoulias, A. K., Chowdhury, S., Horowitz, L. W., Naik, V., O'Connor, F. M., Keeble, J., Sager, P. L., van Noije, T., Zhou, P., Turnock, S., West, J. J., Lelieveld, J., and Pozzer, A.: Strong increase in mortality attributable to ozone pollution under a climate change and demographic scenario, Environ. Res. Lett., 19, 024041, https://doi.org/10.1088/1748-9326/ad2162, 2024.

Allen, R. J., Turnock, S., Nabat, P., Neubauer, D., Lohmann, U., Olivié, D., Oshima, N., Michou, M., Wu, T., Zhang, J., Takemura, T., Schulz, M., Tsigaridis, K., Bauer, S. E., Emmons, L., Horowitz, L., Naik, V., van Noije, T., Bergman, T., Lamarque, J.-F., Zanis, P., Tegen, I., Westervelt, D. M., Le Sager, P., Good, P., Shim, S., O'Connor, F., Akritidis, D., Georgoulias, A. K., Deushi, M., Sentman, L. T., John, J. G., Fujimori, S., and Collins, W. J.: Climate and air quality impacts due to mitigation of non-methane near-term climate forcers, Atmos. Chem. Phys., 20, 9641–9663, https://doi.org/10.5194/acp-20-9641-2020, 2020.

Allen, R. J., Horowitz, L. W., Naik, V., Oshima, N., O'Connor, F. M., Turnock, S., Shim, S., Le Sager, P., Van Noije, T., Tsigaridis, K., Bauer, S. E., Sentman, L. T., John, J. G., Broderick, C., Deushi, M., Folberth, G. A., Fujimori, S., and Collins, W. J.: Significant climate benefits from near-term climate forcer mitigation in spite of aerosol reductions, Environ. Res. Lett., 16, 034010, https://doi.org/10.1088/1748-9326/abe06b, 2021.

Allen, R. J., Zhao, X., Randles, C. A., Kramer, R. J., Samset, B. H., and Smith, C. J.: Surface warming and wetting due to methane's long-wave radiative effects muted by short-wave absorption, Nat. Geosci., 16, 314–320, https://doi.org/10.1038/s41561-023-01144-z, 2023.

Allen, R. J., Gomez, J., Horowitz, L. W., and Shevliakova, E.: Enhanced future vegetation growth with elevated carbon dioxide concentrations could increase fire activity, Commun. Earth Environ., 5, 54, https://doi.org/10.1038/s43247-024-01228-7, 2024a.

Allen, R. J., Zhao, X., Randles, C. A., Kramer, R. J., Samset, B. H., and Smith, C. J.: Present-day methane shortwave absorption mutes surface warming relative to preindustrial conditions, Atmos. Chem. Phys., 24, 11207–11226, https://doi.org/10.5194/acp-24-11207-2024, 2024b.

Amiri-Farahani, A., Allen, R. J., Li, K.-F., Nabat, P., and Westervelt, D. M.: A La Niña-Like Climate Response to South African Biomass Burning Aerosol in CESM Simulations, J. Geophys. Res.-Atmos., 125, e2019JD031832, https://doi.org/10.1029/2019JD031832, 2020.

Andrews, M. B., Ridley, J. K., Wood, R. A., Andrews, T., Blockley, E. W., Booth, B., Burke, E., Dittus, A. J., Florek, P., Gray, L. J., Haddad, S., Hardiman, S. C., Hermanson, L., Hodson, D., Hogan, E., Jones, G. S., Knight, J. R., Kuhlbrodt, T., Misios, S., Mizielinski, M. S., Ringer, M. A., Robson, J., and Sutton, R. T.: Historical Simulations With HadGEM3-GC3.1 for CMIP6, J. Adv. Model. Earth Sy., 12, e2019MS001995, https://doi.org/10.1029/2019MS001995, 2020.

Anenberg, S. C., West, J. J., Fiore, A. M., Jaffe, D. A., Prather, M. J., Bergmann, D., Cuvelier, K., Dentener, F. J., Duncan, B. N., Gauss, M., Hess, P., Jonson, J. E., Lupu, A., MacKenzie, I. A., Marmer, E., Park, R. J., Sanderson, M. G., Schultz, M., Shindell, D. T., Szopa, S., Vivanco, M. G., Wild, O., and Zeng, G.: Intercontinental impacts of ozone pollution on human mortality, Environ. Sci. Technol., 43, 6482–6487, https://doi.org/10.1021/es900518z, 2009.

Archibald, A., Collins, W., Evans, M., Griffiths, P., O'Connor, F., Wild, O., and Young, P.: Ace in the hole or a house of cards: Will a DeCK experiment help atmospheric chemistry?, EGU General Assembly 2022, Vienna, Austria, 23–27 May 2022, EGU22-9442, https://doi.org/10.5194/egusphere-egu22-9442, 2022.

Arora, V. K., Katavouta, A., Williams, R. G., Jones, C. D., Brovkin, V., Friedlingstein, P., Schwinger, J., Bopp, L., Boucher, O., Cadule, P., Chamberlain, M. A., Christian, J. R., Delire, C., Fisher, R. A., Hajima, T., Ilyina, T., Joetzjer, E., Kawamiya, M., Koven, C. D., Krasting, J. P., Law, R. M., Lawrence, D. M., Lenton, A., Lindsay, K., Pongratz, J., Raddatz, T., Séférian, R., Tachiiri, K., Tjiputra, J. F., Wiltshire, A., Wu, T., and Ziehn, T.: Carbon–concentration and carbon–climate feedbacks in CMIP6 models and their comparison to CMIP5 models, Biogeosciences, 17, 4173–4222, https://doi.org/10.5194/bg-17-4173-2020, 2020.

Bader, D. C., Leung, R., Taylor, M., and McCoy, R. B.: E3SM-Project E3SM1.0 model output prepared for CMIP6 CMIP historical, Earth System Grid Federation [data set], https://doi.org/10.22033/ESGF/CMIP6.4497, 2019a.

Bader, D. C., Leung, R., Taylor, M., and McCoy, R. B.: E3SM-Project E3SM1.1 model output prepared for CMIP6

CMIP historical, Earth System Grid Federation [data set], https://doi.org/10.22033/ESGF/CMIP6.11485, 2019b.

Balaji, V., Taylor, K. E., Juckes, M., Lawrence, B. N., Durack, P. J., Lautenschlager, M., Blanton, C., Cinquini, L., Denvil, S., Elkington, M., Guglielmo, F., Guilyardi, E., Hassell, D., Kharin, S., Kindermann, S., Nikonov, S., Radhakrishnan, A., Stockhause, M., Weigel, T., and Williams, D.: Requirements for a global data infrastructure in support of CMIP6, Geosci. Model Dev., 11, 3659–3680, https://doi.org/10.5194/gmd-11-3659-2018, 2018.

Bao, Y., Song, Z., and Qiao, F.: FIO-ESM Version 2.0: Model Description and Evaluation, J. Geophys. Res.-Oceans, 125, e2019JC016036, https://doi.org/10.1029/2019JC016036, e2019JC016036 2019JC016036, 2020.

Bellouin, N., Quaas, J., Gryspeerdt, E., Kinne, S., Stier, P., Watson-Parris, D., Boucher, O., Carslaw, K. S., Christensen, M., Daniau, A. L., Dufresne, J. L., Feingold, G., Fiedler, S., Forster, P., Gettelman, A., Haywood, J. M., Lohmann, U., Malavelle, F., Mauritsen, T., McCoy, D. T., Myhre, G., Mülmenstädt, J., Neubauer, D., Possner, A., Rugenstein, M., Sato, Y., Schulz, M., Schwartz, S. E., Sourdeval, O., Storelvmo, T., Toll, V., Winker, D., and Stevens, B.: Bounding global aerosol radiative forcing of climate change, Rev. Geophys., 58, e2019RG000660, https://doi.org/10.1029/2019RG000660, 2020.

Bentsen, M., Oliviè, D. J. L., Seland, y., Toniazzo, T., Gjermundsen, A., Graff, L. S., Debernard, J. B., Gupta, A. K., He, Y., Kirkevåg, A., Schwinger, J., Tjiputra, J., Aas, K. S., Bethke, I., Fan, Y., Griesfeller, J., Grini, A., Guo, C., Ilicak, M., Karset, I. H. H., Landgren, O. A., Liakka, J., Moseid, K. O., Nummelin, A., Spensberger, C., Tang, H., Zhang, Z., Heinze, C., Iversen, T., and Schulz, M.: NCC NorESM2-MM model output prepared for CMIP6 CMIP historical, Earth System Grid Federation [data set], https://doi.org/10.22033/ESGF/CMIP6.8040, 2019.

Bethke, I., Wang, Y., Counillon, F., Kimmritz, M., Fransner, F., Samuelsen, A., Langehaug, H. R., Chiu, P.-G., Bentsen, M., Guo, C., Tjiputra, J., Kirkevåg, A., Oliviè, D. J. L., Seland, y., Fan, Y., Lawrence, P., Eldevik, T., and Keenlyside, N.: NCC NorCPM1 model output prepared for CMIP6 CMIP historical, Earth System Grid Federation [data set], https://doi.org/10.22033/ESGF/CMIP6.10894, 2019.

Bethke, I., Wang, Y., Counillon, F., Keenlyside, N., Kimmritz, M., Fransner, F., Samuelsen, A., Langehaug, H., Svendsen, L., Chiu, P.-G., Passos, L., Bentsen, M., Guo, C., Gupta, A., Tjiputra, J., Kirkevåg, A., Olivié, D., Seland, Ø., Solsvik Vågane, J., Fan, Y., and Eldevik, T.: NorCPM1 and its contribution to CMIP6 DCPP, Geosci. Model Dev., 14, 7073–7116, https://doi.org/10.5194/gmd-14-7073-2021, 2021.

Bi, D., Dix, M., Marsland, S., O'Farrell, S., Sullivan, A., Bodman, R., Law, R., Harman, I., Srbinovsky, J., Rashid, H. A., Dobrohotoff, P., Mackallah, C., Yan, H., Hirst, A., Savita, A., Dias, F. B., Woodhouse, M., Fiedler, R., and Heerdegen, A.: Configuration and spin-up of ACCESS-CM2, the new generation Australian Community Climate and Earth System Simulator Coupled Model, Journal of Southern Hemisphere Earth Systems Science, 70, 225–251, https://doi.org/10.1071/ES19040, 2020.

Blichner, S.-M. and Berntsen, T.: Chapter 6 of the Working Group I Contribution to the IPCC Sixth Assessment Report – data for Figure 6.12 (v20220815), NERC Centre for Environmental Data Analysis (CEDA), https://doi.org/10.5285/8855e410adf547b4afd039a5b88487f4, 2023.

Booth, B. B. B., Harris, G. R., Jones, A., Wilcox, L., Hawcroft, M., and Carslaw, K. S.: Comments on "Rethinking the Lower Bound on Aerosol Radiative Forcing", J. Climate, 31, 9407–9412, https://doi.org/10.1175/JCLI-D-17-0369.1, 2018.

Boucher, O., Randall, D., Artaxo, P., Bretherton, C., Feingold, G., Forster, P., Kerminen, V.-M., Kondo, Y., Liao, H., Lohmann, U., Rasch, P., Satheesh, S., Sherwood, S., Stevens, B., and Zhang, X.: Clouds and aerosols, in: Climate change 2013: The physical science basis. Contribution of working group I to the fifth assessment report of the intergovernmental panel on climate change, section: 7 Type: Book section, edited by: Stocker, T., Qin, D., Plattner, G.-K., Tignor, M., Allen, S., Boschung, J., Nauels, A., Xia, Y., Bex, V., and Midgley, P., Cambridge University Press, Cambridge, UK and New York, NY, USA, https://doi.org/10.1017/CBO9781107415324.016, 2013.

Boucher, O., Servonnat, J., Albright, A. L., Aumont, O., Balkanski, Y., Bastrikov, V., Bekki, S., Bonnet, R., Bony, S., Bopp, L., Braconnot, P., Brockmann, P., Cadule, P., Caubel, A., Cheruy, F., Codron, F., Cozic, A., Cugnet, D., D'Andrea, F., Davini, P., de Lavergne, C., Denvil, S., Deshayes, J., Devilliers, M., Ducharne, A., Dufresne, J.-L., Dupont, E., Éthé, C., Fairhead, L., Falletti, L., Flavoni, S., Foujols, M.-A., Gardoll, S., Gastineau, G., Ghattas, J., Grandpeix, J.-Y., Guenet, B., Guez, Lionel, E., Guilyardi, E., Guimberteau, M., Hauglustaine, D., Hourdin, F., Idelkadi, A., Joussaume, S., Kageyama, M., Khodri, M., Krinner, G., Lebas, N., Levavasseur, G., Lévy, C., Li, L., Lott, F., Lurton, T., Luyssaert, S., Madec, G., Madeleine, J.-B., Maignan, F., Marchand, M., Marti, O., Mellul, L., Meurdesoif, Y., Mignot, J., Musat, I., Ottlé, C., Peylin, P., Planton, Y., Polcher, J., Rio, C., Rochetin, N., Rousset, C., Sepulchre, P., Sima, A., Swingedouw, D., Thiéblemont, R., Traore, A. K., Vancoppenolle, M., Vial, J., Vialard, J., Viovy, N., and Vuichard, N.: Presentation and Evaluation of the IPSL-CM6A-LR Climate Model, J. Adv. Model. Earth Sy., 12, e2019MS002010, https://doi.org/10.1029/2019MS002010, 2020.

Boucher, O., Denvil, S., Levavasseur, G., Cozic, A., Caubel, A., Foujols, M.-A., Meurdesoif, Y., Balkanski, Y., Checa-Garcia, R., Hauglustaine, D., Bekki, S., and Marchand, M.: IPSL IPSL-CM6A-LR-INCA model output prepared for CMIP6 CMIP historical, Earth System Grid Federation [data set], https://doi.org/10.22033/ESGF/CMIP6.13601, 2021.

Brown, F., Folberth, G. A., Sitch, S., Bauer, S., Bauters, M., Boeckx, P., Cheesman, A. W., Deushi, M., Dos Santos Vieira, I., Galy-Lacaux, C., Haywood, J., Keeble, J., Mercado, L. M., O'Connor, F. M., Oshima, N., Tsigaridis, K., and Verbeeck, H.: The ozone–climate penalty over South America and Africa by 2100, Atmos. Chem. Phys., 22, 12331–12352, https://doi.org/10.5194/acp-22-12331-2022, 2022.

Burrows, S. M., Maltrud, M., Yang, X., Zhu, Q., Jeffery, N., Shi, X., Ricciuto, D., Wang, S., Bisht, G., Tang, J., Wolfe, J., Harrop, B. E., Singh, B., Brent, L., Baldwin, S., Zhou, T., Cameron-Smith, P., Keen, N., Collier, N., Xu, M., Hunke, E. C., Elliott, S. M., Turner, A. K., Li, H., Wang, H., Golaz, J.-C., Bond-Lamberty, B., Hoffman, F. M., Riley, W. J., Thornton, P. E., Calvin, K., and Leung, L. R.: The DOE E3SM v1.1 Biogeochemistry Configuration: Description and Simulated Ecosystem-Climate Responses to Historical Changes

in Forcing, J. Adv. Model. Earth Sy., 12, e2019MS001766, https://doi.org/10.1029/2019MS001766, 2020.

Byun, Y.-H., Lim, Y.-J., Sung, H. M., Kim, J., Sun, M., and Kim, B.-H.: NIMS-KMA KACE1.0-G model output prepared for CMIP6 CMIP historical, Earth System Grid Federation [data set], https://doi.org/10.22033/ESGF/CMIP6.8378, 2019.

Cao, J. and Wang, B.: NUIST NESMv3 model output prepared for CMIP6 CMIP historical, Earth System Grid Federation [data set], https://doi.org/10.22033/ESGF/CMIP6.8769, 2019.

Cao, J., Wang, B., Yang, Y.-M., Ma, L., Li, J., Sun, B., Bao, Y., He, J., Zhou, X., and Wu, L.: The NUIST Earth System Model (NESM) version 3: description and preliminary evaluation, Geosci. Model Dev., 11, 2975–2993, https://doi.org/10.5194/gmd-11-2975-2018, 2018.

Carslaw, K. S., Lee, L. A., Reddington, C. L., Pringle, K. J., Rap, A., Forster, P. M., Mann, G. W., Spracklen, D. V., Woodhouse, M. T., Regayre, L. A., and Pierce, J. R.: Large Contribution of Natural Aerosols to Uncertainty in Indirect Forcing, Nature, 503, 67–71, https://doi.org/10.1038/nature12674, 2013.

Chen, H.-M., Li, J., Su, J.-Z., Hua, L.-J., Rong, X.-Y., Xin, Y.-F., and Zhang, Z.-Q.: Introduction of CAMS-CSM model and its participation in CMIP6, Advances in Climate Change Research, 15, 540–544, 2019.

Cherchi, A., Fogli, P. G., Lovato, T., Peano, D., Iovino, D., Gualdi, S., Masina, S., Scoccimarro, E., Materia, S., Bellucci, A., and Navarra, A.: Global Mean Climate and Main Patterns of Variability in the CMCC-CM2 Coupled Model, J. Adv. Model. Earth Sy., 11, 185–209, https://doi.org/10.1029/2018MS001369, 2019.

Collins, W. J., Lamarque, J.-F., Schulz, M., Boucher, O., Eyring, V., Hegglin, M. I., Maycock, A., Myhre, G., Prather, M., Shindell, D., and Smith, S. J.: AerChemMIP: quantifying the effects of chemistry and aerosols in CMIP6, Geosci. Model Dev., 10, 585–607, https://doi.org/10.5194/gmd-10-585-2017, 2017.

Collins, W. J., O'Connor, F. M., Barker, C. R., Byrom, R. E., Eastham, S. D., Hodnebrog, Ø., Jöckel, P., Marais, E. A., Mertens, M., Myhre, G., Nützel, M., Olivié, D., Bieltvedt Skeie, R., Stecher, L., Horowitz, L. W., Naik, V., Faluvegi, G., Im, U., Murray, L. T., Shindell, D., Tsigaridis, K., Abraham, N. L., and Keeble, J.: Climate Forcing due to Future Ozone Changes: An intercomparison of metrics and methods, EGUsphere [preprint], https://doi.org/10.5194/egusphere-2024-3698, 2024.

Coupled Model Intercomparison Project Phase 6 (CMIP6): Scenario Model Intercomparison Project (ScenarioMIP) [data set], https://esgf-node.llnl.gov/search/cmip6/, last access: 22 March 2025.

Danabasoglu, G.: NCAR CESM2-FV2 model output prepared for CMIP6 CMIP historical, Earth System Grid Federation [data set], https://doi.org/10.22033/ESGF/CMIP6.11297, 2019a.

Danabasoglu, G.: NCAR CESM2-WACCM-FV2 model output prepared for CMIP6 CMIP historical, Earth System Grid Federation [data set], https://doi.org/10.22033/ESGF/CMIP6.11298, 2019b.

Danabasoglu, G.: NCAR CESM2-WACCM model output prepared for CMIP6 CMIP historical, Earth System Grid Federation [data set], https://doi.org/10.22033/ESGF/CMIP6.10071, 2019c.

Danabasoglu, G.: NCAR CESM2 model output prepared for CMIP6 CMIP historical, Earth System Grid Federation [data set], https://doi.org/10.22033/ESGF/CMIP6.7627, 2019d.

Danabasoglu, G., Lamarque, J.-F., Bacmeister, J., Bailey, D. A., DuVivier, A. K., Edwards, J., Emmons, L. K., Fasullo, J., Garcia, R., Gettelman, A., Hannay, C., Holland, M. M., Large, W. G., Lauritzen, P. H., Lawrence, D. M., Lenaerts, J. T. M., Lindsay, K., Lipscomb, W. H., Mills, M. J., Neale, R., Oleson, K. W., Otto-Bliesner, B., Phillips, A. S., Sacks, W., Tilmes, S., van Kampenhout, L., Vertenstein, M., Bertini, A., Dennis, J., Deser, C., Fischer, C., Fox-Kemper, B., Kay, J. E., Kinnison, D., Kushner, P. J., Larson, V. E., Long, M. C., Mickelson, S., Moore, J. K., Nienhouse, E., Polvani, L., Rasch, P. J., and Strand, W. G.: The Community Earth System Model Version 2 (CESM2), J. Adv. Model. Earth Sy., 12, e2019MS001916, https://doi.org/10.1029/2019MS001916, 2020.

Danek, C., Shi, X., Stepanek, C., Yang, H., Barbi, D., Hegewald, J., and Lohmann, G.: AWI AWI-ESM1.1LR model output prepared for CMIP6 CMIP historical, Earth System Grid Federation [data set], https://doi.org/10.22033/ESGF/CMIP6.9328, 2020.

Deng, J., Dai, A., and Xu, H.: Nonlinear Climate Responses to Increasing CO_2 and Anthropogenic Aerosols Simulated by CESM1, J. Climate, 33, 281–301, https://doi.org/10.1175/JCLI-D-19-0195.1, 2020.

DeRepentigny, P., Jahn, A., Holland, M. M., and Smith, A.: Arctic Sea Ice in Two Configurations of the CESM2 During the 20th and 21st Centuries, J. Geophys. Res.-Oceans, 125, e2020JC016133, https://doi.org/10.1029/2020JC016133, 2020.

Diamond, M. S., Gristey, J. J., Kay, J. E., and Feingold, G.: Anthropogenic aerosol and cryosphere changes drive Earth's strong but transient clear-sky hemispheric albedo asymmetry, Commun. Earth Environ., 3, 1–10, https://doi.org/10.1038/s43247-022-00546-y, 2022.

Dix, M., Bi, D., Dobrohotoff, P., Fiedler, R., Harman, I., Law, R., Mackallah, C., Marsland, S., O'Farrell, S., Rashid, H., Srbinovsky, J., Sullivan, A., Trenham, C., Vohralik, P., Watterson, I., Williams, G., Woodhouse, M., Bodman, R., Dias, F. B., Domingues, C., Hannah, N., Heerdegen, A., Savita, A., Wales, S., Allen, C., Druken, K., Evans, B., Richards, C., Ridzwan, S. M., Roberts, D., Smillie, J., Snow, K., Ward, M., and Yang, R.: CSIRO-ARCCSS ACCESS-CM2 model output prepared for CMIP6 CMIP historical, Earth System Grid Federation [data set], https://doi.org/10.22033/ESGF/CMIP6.4271, 2019.

Döscher, R., Acosta, M., Alessandri, A., Anthoni, P., Arsouze, T., Bergman, T., Bernardello, R., Boussetta, S., Caron, L.-P., Carver, G., Castrillo, M., Catalano, F., Cvijanovic, I., Davini, P., Dekker, E., Doblas-Reyes, F. J., Docquier, D., Echevarria, P., Fladrich, U., Fuentes-Franco, R., Gröger, M., v. Hardenberg, J., Hieronymus, J., Karami, M. P., Keskinen, J.-P., Koenigk, T., Makkonen, R., Massonnet, F., Ménégoz, M., Miller, P. A., Moreno-Chamarro, E., Nieradzik, L., van Noije, T., Nolan, P., O'Donnell, D., Ollinaho, P., van den Oord, G., Ortega, P., Prims, O. T., Ramos, A., Reerink, T., Rousset, C., Ruprich-Robert, Y., Le Sager, P., Schmith, T., Schrödner, R., Serva, F., Sicardi, V., Sloth Madsen, M., Smith, B., Tian, T., Tourigny, E., Uotila, P., Vancoppenolle, M., Wang, S., Wårlind, D., Willén, U., Wyser, K., Yang, S., Yepes-Arbós, X., and Zhang, Q.: The EC-Earth3 Earth system model for the Coupled Model Intercomparison Project 6, Geosci. Model Dev., 15, 2973–3020, https://doi.org/10.5194/gmd-15-2973-2022, 2022.

Dunne, J. P., Horowitz, L. W., Adcroft, A. J., Ginoux, P., Held, I. M., John, J. G., Krasting, J. P., Malyshev, S., Naik, V., Paulot, F., Shevliakova, E., Stock, C. A., Zadeh, N., Balaji, V., Blanton, C., Dunne, K. A., Dupuis, C., Durachta, J., Dussin, R., Gau-

thier, P. P. G., Griffies, S. M., Guo, H., Hallberg, R. W., Harrison, M., He, J., Hurlin, W., McHugh, C., Menzel, R., Milly, P. C. D., Nikonov, S., Paynter, D. J., Ploshay, J., Radhakrishnan, A., Rand, K., Reichl, B. G., Robinson, T., Schwarzkopf, D. M., Sentman, L. T., Underwood, S., Vahlenkamp, H., Winton, M., Wittenberg, A. T., Wyman, B., Zeng, Y., and Zhao, M.: The GFDL Earth System Model Version 4.1 (GFDL-ESM 4.1): Overall Coupled Model Description and Simulation Characteristics, J. Adv. Model. Earth Sy., 12, e2019MS002015, https://doi.org/10.1029/2019MS002015, 2020.

EC-Earth Consortium (EC-Earth): EC-Earth-Consortium EC-Earth3-Veg model output prepared for CMIP6 CMIP historical, Earth System Grid Federation [data set], https://doi.org/10.22033/ESGF/CMIP6.4706, 2019a.

EC-Earth Consortium (EC-Earth): EC-Earth-Consortium EC-Earth3 model output prepared for CMIP6 CMIP historical, Earth System Grid Federation [data set], https://doi.org/10.22033/ESGF/CMIP6.4700, 2019b.

EC-Earth Consortium (EC-Earth): EC-Earth-Consortium EC-Earth3-AerChem model output prepared for CMIP6 CMIP historical, Earth System Grid Federation [data set], https://doi.org/10.22033/ESGF/CMIP6.4701, 2020.

Ekman, A. M. L.: Do sophisticated parameterizations of aerosol-cloud interactions in CMIP5 models improve the representation of recent observed temperature trends?, J. Geophys. Res.-Atmospheres, 119, 817–832, https://doi.org/10.1002/2013JD020511, 2014.

Emberson, L.: Effects of ozone on agriculture, forests and grasslands, Philos. T. Roy. Soc. A:, 378, 20190327, https://doi.org/10.1098/rsta.2019.0327, 2020.

Eyring, V., Bony, S., Meehl, G. A., Senior, C. A., Stevens, B., Stouffer, R. J., and Taylor, K. E.: Overview of the Coupled Model Intercomparison Project Phase 6 (CMIP6) experimental design and organization, Geosci. Model Dev., 9, 1937–1958, https://doi.org/10.5194/gmd-9-1937-2016, 2016.

Fiedler, S., Naik, V., O'Connor, F. M., Smith, C. J., Griffiths, P., Kramer, R. J., Takemura, T., Allen, R. J., Im, U., Kasoar, M., Modak, A., Turnock, S., Voulgarakis, A., Watson-Parris, D., Westervelt, D. M., Wilcox, L. J., Zhao, A., Collins, W. J., Schulz, M., Myhre, G., and Forster, P. M.: Interactions between atmospheric composition and climate change – progress in understanding and future opportunities from AerChemMIP, PDRMIP, and RFMIP, Geosci. Model Dev., 17, 2387–2417, https://doi.org/10.5194/gmd-17-2387-2024, 2024.

Finney, D. L., Doherty, R. M., Wild, O., Young, P. J., and Butler, A.: Response of lightning NO_x emissions and ozone production to climate change: Insights from the Atmospheric Chemistry and Climate Model Intercomparison Project, Geophys. Res. Lett., 43, 5492–5500, https://doi.org/10.1002/2016GL068825, 2016.

Fiore, A. M., Milly, G. P., Hancock, S. E., Quiñones, L., Bowden, J. H., Helstrom, E., Lamarque, J.-F., Schnell, J., West, J. J., and Xu, Y.: Characterizing Changes in Eastern U.S. Pollution Events in a Warming World, J. Geophys. Res.-Atmospheres, 127, e2021JD035985, https://doi.org/10.1029/2021JD035985, 2022.

Forster, P., Storelvmo, T., Armour, K., Collins, W., Dufresne, J.-L., Frame, D., Lunt, D., Mauritsen, T., Palmer, M., Watanabe, M., Wild, M., and Zhang, H.: The earth's energy budget, climate feedbacks, and climate sensitivity, in: Climate change 2021: The physical science basis. Contribution of working group I to the sixth assessment report of the intergovernmental panel on climate change, section: 7 Type: Book section, edited by: Masson-Delmotte, V., Zhai, P., Pirani, A., Connors, S. L., Péan, C., Berger, S., Caud, N., Chen, Y., Goldfarb, L., Gomis, M. I., Huang, M., Leitzell, K., Lonnoy, E., Matthews, J. B. R., Maycock, T. K., Waterfield, T., Yelekçi, O., Yu, R., and Zhou, B., Cambridge University Press, Cambridge, UK and New York, NY, USA, https://doi.org/10.1017/9781009157896.009, 2021.

Forster, P. M., Andrews, T., Good, P., Gregory, J. M., Jackson, L. S., and Zelinka, M.: Evaluating adjusted forcing and model spread for historical and future scenarios in the CMIP5 generation of climate models, J. Geophys. Res.-Atmos., 118, 1139–1150, https://doi.org/10.1002/jgrd.50174, 2013.

Forster, P. M., Richardson, T., Maycock, A. C., Smith, C. J., Samset, B. H., Myhre, G., Andrews, T., Pincus, R., and Schulz, M.: Recommendations for diagnosing effective radiative forcing from climate models for CMIP6, J. Geophys. Res.-Atmos., 121, 12460–12475, https://doi.org/10.1002/2016JD025320, 2016.

Forster, P. M., Smith, C. J., Walsh, T., Lamb, W. F., Lamboll, R., Hauser, M., Ribes, A., Rosen, D., Gillett, N., Palmer, M. D., Rogelj, J., von Schuckmann, K., Seneviratne, S. I., Trewin, B., Zhang, X., Allen, M., Andrew, R., Birt, A., Borger, A., Boyer, T., Broersma, J. A., Cheng, L., Dentener, F., Friedlingstein, P., Gutiérrez, J. M., Gütschow, J., Hall, B., Ishii, M., Jenkins, S., Lan, X., Lee, J.-Y., Morice, C., Kadow, C., Kennedy, J., Killick, R., Minx, J. C., Naik, V., Peters, G. P., Pirani, A., Pongratz, J., Schleussner, C.-F., Szopa, S., Thorne, P., Rohde, R., Rojas Corradi, M., Schumacher, D., Vose, R., Zickfeld, K., Masson-Delmotte, V., and Zhai, P.: Indicators of Global Climate Change 2022: annual update of large-scale indicators of the state of the climate system and human influence, Earth Syst. Sci. Data, 15, 2295–2327, https://doi.org/10.5194/essd-15-2295-2023, 2023.

Fyfe, J. C., Kharin, V. V., Santer, B. D., Cole, J. N. S., and Gillett, N. P.: Significant impact of forcing uncertainty in a large ensemble of climate model simulations, P. Natl. Acad. Sci. USA, 118, e2016549118, https://doi.org/10.1073/pnas.2016549118, 2021.

Gaudel, A., Cooper, O. R., Ancellet, G., Barret, B., Boynard, A., Burrows, J. P., Clerbaux, C., Coheur, P.-F., Cuesta, J., Cuevas, E., Doniki, S., Dufour, G., Ebojie, F., Foret, G., Garcia, O., Granados-Muñoz, M. J., Hannigan, J. W., Hase, F., Hassler, B., Huang, G., Hurtmans, D., Jaffe, D., Jones, N., Kalabokas, P., Kerridge, B., Kulawik, S., Latter, B., Leblanc, T., Le Flochmoën, E., Lin, W., Liu, J., Liu, X., Mahieu, E., McClure-Begley, A., Neu, J. L., Osman, M., Palm, M., Petetin, H., Petropavlovskikh, I., Querel, R., Rahpoe, N., Rozanov, A., Schultz, M. G., Schwab, J., Siddans, R., Smale, D., Steinbacher, M., Tanimoto, H., Tarasick, D. W., Thouret, V., Thompson, A. M., Trickl, T., Weatherhead, E., Wespes, C., Worden, H. M., Vigouroux, C., Xu, X., Zeng, G., and Ziemke, J.: Tropospheric Ozone Assessment Report: Present-day distribution and trends of tropospheric ozone relevant to climate and global atmospheric chemistry model evaluation, Elem. Sci. Anth., 6, 39, https://doi.org/10.1525/elementa.291, 2018.

Ghan, S. J.: Technical Note: Estimating aerosol effects on cloud radiative forcing, Atmos. Chem. Phys., 13, 9971–9974, https://doi.org/10.5194/acp-13-9971-2013, 2013.

Gidden, M. J., Riahi, K., Smith, S. J., Fujimori, S., Luderer, G., Kriegler, E., van Vuuren, D. P., van den Berg, M., Feng, L., Klein, D., Calvin, K., Doelman, J. C., Frank, S., Fricko, O.,

Harmsen, M., Hasegawa, T., Havlik, P., Hilaire, J., Hoesly, R., Horing, J., Popp, A., Stehfest, E., and Takahashi, K.: Global emissions pathways under different socioeconomic scenarios for use in CMIP6: a dataset of harmonized emissions trajectories through the end of the century, Geosci. Model Dev., 12, 1443–1475, https://doi.org/10.5194/gmd-12-1443-2019, 2019.

Gillett, N. P., Shiogama, H., Funke, B., Hegerl, G., Knutti, R., Matthes, K., Santer, B. D., Stone, D., and Tebaldi, C.: The Detection and Attribution Model Intercomparison Project (DAMIP v1.0) contribution to CMIP6, Geosci. Model Dev., 9, 3685–3697, https://doi.org/10.5194/gmd-9-3685-2016, 2016.

Gliß, J., Mortier, A., Schulz, M., Andrews, E., Balkanski, Y., Bauer, S. E., Benedictow, A. M. K., Bian, H., Checa-Garcia, R., Chin, M., Ginoux, P., Griesfeller, J. J., Heckel, A., Kipling, Z., Kirkevåg, A., Kokkola, H., Laj, P., Le Sager, P., Lund, M. T., Lund Myhre, C., Matsui, H., Myhre, G., Neubauer, D., van Noije, T., North, P., Olivié, D. J. L., Rémy, S., Sogacheva, L., Takemura, T., Tsigaridis, K., and Tsyro, S. G.: AeroCom phase III multi-model evaluation of the aerosol life cycle and optical properties using ground- and space-based remote sensing as well as surface in situ observations, Atmos. Chem. Phys., 21, 87–128, https://doi.org/10.5194/acp-21-87-2021, 2021.

Golaz, J.-C., Caldwell, P. M., Van Roekel, L. P., Petersen, M. R., Tang, Q., Wolfe, J. D., Abeshu, G., Anantharaj, V., Asay-Davis, X. S., Bader, D. C., Baldwin, S. A., Bisht, G., Bogenschutz, P. A., Branstetter, M., Brunke, M. A., Brus, S. R., Burrows, S. M., Cameron-Smith, P. J., Donahue, A. S., Deakin, M., Easter, R. C., Evans, K. J., Feng, Y., Flanner, M., Foucar, J. G., Fyke, J. G., Griffin, B. M., Hannay, C., Harrop, B. E., Hoffman, M. J., Hunke, E. C., Jacob, R. L., Jacobsen, D. W., Jeffery, N., Jones, P. W., Keen, N. D., Klein, S. A., Larson, V. E., Leung, L. R., Li, H.-Y., Lin, W., Lipscomb, W. H., Ma, P.-L., Mahajan, S., Maltrud, M. E., Mametjanov, A., McClean, J. L., McCoy, R. B., Neale, R. B., Price, S. F., Qian, Y., Rasch, P. J., Reeves Eyre, J. E. J., Riley, W. J., Ringler, T. D., Roberts, A. F., Roesler, E. L., Salinger, A. G., Shaheen, Z., Shi, X., Singh, B., Tang, J., Taylor, M. A., Thornton, P. E., Turner, A. K., Veneziani, M., Wan, H., Wang, H., Wang, S., Williams, D. N., Wolfram, P. J., Worley, P. H., Xie, S., Yang, Y., Yoon, J.-H., Zelinka, M. D., Zender, C. S., Zeng, X., Zhang, C., Zhang, K., Zhang, Y., Zheng, X., Zhou, T., and Zhu, Q.: The DOE E3SM Coupled Model Version 1: Overview and Evaluation at Standard Resolution, J. Adv. Model. Earth Sy., 11, 2089–2129, https://doi.org/10.1029/2018MS001603, 2019.

Griffiths, P., Shin, Y., Keeble, J., and Archibald, A.: Tropospheric ozone budget in AerChemMIP experiments, EGU General Assembly 2023, Vienna, Austria, 24–28 April 2023, EGU23-7364, https://doi.org/10.5194/egusphere-egu23-7364, 2023.

Griffiths, P. T., Murray, L. T., Zeng, G., Shin, Y. M., Abraham, N. L., Archibald, A. T., Deushi, M., Emmons, L. K., Galbally, I. E., Hassler, B., Horowitz, L. W., Keeble, J., Liu, J., Moeini, O., Naik, V., O'Connor, F. M., Oshima, N., Tarasick, D., Tilmes, S., Turnock, S. T., Wild, O., Young, P. J., and Zanis, P.: Tropospheric ozone in CMIP6 simulations, Atmos. Chem. Phys., 21, 4187–4218, https://doi.org/10.5194/acp-21-4187-2021, 2021.

Guilyardi, E., Balaji, V., Lawrence, B., Callaghan, S., Deluca, C., Denvil, S., Lautenschlager, M., Morgan, M., Murphy, S., and Taylor, K. E.: Documenting Climate Models and Their Simulations, B. Am. Meteorol. Soc., 94, 623–627, https://doi.org/10.1175/BAMS-D-11-00035.1, 2013.

Guo, H., John, J. G., Blanton, C., McHugh, C., Nikonov, S., Radhakrishnan, A., Rand, K., Zadeh, N. T., Balaji, V., Durachta, J., Dupuis, C., Menzel, R., Robinson, T., Underwood, S., Vahlenkamp, H., Bushuk, M., Dunne, K. A., Dussin, R., Gauthier, P. P., Ginoux, P., Griffies, S. M., Hallberg, R., Harrison, M., Hurlin, W., Lin, P., Malyshev, S., Naik, V., Paulot, F., Paynter, D. J., Ploshay, J., Reichl, B. G., Schwarzkopf, D. M., Seman, C. J., Shao, A., Silvers, L., Wyman, B., Yan, X., Zeng, Y., Adcroft, A., Dunne, J. P., Held, I. M., Krasting, J. P., Horowitz, L. W., Milly, P., Shevliakova, E., Winton, M., Zhao, M., and Zhang, R.: NOAA-GFDL GFDL-CM4 model output historical, Earth System Grid Federation [data set], https://doi.org/10.22033/ESGF/CMIP6.8594, 2018.

Hajima, T., Abe, M., Arakawa, O., Suzuki, T., Komuro, Y., Ogura, T., Ogochi, K., Watanabe, M., Yamamoto, A., Tatebe, H., Noguchi, M. A., Ohgaito, R., Ito, A., Yamazaki, D., Ito, A., Takata, K., Watanabe, S., Kawamiya, M., and Tachiiri, K.: MIROC MIROC-ES2L model output prepared for CMIP6 CMIP historical, Earth System Grid Federation [data set], https://doi.org/10.22033/ESGF/CMIP6.5602, 2019.

Hajima, T., Watanabe, M., Yamamoto, A., Tatebe, H., Noguchi, M. A., Abe, M., Ohgaito, R., Ito, A., Yamazaki, D., Okajima, H., Ito, A., Takata, K., Ogochi, K., Watanabe, S., and Kawamiya, M.: Development of the MIROC-ES2L Earth system model and the evaluation of biogeochemical processes and feedbacks, Geosci. Model Dev., 13, 2197–2244, https://doi.org/10.5194/gmd-13-2197-2020, 2020.

Hassan, T., Allen, R. J., Liu, W., Shim, S., van Noije, T., Le Sager, P., Oshima, N., Deushi, M., Randles, C. A., and O'Connor, F. M.: Air quality improvements are projected to weaken the Atlantic meridional overturning circulation through radiative forcing effects, Commun. Earth Environ., 3, 149, https://doi.org/10.1038/s43247-022-00476-9, 2022.

He, B., Yu, Y., Bao, Q., Lin, P., Liu, H., Li, J., Wang, L., Liu, Y., Wu, G., Chen, K., Guo, Y., Zhao, S., Zhang, X., Song, M., and Xie, J.: CAS FGOALS-f3-L model dataset descriptions for CMIP6 DECK experiments, Atmos. Ocean. Sci. Lett., 13, 582–588, https://doi.org/10.1080/16742834.2020.1778419, 2020.

Held, I. M., Guo, H., Adcroft, A., Dunne, J. P., Horowitz, L. W., Krasting, J., Shevliakova, E., Winton, M., Zhao, M., Bushuk, M., Wittenberg, A. T., Wyman, B., Xiang, B., Zhang, R., Anderson, W., Balaji, V., Donner, L., Dunne, K., Durachta, J., Gauthier, P. P. G., Ginoux, P., Golaz, J.-C., Griffies, S. M., Hallberg, R., Harris, L., Harrison, M., Hurlin, W., John, J., Lin, P., Lin, S.-J., Malyshev, S., Menzel, R., Milly, P. C. D., Ming, Y., Naik, V., Paynter, D., Paulot, F., Rammaswamy, V., Reichl, B., Robinson, T., Rosati, A., Seman, C., Silvers, L. G., Underwood, S., and Zadeh, N.: Structure and Performance of GFDL's CM4.0 Climate Model, J. Adv. Model. Earth Sy., 11, 3691–3727, https://doi.org/10.1029/2019MS001829, 2019.

Hoesly, R. M., Smith, S. J., Feng, L., Klimont, Z., Janssens-Maenhout, G., Pitkanen, T., Seibert, J. J., Vu, L., Andres, R. J., Bolt, R. M., Bond, T. C., Dawidowski, L., Kholod, N., Kurokawa, J.-I., Li, M., Liu, L., Lu, Z., Moura, M. C. P., O'Rourke, P. R., and Zhang, Q.: Historical (1750–2014) anthropogenic emissions of reactive gases and aerosols from the Community Emissions Data System (CEDS), Geosci. Model Dev., 11, 369–408, https://doi.org/10.5194/gmd-11-369-2018, 2018.

Holland, M. M., Hannay, C., Fasullo, J., Jahn, A., Kay, J. E., Mills, M., Simpson, I. R., Wieder, W., Lawrence, P., Kluzek, E., and Bailey, D.: New model ensemble reveals how forcing uncertainty and model structure alter climate simulated across CMIP generations of the Community Earth System Model, Geosci. Model Dev., 17, 1585–1602, https://doi.org/10.5194/gmd-17-1585-2024, 2024.

Huang, W.: THU CIESM model output prepared for CMIP6 CMIP historical, Earth System Grid Federation [data set], https://doi.org/10.22033/ESGF/CMIP6.8843, 2019.

IPCC: Summary for policymakers, in: Climate change 2021: The physical science basis. Contribution of working group I to the sixth assessment report of the intergovernmental panel on climate change, type: Book section, edited by: Masson-Delmotte, V., Zhai, P., Pirani, A., Connors, S. L., Péan, C., Berger, S., Caud, N., Chen, Y., Goldfarb, L., Gomis, M. I., Huang, M., Leitzell, K., Lonnoy, E., Matthews, J. B. R., Maycock, T. K., Waterfield, T., Yelekçi, O., Yu, R., and Zhou, B., Cambridge University Press, Cambridge, UK and New York, NY, USA, https://doi.org/10.1017/9781009157896.001, 2021.

Jungclaus, J., Bittner, M., Wieners, K.-H., Wachsmann, F., Schupfner, M., Legutke, S., Giorgetta, M., Reick, C., Gayler, V., Haak, H., de Vrese, P., Raddatz, T., Esch, M., Mauritsen, T., von Storch, J.-S., Behrens, J., Brovkin, V., Claussen, M., Crueger, T., Fast, I., Fiedler, S., Hagemann, S., Hohenegger, C., Jahns, T., Kloster, S., Kinne, S., Lasslop, G., Kornblueh, L., Marotzke, J., Matei, D., Meraner, K., Mikolajewicz, U., Modali, K., Müller, W., Nabel, J., Notz, D., Peters-von Gehlen, K., Pincus, R., Pohlmann, H., Pongratz, J., Rast, S., Schmidt, H., Schnur, R., Schulzweida, U., Six, K., Stevens, B., Voigt, A., and Roeckner, E.: MPI-M MPI-ESM1.2-HR model output prepared for CMIP6 CMIP historical, Earth System Grid Federation [data set], https://doi.org/10.22033/ESGF/CMIP6.6594, 2019.

Kalisoras, A., Georgoulias, A. K., Akritidis, D., Allen, R. J., Naik, V., Kuo, C., Szopa, S., Nabat, P., Olivié, D., van Noije, T., Le Sager, P., Neubauer, D., Oshima, N., Mulcahy, J., Horowitz, L. W., and Zanis, P.: Decomposing the effective radiative forcing of anthropogenic aerosols based on CMIP6 Earth system models, Atmos. Chem. Phys., 24, 7837–7872, https://doi.org/10.5194/acp-24-7837-2024, 2024.

Karset, I. H. H., Berntsen, T. K., Storelvmo, T., Alterskjær, K., Grini, A., Olivié, D., Kirkevåg, A., Seland, Ø., Iversen, T., and Schulz, M.: Strong impacts on aerosol indirect effects from historical oxidant changes, Atmos. Chem. Phys., 18, 7669–7690, https://doi.org/10.5194/acp-18-7669-2018, 2018.

Kelley, M., Schmidt, G. A., Nazarenko, L. S., Bauer, S. E., Ruedy, R., Russell, G. L., Ackerman, A. S., Aleinov, I., Bauer, M., Bleck, R., Canuto, V., Cesana, G., Cheng, Y., Clune, T. L., Cook, B. I., Cruz, C. A., Del Genio, A. D., Elsaesser, G. S., Faluvegi, G., Kiang, N. Y., Kim, D., Lacis, A. A., Leboissetier, A., LeGrande, A. N., Lo, K. K., Marshall, J., Matthews, E. E., McDermid, S., Mezuman, K., Miller, R. L., Murray, L. T., Oinas, V., Orbe, C., García-Pando, C. P., Perlwitz, J. P., Puma, M. J., Rind, D., Romanou, A., Shindell, D. T., Sun, S., Tausnev, N., Tsigaridis, K., Tselioudis, G., Weng, E., Wu, J., and Yao, M.-S.: GISS-E2.1: Configurations and Climatology, J. Adv. Model. Earth Sy., 12, e2019MS002025, https://doi.org/10.1029/2019MS002025, 2020.

Kim, Y., Noh, Y., Kim, D., Lee, M.-I., Lee, H. J., Kim, S. Y., and Kim, D.: KIOST KIOST-ESM model output prepared for CMIP6 CMIP historical, Earth System Grid Federation [data set], https://doi.org/10.22033/ESGF/CMIP6.5296, 2019.

Kok, J. F., Adebiyi, A. A., Albani, S., Balkanski, Y., Checa-Garcia, R., Chin, M., Colarco, P. R., Hamilton, D. S., Huang, Y., Ito, A., Klose, M., Leung, D. M., Li, L., Mahowald, N. M., Miller, R. L., Obiso, V., Pérez García-Pando, C., Rocha-Lima, A., Wan, J. S., and Whicker, C. A.: Improved representation of the global dust cycle using observational constraints on dust properties and abundance, Atmos. Chem. Phys., 21, 8127–8167, https://doi.org/10.5194/acp-21-8127-2021, 2021.

Krasting, J. P., John, J. G., Blanton, C., McHugh, C., Nikonov, S., Radhakrishnan, A., Rand, K., Zadeh, N. T., Balaji, V., Durachta, J., Dupuis, C., Menzel, R., Robinson, T., Underwood, S., Vahlenkamp, H., Dunne, K. A., Gauthier, P. P., Ginoux, P., Griffies, S. M., Hallberg, R., Harrison, M., Hurlin, W., Malyshev, S., Naik, V., Paulot, F., Paynter, D. J., Ploshay, J., Reichl, B. G., Schwarzkopf, D. M., Seman, C. J., Silvers, L., Wyman, B., Zeng, Y., Adcroft, A., Dunne, J. P., Dussin, R., Guo, H., He, J., Held, I. M., Horowitz, L. W., Lin, P., Milly, P., Shevliakova, E., Stock, C., Winton, M., Wittenberg, A. T., Xie, Y., and Zhao, M.: NOAA-GFDL GFDL-ESM4 model output prepared for CMIP6 CMIP historical, Earth System Grid Federation [data set], https://doi.org/10.22033/ESGF/CMIP6.8597, 2018.

Kuhlbrodt, T., Jones, C. G., Sellar, A., Storkey, D., Blockley, E., Stringer, M., Hill, R., Graham, T., Ridley, J., Blaker, A., Calvert, D., Copsey, D., Ellis, R., Hewitt, H., Hyder, P., Ineson, S., Mulcahy, J., Siahaan, A., and Walton, J.: The Low-Resolution Version of HadGEM3 GC3.1: Development and Evaluation for Global Climate, J. Adv. Model. Earth Sy., 10, 2865–2888, https://doi.org/10.1029/2018MS001370, 2018.

Lamarque, J.-F., Shindell, D. T., Josse, B., Young, P. J., Cionni, I., Eyring, V., Bergmann, D., Cameron-Smith, P., Collins, W. J., Doherty, R., Dalsoren, S., Faluvegi, G., Folberth, G., Ghan, S. J., Horowitz, L. W., Lee, Y. H., MacKenzie, I. A., Nagashima, T., Naik, V., Plummer, D., Righi, M., Rumbold, S. T., Schulz, M., Skeie, R. B., Stevenson, D. S., Strode, S., Sudo, K., Szopa, S., Voulgarakis, A., and Zeng, G.: The Atmospheric Chemistry and Climate Model Intercomparison Project (ACCMIP): overview and description of models, simulations and climate diagnostics, Geosci. Model Dev., 6, 179–206, https://doi.org/10.5194/gmd-6-179-2013, 2013.

Lawrence, D. M., Hurtt, G. C., Arneth, A., Brovkin, V., Calvin, K. V., Jones, A. D., Jones, C. D., Lawrence, P. J., de Noblet-Ducoudré, N., Pongratz, J., Seneviratne, S. I., and Shevliakova, E.: The Land Use Model Intercomparison Project (LUMIP) contribution to CMIP6: rationale and experimental design, Geosci. Model Dev., 9, 2973–2998, https://doi.org/10.5194/gmd-9-2973-2016, 2016.

Leach, N. J., Jenkins, S., Nicholls, Z., Smith, C. J., Lynch, J., Cain, M., Walsh, T., Wu, B., Tsutsui, J., and Allen, M. R.: FaIRv2.0.0: a generalized impulse response model for climate uncertainty and future scenario exploration, Geosci. Model Dev., 14, 3007–3036, https://doi.org/10.5194/gmd-14-3007-2021, 2021.

Lee, J., Kim, J., Sun, M.-A., Kim, B.-H., Moon, H., Sung, H. M., Kim, J., and Byun, Y.-H.: Evaluation of the Korea Meteorological Administration Advanced Community Earth-

System model (K-ACE), Asia-Pac. J. Atmos. Sci., 56, 381–395, https://doi.org/10.1007/s13143-019-00144-7, 2020a.

Lee, J., Gleckler, P. J., Ahn, M.-S., Ordonez, A., Ullrich, P. A., Sperber, K. R., Taylor, K. E., Planton, Y. Y., Guilyardi, E., Durack, P., Bonfils, C., Zelinka, M. D., Chao, L.-W., Dong, B., Doutriaux, C., Zhang, C., Vo, T., Boutte, J., Wehner, M. F., Pendergrass, A. G., Kim, D., Xue, Z., Wittenberg, A. T., and Krasting, J.: Systematic and objective evaluation of Earth system models: PCMDI Metrics Package (PMP) version 3, Geosci. Model Dev., 17, 3919–3948, https://doi.org/10.5194/gmd-17-3919-2024, 2024.

Lee, L. A., Carslaw, K. S., Pringle, K. J., Mann, G. W., and Spracklen, D. V.: Emulation of a complex global aerosol model to quantify sensitivity to uncertain parameters, Atmos. Chem. Phys., 11, 12253–12273, https://doi.org/10.5194/acp-11-12253-2011, 2011.

Lee, W.-L. and Liang, H.-C.: AS-RCEC TaiESM1.0 model output prepared for CMIP6 CMIP historical, Earth System Grid Federation [data set], https://doi.org/10.22033/ESGF/CMIP6.9755, 2020.

Lee, W.-L., Wang, Y.-C., Shiu, C.-J., Tsai, I., Tu, C.-Y., Lan, Y.-Y., Chen, J.-P., Pan, H.-L., and Hsu, H.-H.: Taiwan Earth System Model Version 1: description and evaluation of mean state, Geosci. Model Dev., 13, 3887–3904, https://doi.org/10.5194/gmd-13-3887-2020, 2020.b.

Li, L.: CAS FGOALS-g3 model output prepared for CMIP6 CMIP historical, Earth System Grid Federation [data set], https://doi.org/10.22033/ESGF/CMIP6.3356, 2019.

Li, L., Yu, Y., Tang, Y., Lin, P., Xie, J., Song, M., Dong, L., Zhou, T., Liu, L., Wang, L., Pu, Y., Chen, X., Chen, L., Xie, Z., Liu, H., Zhang, L., Huang, X., Feng, T., Zheng, W., Xia, K., Liu, H., Liu, J., Wang, Y., Wang, L., Jia, B., Xie, F., Wang, B., Zhao, S., Yu, Z., Zhao, B., and Wei, J.: The Flexible Global Ocean-Atmosphere-Land System Model Grid-Point Version 3 (FGOALS-g3): Description and Evaluation, J. Adv. Model. Earth Sy., 12, e2019MS002012, https://doi.org/10.1029/2019MS002012, 2020.

Li, Y., Wang, Z., Lei, Y., Che, H., and Zhang, X.: Impacts of reductions in non-methane short-lived climate forcers on future climate extremes and the resulting population exposure risks in eastern and southern Asia, Atmos. Chem. Phys., 23, 2499–2523, https://doi.org/10.5194/acp-23-2499-2023, 2023.

Lin, Y., Huang, X., Liang, Y., Qin, Y., Xu, S., Huang, W., Xu, F., Liu, L., Wang, Y., Peng, Y., Wang, L., Xue, W., Fu, H., Zhang, G. J., Wang, B., Li, R., Zhang, C., Lu, H., Yang, K., Luo, Y., Bai, Y., Song, Z., Wang, M., Zhao, W., Zhang, F., Xu, J., Zhao, X., Lu, C., Chen, Y., Luo, Y., Hu, Y., Tang, Q., Chen, D., Yang, G., and Gong, P.: Community Integrated Earth System Model (CIESM): Description and Evaluation, J. Adv. Model. Earth Sy., 12, e2019MS002036, https://doi.org/10.1029/2019MS002036, 2020.

Liu, L., Shawki, D., Voulgarakis, A., Kasoar, M., Samset, B. H., Myhre, G., Forster, P. M., Hodnebrog, Ø., Sillmann, J., Aalbergsjø, S. G., Boucher, O., Faluvegi, G., Iversen, T., Kirkevåg, A., Lamarque, J.-F., Olivié, D., Richardson, T., Shindell, D., and Takemura, T.: A PDRMIP Multimodel Study on the Impacts of Regional Aerosol Forcings on Global and Regional Precipitation, J. Climate, 31, 4429–4447, https://doi.org/10.1175/JCLI-D-17-0439.1, 2018.

Liu, Z., Doherty, R. M., Wild, O., O'Connor, F. M., and Turnock, S. T.: Correcting ozone biases in a global chemistry–climate model: implications for future ozone, Atmos. Chem. Phys., 22, 12543–12557, https://doi.org/10.5194/acp-22-12543-2022, 2022.

Lovato, T. and Peano, D.: CMCC CMCC-CM2-SR5 model output prepared for CMIP6 CMIP historical, Earth System Grid Federation [data set], https://doi.org/10.22033/ESGF/CMIP6.3825, 2020.

Mauritsen, T., Bader, J., Becker, T., Behrens, J., Bittner, M., Brokopf, R., Brovkin, V., Claussen, M., Crueger, T., Esch, M., Fast, I., Fiedler, S., Fläschner, D., Gayler, V., Giorgetta, M., Goll, D. S., Haak, H., Hagemann, S., Hedemann, C., Hohenegger, C., Ilyina, T., Jahns, T., Jimenéz-de-la Cuesta, D., Jungclaus, J., Kleinen, T., Kloster, S., Kracher, D., Kinne, S., Kleberg, D., Lasslop, G., Kornblueh, L., Marotzke, J., Matei, D., Meraner, K., Mikolajewicz, U., Modali, K., Möbis, B., Müller, W. A., Nabel, J. E. M. S., Nam, C. C. W., Notz, D., Nyawira, S.-S., Paulsen, H., Peters, K., Pincus, R., Pohlmann, H., Pongratz, J., Popp, M., Raddatz, T. J., Rast, S., Redler, R., Reick, C. H., Rohrschneider, T., Schemann, V., Schmidt, H., Schnur, R., Schulzweida, U., Six, K. D., Stein, L., Stemmler, I., Stevens, B., von Storch, J.-S., Tian, F., Voigt, A., Vrese, P., Wieners, K.-H., Wilkenskjeld, S., Winkler, A., and Roeckner, E.: Developments in the MPI-M Earth System Model version 1.2 (MPI-ESM1.2) and Its Response to Increasing CO_2, J. Adv. Model. Earth Sy., 11, 998–1038, https://doi.org/10.1029/2018MS001400, 2019.

Meehl, G. A., Moss, R., Taylor, K. E., Eyring, V., Stouffer, R. J., Bony, S., and Stevens, B.: Climate Model Intercomparisons: Preparing for the Next Phase, Eos, 95, 77–78, https://doi.org/10.1002/2014EO090001, 2014.

Melton, J. R., Wania, R., Hodson, E. L., Poulter, B., Ringeval, B., Spahni, R., Bohn, T., Avis, C. A., Beerling, D. J., Chen, G., Eliseev, A. V., Denisov, S. N., Hopcroft, P. O., Lettenmaier, D. P., Riley, W. J., Singarayer, J. S., Subin, Z. M., Tian, H., Zürcher, S., Brovkin, V., van Bodegom, P. M., Kleinen, T., Yu, Z. C., and Kaplan, J. O.: Present state of global wetland extent and wetland methane modelling: conclusions from a model intercomparison project (WETCHIMP), Biogeosciences, 10, 753–788, https://doi.org/10.5194/bg-10-753-2013, 2013.

Menary, M. B., Robson, J., Allan, R. P., Booth, B. B. B., Cassou, C., Gastineau, G., Gregory, J., Hodson, D., Jones, C., Mignot, J., Ringer, M., Sutton, R., Wilcox, L., and Zhang, R.: Aerosol-Forced AMOC Changes in CMIP6 Historical Simulations, Geophys. Res. Lett., 47, e2020GL088166, https://doi.org/10.1029/2020GL088166, 2020.

Miller, R. L., Schmidt, G. A., Nazarenko, L. S., Bauer, S. E., Kelley, M., Ruedy, R., Russell, G. L., Ackerman, A. S., Aleinov, I., Bauer, M., Bleck, R., Canuto, V., Cesana, G., Cheng, Y., Clune, T. L., Cook, B. I., Cruz, C. A., Del Genio, A. D., Elsaesser, G. S., Faluvegi, G., Kiang, N. Y., Kim, D., Lacis, A. A., Leboissetier, A., LeGrande, A. N., Lo, K. K., Marshall, J., Matthews, E. E., McDermid, S., Mezuman, K., Murray, L. T., Oinas, V., Orbe, C., Pérez García-Pando, C., Perlwitz, J. P., Puma, M. J., Rind, D., Romanou, A., Shindell, D. T., Sun, S., Tausnev, N., Tsigaridis, K., Tselioudis, G., Weng, E., Wu, J., and Yao, M.-S.: CMIP6 Historical Simulations (1850–2014) With GISS-E2.1, J. Adv. Model. Earth Sy., 13, e2019MS002034, https://doi.org/10.1029/2019MS002034, 2021.

Monerie, P.-A., Robson, J. I., Dunstone, N. J., and Turner, A. G.: Skilful seasonal predictions of global monsoon summer precipitation with DePreSys3, Environ. Res. Lett., 16, 104035, https://doi.org/10.1088/1748-9326/ac2a65, 2021.

Morgenstern, O., O'Connor, F. M., Johnson, B. T., Zeng, G., Mulcahy, J. P., Williams, J., Teixeira, J., Michou, M., Nabat, P., Horowitz, L. W., Naik, V., Sentman, L. T., Deushi, M., Bauer, S. E., Tsigaridis, K., Shindell, D. T., and Kinnison, D. E.: Reappraisal of the Climate Impacts of Ozone-Depleting Substances, Geophys. Res. Lett., 47, e2020GL088295, https://doi.org/10.1029/2020GL088295, 2020.

Mortier, A., Gliß, J., Schulz, M., Aas, W., Andrews, E., Bian, H., Chin, M., Ginoux, P., Hand, J., Holben, B., Zhang, H., Kipling, Z., Kirkevåg, A., Laj, P., Lurton, T., Myhre, G., Neubauer, D., Olivié, D., von Salzen, K., Skeie, R. B., Takemura, T., and Tilmes, S.: Evaluation of climate model aerosol trends with ground-based observations over the last 2 decades – an AeroCom and CMIP6 analysis, Atmos. Chem. Phys., 20, 13355–13378, https://doi.org/10.5194/acp-20-13355-2020, 2020.

Moseid, K. O., Schulz, M., Storelvmo, T., Julsrud, I. R., Olivié, D., Nabat, P., Wild, M., Cole, J. N. S., Takemura, T., Oshima, N., Bauer, S. E., and Gastineau, G.: Bias in CMIP6 models as compared to observed regional dimming and brightening, Atmos. Chem. Phys., 20, 16023–16040, https://doi.org/10.5194/acp-20-16023-2020, 2020.

Murray, L. T., Logan, J. A., and Jacob, D. J.: Interannual variability in tropical tropospheric ozone and OH: The role of lightning: Iav In Ozone And Oh-Role Of Lightning, J. Geophys. Res.-Atmos., 118, 11468–11480, https://doi.org/10.1002/jgrd.50857, 2013.

Myhre, G., Forster, P. M., Samset, B. H., Hodnebrog, Ø., Sillmann, J., Aalbergsjø, S. G., Andrews, T., Boucher, O., Faluvegi, G., Fläschner, D., Iversen, T., Kasoar, M., Kharin, V., Kirkevåg, A., Lamarque, J.-F., Olivié, D., Richardson, T. B., Shindell, D., Shine, K. P., Stjern, C. W., Takemura, T., Voulgarakis, A., and Zwiers, F.: PDRMIP: A Precipitation Driver and Response Model Intercomparison Project – Protocol and Preliminary Results, B. Am. Meteorol. Soc., 98, 1185–1198, https://doi.org/10.1175/BAMS-D-16-0019.1, 2017.

NASA Goddard Institute for Space Studies (NASA/GISS): NASA-GISS GISS-E2.1G model output prepared for CMIP6 CMIP historical, Earth System Grid Federation [data set], https://doi.org/10.22033/ESGF/CMIP6.7127, 2018.

NASA Goddard Institute for Space Studies (NASA/GISS): NASA-GISS GISS-E2-1-G-CC model output prepared for CMIP6 CMIP historical, Earth System Grid Federation [data set], https://doi.org/10.22033/ESGF/CMIP6.11762, 2019a.

NASA Goddard Institute for Space Studies (NASA/GISS): NASA-GISS GISS-E2.1H model output prepared for CMIP6 CMIP historical, Earth System Grid Federation [data set], https://doi.org/10.22033/ESGF/CMIP6.7128, 2019b.

Neubauer, D., Ferrachat, S., Siegenthaler-Le Drian, C., Stoll, J., Folini, D. S., Tegen, I., Wieners, K.-H., Mauritsen, T., Stemmler, I., Barthel, S., Bey, I., Daskalakis, N., Heinold, B., Kokkola, H., Partridge, D., Rast, S., Schmidt, H., Schutgens, N., Stanelle, T., Stier, P., Watson-Parris, D., and Lohmann, U.: HAMMOZ-Consortium MPI-ESM1.2-HAM model output prepared for CMIP6 CMIP historical, Earth System Grid Federation [data set], https://doi.org/10.22033/ESGF/CMIP6.5016, 2019.

O'Connor, F. M., Abraham, N. L., Dalvi, M., Folberth, G. A., Griffiths, P. T., Hardacre, C., Johnson, B. T., Kahana, R., Keeble, J., Kim, B., Morgenstern, O., Mulcahy, J. P., Richardson, M., Robertson, E., Seo, J., Shim, S., Teixeira, J. C., Turnock, S. T., Williams, J., Wiltshire, A. J., Woodward, S., and Zeng, G.: Assessment of pre-industrial to present-day anthropogenic climate forcing in UKESM1, Atmos. Chem. Phys., 21, 1211–1243, https://doi.org/10.5194/acp-21-1211-2021, 2021.

O'Connor, F. M., Johnson, B. T., Jamil, O., Andrews, T., Mulcahy, J. P., and Manners, J.: Apportionment of the Pre-Industrial to Present-Day Climate Forcing by Methane Using UKESM1: The Role of the Cloud Radiative Effect, J. Adv. Model. Earth Sy., 14, e2022MS002991, https://doi.org/10.1029/2022MS002991, 2022.

O'Neill, B. C., Tebaldi, C., van Vuuren, D. P., Eyring, V., Friedlingstein, P., Hurtt, G., Knutti, R., Kriegler, E., Lamarque, J.-F., Lowe, J., Meehl, G. A., Moss, R., Riahi, K., and Sanderson, B. M.: The Scenario Model Intercomparison Project (ScenarioMIP) for CMIP6, Geosci. Model Dev., 9, 3461–3482, https://doi.org/10.5194/gmd-9-3461-2016, 2016.

Oshima, N., Yukimoto, S., Deushi, M., Koshiro, T., Kawai, H., Tanaka, T. Y., and Yoshida, K.: Global and Arctic effective radiative forcing of anthropogenic gases and aerosols in MRI-ESM2.0, Prog. Earth Planet. Sci., 7, 38, https://doi.org/10.1186/s40645-020-00348-w, 2020.

Pak, G., Noh, Y., Lee, M.-I., Yeh, S.-W., Kim, D., Kim, S.-Y., Lee, J.-L., Lee, H. J., Hyun, S.-H., Lee, K.-Y., Lee, J.-H., Park, Y.-G., Jin, H., Park, H., and Kim, Y. H.: Korea Institute of Ocean Science and Technology Earth System Model and Its Simulation Characteristics, Ocean Sci. J., 56, 18–45, https://doi.org/10.1007/s12601-021-00001-7, 2021.

Park, S. and Shin, J.: SNU SAM0-UNICON model output prepared for CMIP6 CMIP historical, Earth System Grid Federation [data set], https://doi.org/10.22033/ESGF/CMIP6.7789, 2019.

Park, S., Shin, J., Kim, S., Oh, E., and Kim, Y.: Global Climate Simulated by the Seoul National University Atmosphere Model Version 0 with a Unified Convection Scheme (SAM0-UNICON), J. Climate, 32, 2917–2949, https://doi.org/10.1175/JCLI-D-18-0796.1, 2019.

Pascoe, C., Lawrence, B. N., Guilyardi, E., Juckes, M., and Taylor, K. E.: Documenting numerical experiments in support of the Coupled Model Intercomparison Project Phase 6 (CMIP6), Geosci. Model Dev., 13, 2149–2167, https://doi.org/10.5194/gmd-13-2149-2020, 2020.

Persad, G., Samset, B. H., Wilcox, L. J., Allen, R. J., Bollasina, M. A., Booth, B. B. B., Bonfils, C., Crocker, T., Joshi, M., Lund, M. T., Marvel, K., Merikanto, J., Nordling, K., Undorf, S., van Vuuren, D. P., Westervelt, D. M., and Zhao, A.: Rapidly evolving aerosol emissions are a dangerous omission from near-term climate risk assessments, Environmental Research: Climate, 2, 032001, https://doi.org/10.1088/2752-5295/acd6af, 2023.

Pincus, R., Forster, P. M., and Stevens, B.: The Radiative Forcing Model Intercomparison Project (RFMIP): experimental protocol for CMIP6, Geosci. Model Dev., 9, 3447–3460, https://doi.org/10.5194/gmd-9-3447-2016, 2016.

Prather, M. J., Zhu, X., Tang, Q., Hsu, J., and Neu, J. L.: An atmospheric chemist in search of the tropopause, J. Geophys. Res., 116, D04306, https://doi.org/10.1029/2010JD014939, 2011.

Rao, S., Klimont, Z., Smith, S. J., Van Dingenen, R., Dentener, F., Bouwman, L., Riahi, K., Amann, M., Bodirsky, B. L., van Vuuren, D. P., Aleluia Reis, L., Calvin, K., Drouet, L., Fricko, O., Fujimori, S., Gernaat, D., Havlik, P., Harmsen, M., Hasegawa, T., Heyes, C., Hilaire, J., Luderer, G., Masui, T., Stehfest, E., Strefler, J., van der Sluis, S., and Tavoni, M.: Future air pollution in the Shared Socio-economic Pathways, Global Environ. Chang., 42, 346–358, https://doi.org/10.1016/j.gloenvcha.2016.05.012, 2017.

Riahi, K., van Vuuren, D. P., Kriegler, E., Edmonds, J., O'Neill, B. C., Fujimori, S., Bauer, N., Calvin, K., Dellink, R., Fricko, O., Lutz, W., Popp, A., Cuaresma, J. C., Kc, S., Leimbach, M., Jiang, L., Kram, T., Rao, S., Emmerling, J., Ebi, K., Hasegawa, T., Havlik, P., Humpenöder, F., Da Silva, L. A., Smith, S., Stehfest, E., Bosetti, V., Eom, J., Gernaat, D., Masui, T., Rogelj, J., Strefler, J., Drouet, L., Krey, V., Luderer, G., Harmsen, M., Takahashi, K., Baumstark, L., Doelman, J. C., Kainuma, M., Klimont, Z., Marangoni, G., Lotze-Campen, H., Obersteiner, M., Tabeau, A., and Tavoni, M.: The Shared Socioeconomic Pathways and their energy, land use, and greenhouse gas emissions implications: An overview, Global Environ. Chang., 42, 153–168, https://doi.org/10.1016/j.gloenvcha.2016.05.009, 2017.

Ridley, J., Menary, M., Kuhlbrodt, T., Andrews, M., and Andrews, T.: MOHC HadGEM3-GC31-LL model output prepared for CMIP6 CMIP historical, Earth System Grid Federation [data set], https://doi.org/10.22033/ESGF/CMIP6.6109, 2019a.

Ridley, J., Menary, M., Kuhlbrodt, T., Andrews, M., and Andrews, T.: MOHC HadGEM3-GC31-MM model output prepared for CMIP6 CMIP historical, Earth System Grid Federation [data set], https://doi.org/10.22033/ESGF/CMIP6.6112, 2019b.

Rong, X.: CAMS CAMS_CSM1.0 model output prepared for CMIP6 CMIP historical, Earth System Grid Federation [data set], https://doi.org/10.22033/ESGF/CMIP6.9754, 2019.

Rong, X., Li, J., Chen, H., Xin, Y., Su, J., Hua, L., Zhou, T., Qi, Y., Zhang, Z., Zhang, G., and Li, J.: The CAMS Climate System Model and a Basic Evaluation of Its Climatology and Climate Variability Simulation, J. Meteorol. Res., 32, 839–861, https://doi.org/10.1007/s13351-018-8058-x, 2018.

Samset, B. H., Myhre, G., Forster, P. M., Hodnebrog, Ø., Andrews, T., Faluvegi, G., Fläschner, D., Kasoar, M., Kharin, V., Kirkevåg, A., Lamarque, J.-F., Olivié, D., Richardson, T., Shindell, D., Shine, K. P., Takemura, T., and Voulgarakis, A.: Fast and slow precipitation responses to individual climate forcers: A PDRMIP multimodel study, Geophys. Res. Lett., 43, 2782–2791, https://doi.org/10.1002/2016GL068064, 2016.

Schlund, M., Lauer, A., Gentine, P., Sherwood, S. C., and Eyring, V.: Emergent constraints on equilibrium climate sensitivity in CMIP5: do they hold for CMIP6?, Earth Syst. Dynam., 11, 1233–1258, https://doi.org/10.5194/esd-11-1233-2020, 2020.

Schlund, M., Hassler, B., Lauer, A., Andela, B., Jöckel, P., Kazeroni, R., Loosveldt Tomas, S., Medeiros, B., Predoi, V., Sénési, S., Servonnat, J., Stacke, T., Vegas-Regidor, J., Zimmermann, K., and Eyring, V.: Evaluation of native Earth system model output with ESMValTool v2.6.0, Geosci. Model Dev., 16, 315–333, https://doi.org/10.5194/gmd-16-315-2023, 2023.

Scoccimarro, E., Bellucci, A., and Peano, D.: CMCC CMCC-CM2-HR4 model output prepared for CMIP6 CMIP historical, Earth System Grid Federation [data set], https://doi.org/10.22033/ESGF/CMIP6.3823, 2020.

Seferian, R.: CNRM-CERFACS CNRM-ESM2-1 model output prepared for CMIP6 CMIP historical, Earth System Grid Federation [data set], https://doi.org/10.22033/ESGF/CMIP6.4068, 2018.

Séférian, R., Nabat, P., Michou, M., Saint-Martin, D., Voldoire, A., Colin, J., Decharme, B., Delire, C., Berthet, S., Chevallier, M., Sénési, S., Franchisteguy, L., Vial, J., Mallet, M., Joetzjer, E., Geoffroy, O., Guérémy, J.-F., Moine, M.-P., Msadek, R., Ribes, A., Rocher, M., Roehrig, R., Salas-y Mélia, D., Sanchez, E., Terray, L., Valcke, S., Waldman, R., Aumont, O., Bopp, L., Deshayes, J., Éthé, C., and Madec, G.: Evaluation of CNRM Earth System Model, CNRM-ESM2-1: Role of Earth System Processes in Present-Day and Future Climate, J. Adv. Model. Earth Sy., 11, 4182–4227, https://doi.org/10.1029/2019MS001791, 2019.

Seland, Ø., Bentsen, M., Olivié, D., Toniazzo, T., Gjermundsen, A., Graff, L. S., Debernard, J. B., Gupta, A. K., He, Y.-C., Kirkevåg, A., Schwinger, J., Tjiputra, J., Aas, K. S., Bethke, I., Fan, Y., Griesfeller, J., Grini, A., Guo, C., Ilicak, M., Karset, I. H. H., Landgren, O., Liakka, J., Moseid, K. O., Nummelin, A., Spensberger, C., Tang, H., Zhang, Z., Heinze, C., Iversen, T., and Schulz, M.: Overview of the Norwegian Earth System Model (NorESM2) and key climate response of CMIP6 DECK, historical, and scenario simulations, Geosci. Model Dev., 13, 6165–6200, https://doi.org/10.5194/gmd-13-6165-2020, 2020.

Seland, Y., Bentsen, M., Oliviè, D. J. L., Toniazzo, T., Gjermundsen, A., Graff, L. S., Debernard, J. B., Gupta, A. K., He, Y., Kirkevåg, A., Schwinger, J., Tjiputra, J., Aas, K. S., Bethke, I., Fan, Y., Griesfeller, J., Grini, A., Guo, C., Ilicak, M., Karset, I. H. H., Landgren, O. A., Liakka, J., Moseid, K. O., Nummelin, A., Spensberger, C., Tang, H., Zhang, Z., Heinze, C., Iversen, T., and Schulz, M.: NCC NorESM2-LM model output prepared for CMIP6 CMIP historical, Earth System Grid Federation [data set], https://doi.org/10.22033/ESGF/CMIP6.8036, 2019.

Sellar, A. A., Jones, C. G., Mulcahy, J. P., Tang, Y., Yool, A., Wiltshire, A., O'Connor, F. M., Stringer, M., Hill, R., Palmieri, J., Woodward, S., de Mora, L., Kuhlbrodt, T., Rumbold, S. T., Kelley, D. I., Ellis, R., Johnson, C. E., Walton, J., Abraham, N. L., Andrews, M. B., Andrews, T., Archibald, A. T., Berthou, S., Burke, E., Blockley, E., Carslaw, K., Dalvi, M., Edwards, J., Folberth, G. A., Gedney, N., Griffiths, P. T., Harper, A. B., Hendry, M. A., Hewitt, A. J., Johnson, B., Jones, A., Jones, C. D., Keeble, J., Liddicoat, S., Morgenstern, O., Parker, R. J., Predoi, V., Robertson, E., Siahaan, A., Smith, R. S., Swaminathan, R., Woodhouse, M. T., Zeng, G., and Zerroukat, M.: UKESM1: Description and Evaluation of the U.K. Earth System Model, J. Adv. Model. Earth Sy., 11, 4513–4558, https://doi.org/10.1029/2019MS001739, 2019.

Shim, S., Sung, H., Kwon, S., Kim, J., Lee, J., Sun, M., Song, J., Ha, J., Byun, Y., Kim, Y., Turnock, S. T., Stevenson, D. S., Allen, R. J., O'Connor, F. M., Teixeira, J. C., Williams, J., Johnson, B., Keeble, J., Mulcahy, J., and Zeng, G.: Regional Features of Long-Term Exposure to $PM_{2.5}$ Air Quality over Asia under SSP Scenarios Based on CMIP6 Models, Int. J. Env. Res. Pub. He., 18, 6817–6834, https://doi.org/10.3390/ijerph18136817, 2021.

Shindell, D. T., Lamarque, J.-F., Schulz, M., Flanner, M., Jiao, C., Chin, M., Young, P. J., Lee, Y. H., Rotstayn, L., Mahowald, N., Milly, G., Faluvegi, G., Balkanski, Y., Collins, W. J., Conley, A. J., Dalsoren, S., Easter, R., Ghan, S., Horowitz, L., Liu, X., Myhre, G., Nagashima, T., Naik, V., Rumbold, S. T., Skeie, R., Sudo, K., Szopa, S., Takemura, T., Voulgarakis, A., Yoon, J.-H.,

and Lo, F.: Radiative forcing in the ACCMIP historical and future climate simulations, Atmos. Chem. Phys., 13, 2939–2974, https://doi.org/10.5194/acp-13-2939-2013, 2013.

Shonk, J. K. P., Turner, A. G., Chevuturi, A., Wilcox, L. J., Dittus, A. J., and Hawkins, E.: Uncertainty in aerosol radiative forcing impacts the simulated global monsoon in the 20th century, Atmos. Chem. Phys., 20, 14903–14915, https://doi.org/10.5194/acp-20-14903-2020, 2020.

Sidorenko, D., Rackow, T., Jung, T., Semmler, T., Barbi, D., Danilov, S., Dethloff, K., Dorn, W., Fieg, K., Goessling, H. F., Handorf, D., Harig, S., Hiller, W., Juricke, S., Losch, M., Schröter, J., Sein, D. V., and Wang, Q.: Towards multi-resolution global climate modeling with ECHAM6–FESOM. Part I: model formulation and mean climate, Clim. Dynam., 44, 757–780, https://doi.org/10.1007/s00382-014-2290-6, 2015.

Simpson, I. R., Rosenbloom, N., Danabasoglu, G., Deser, C., Yeager, S. G., McCluskey, C. S., Yamaguchi, R., Lamarque, J.-F., Tilmes, S., Mills, M. J., and Rodgers, K. B.: The CESM2 Single-Forcing Large Ensemble and Comparison to CESM1: Implications for Experimental Design, J. Climate, 36, 5687–5711, https://doi.org/10.1175/JCLI-D-22-0666.1, 2023.

Skeie, R. B., Myhre, G., Hodnebrog, Ø., Cameron-Smith, P. J., Deushi, M., Hegglin, M. I., Horowitz, L. W., Kramer, R. J., Michou, M., Mills, M. J., Olivié, D. J. L., Connor, F. M. O., Paynter, D., Samset, B. H., Sellar, A., Shindell, D., Takemura, T., Tilmes, S., and Wu, T.: Historical total ozone radiative forcing derived from CMIP6 simulations, npj Clim. Atmos. Sci., 3, 1–10, https://doi.org/10.1038/s41612-020-00131-0, 2020.

Skeie, R. B., Hodnebrog, Ø., and Myhre, G.: Trends in atmospheric methane concentrations since 1990 were driven and modified by anthropogenic emissions, Commun. Earth Environ., 4, 317, https://doi.org/10.1038/s43247-023-00969-1, 2023.

Smith, C., Cummins, D. P., Fredriksen, H.-B., Nicholls, Z., Meinshausen, M., Allen, M., Jenkins, S., Leach, N., Mathison, C., and Partanen, A.-I.: fair-calibrate v1.4.1: calibration, constraining, and validation of the FaIR simple climate model for reliable future climate projections, Geosci. Model Dev., 17, 8569–8592, https://doi.org/10.5194/gmd-17-8569-2024, 2024.

Smith, C. J., Forster, P. M., Allen, M., Leach, N., Millar, R. J., Passerello, G. A., and Regayre, L. A.: FAIR v1.3: a simple emissions-based impulse response and carbon cycle model, Geosci. Model Dev., 11, 2273–2297, https://doi.org/10.5194/gmd-11-2273-2018, 2018.

Smith, C. J., Harris, G. R., Palmer, M. D., Bellouin, N., Collins, W., Myhre, G., Schulz, M., Golaz, J.-C., Ringer, M., Storelvmo, T., and Forster, P. M.: Energy Budget Constraints on the Time History of Aerosol Forcing and Climate Sensitivity, J. Geophys. Res.-Atmos., 126, e2020JD033622, https://doi.org/10.1029/2020JD033622, 2021.

Song, Z., Qiao, F., Bao, Y., Shu, Q., Song, Y., and Yang, X.: FIO-QLNM FIO-ESM2.0 model output prepared for CMIP6 CMIP historical, Earth System Grid Federation [data set], https://doi.org/10.22033/ESGF/CMIP6.9199, 2019.

Steptoe, H., Wilcox, L. J., and Highwood, E. J.: Is there a robust effect of anthropogenic aerosols on the Southern Annular Mode?, J. Geophys. Res.-Atmos., 121, 10029–10042, https://doi.org/10.1002/2015JD024218, 2016.

Stevens, B., Giorgetta, M., Esch, M., Mauritsen, T., Crueger, T., Rast, S., Salzmann, M., Schmidt, H., Bader, J., Block, K., Brokopf, R., Fast, I., Kinne, S., Kornblueh, L., Lohmann, U., Pincus, R., Reichler, T., and Roeckner, E.: Atmospheric component of the MPI-M Earth System Model: ECHAM6, J. Adv. Model. Earth Sy., 5, 146–172, https://doi.org/10.1002/jame.20015, 2013.

Stevenson, D. S., Young, P. J., Naik, V., Lamarque, J.-F., Shindell, D. T., Voulgarakis, A., Skeie, R. B., Dalsoren, S. B., Myhre, G., Berntsen, T. K., Folberth, G. A., Rumbold, S. T., Collins, W. J., MacKenzie, I. A., Doherty, R. M., Zeng, G., van Noije, T. P. C., Strunk, A., Bergmann, D., Cameron-Smith, P., Plummer, D. A., Strode, S. A., Horowitz, L., Lee, Y. H., Szopa, S., Sudo, K., Nagashima, T., Josse, B., Cionni, I., Righi, M., Eyring, V., Conley, A., Bowman, K. W., Wild, O., and Archibald, A.: Tropospheric ozone changes, radiative forcing and attribution to emissions in the Atmospheric Chemistry and Climate Model Intercomparison Project (ACCMIP), Atmos. Chem. Phys., 13, 3063–3085, https://doi.org/10.5194/acp-13-3063-2013, 2013.

Stevenson, D. S., Zhao, A., Naik, V., O'Connor, F. M., Tilmes, S., Zeng, G., Murray, L. T., Collins, W. J., Griffiths, P. T., Shim, S., Horowitz, L. W., Sentman, L. T., and Emmons, L.: Trends in global tropospheric hydroxyl radical and methane lifetime since 1850 from AerChemMIP, Atmos. Chem. Phys., 20, 12905–12920, https://doi.org/10.5194/acp-20-12905-2020, 2020.

Stohl, A., Aamaas, B., Amann, M., Baker, L. H., Bellouin, N., Berntsen, T. K., Boucher, O., Cherian, R., Collins, W., Daskalakis, N., Dusinska, M., Eckhardt, S., Fuglestvedt, J. S., Harju, M., Heyes, C., Hodnebrog, Ø., Hao, J., Im, U., Kanakidou, M., Klimont, Z., Kupiainen, K., Law, K. S., Lund, M. T., Maas, R., MacIntosh, C. R., Myhre, G., Myriokefalitakis, S., Olivié, D., Quaas, J., Quennehen, B., Raut, J.-C., Rumbold, S. T., Samset, B. H., Schulz, M., Seland, Ø., Shine, K. P., Skeie, R. B., Wang, S., Yttri, K. E., and Zhu, T.: Evaluating the climate and air quality impacts of short-lived pollutants, Atmos. Chem. Phys., 15, 10529–10566, https://doi.org/10.5194/acp-15-10529-2015, 2015.

Stouffer, R. J., Eyring, V., Meehl, G. A., Bony, S., Senior, C., Stevens, B., and Taylor, K. E.: CMIP5 Scientific Gaps and Recommendations for CMIP6, B. Am. Meteorol. Soc., 98, 95–105, https://doi.org/10.1175/BAMS-D-15-00013.1, 2017.

Swart, N. C., Cole, J. N., Kharin, V. V., Lazare, M., Scinocca, J. F., Gillett, N. P., Anstey, J., Arora, V., Christian, J. R., Jiao, Y., Lee, W. G., Majaess, F., Saenko, O. A., Seiler, C., Seinen, C., Shao, A., Solheim, L., von Salzen, K., Yang, D., Winter, B., and Sigmond, M.: CCCma CanESM5 model output prepared for CMIP6 CMIP historical, Earth System Grid Federation [data set], https://doi.org/10.22033/ESGF/CMIP6.3610, 2019a.

Swart, N. C., Cole, J. N. S., Kharin, V. V., Lazare, M., Scinocca, J. F., Gillett, N. P., Anstey, J., Arora, V., Christian, J. R., Hanna, S., Jiao, Y., Lee, W. G., Majaess, F., Saenko, O. A., Seiler, C., Seinen, C., Shao, A., Sigmond, M., Solheim, L., von Salzen, K., Yang, D., and Winter, B.: The Canadian Earth System Model version 5 (CanESM5.0.3), Geosci. Model Dev., 12, 4823–4873, https://doi.org/10.5194/gmd-12-4823-2019, 2019b.

Szopa, S., Naik, V., Adhikary, B., Artaxo, P., Berntsen, T., Collins, W., Fuzzi, S., Gallardo, L., Kiendler-Scharr, A., Klimont, Z., Liao, H., Unger, N., and Zanis, P.: Short-lived climate forcers, in: Climate change 2021: The physical science basis. Contribution of working group I to the sixth assessment report of the intergovernmental panel on climate change, section: 6 Type: Book section, edited by: Masson-Delmotte, V., Zhai, P., Pirani, A., Con-

nors, S. L., Péan, C., Berger, S., Caud, N., Chen, Y., Goldfarb, L., Gomis, M. I., Huang, M., Leitzell, K., Lonnoy, E., Matthews, J. B. R., Maycock, T. K., Waterfield, T., Yelekçi, O., Yu, R., and Zhou, B., Cambridge University Press, Cambridge, UK and New York, NY, USA, https://doi.org/10.1017/9781009157896.008, 2021a.

Szopa, S., Naik, V., Adhikary, B., Artaxo, P., Berntsen, T., Collins, W., Fuzzi, S., Gallardo, L., Kiendler-Scharr, A., Klimont, Z., Liao, H., Unger, N., and Zanis, P.: Short-lived climate forcers supplementary material, in: Climate change 2021: The physical science basis. Contribution of working group I to the sixth assessment report of the intergovernmental panel on climate change, section: 6 Type: Book section, edited by Masson-Delmotte, V., Zhai, P., Pirani, A., Connors, S. L., Péan, C., Berger, S., Caud, N., Chen, Y., Goldfarb, L., Gomis, M. I., Huang, M., Leitzell, K., Lonnoy, E., Matthews, J. B. R., Maycock, T. K., Waterfield, T., Yelekçi, O., Yu, R., and Zhou, B., Cambridge University Press, Cambridge, UK and New York, NY, USA, https://www.ipcc.ch/report/ar6/wg1/downloads/report/IPCC_AR6_WGI_Chapter06_SM.pdf (last access: 25 July 2025), 2021b.

Tang, Y., Rumbold, S., Ellis, R., Kelley, D., Mulcahy, J., Sellar, A., Walton, J., and Jones, C.: MOHC UKESM1.0-LL model output prepared for CMIP6 CMIP historical, Earth System Grid Federation [data set], https://doi.org/10.22033/ESGF/CMIP6.6113, 2019.

Tatebe, H. and Watanabe, M.: MIROC MIROC6 model output prepared for CMIP6 CMIP historical, Earth System Grid Federation [data set], https://doi.org/10.22033/ESGF/CMIP6.5603, 2018.

Tatebe, H., Ogura, T., Nitta, T., Komuro, Y., Ogochi, K., Takemura, T., Sudo, K., Sekiguchi, M., Abe, M., Saito, F., Chikira, M., Watanabe, S., Mori, M., Hirota, N., Kawatani, Y., Mochizuki, T., Yoshimura, K., Takata, K., O'ishi, R., Yamazaki, D., Suzuki, T., Kurogi, M., Kataoka, T., Watanabe, M., and Kimoto, M.: Description and basic evaluation of simulated mean state, internal variability, and climate sensitivity in MIROC6, Geosci. Model Dev., 12, 2727–2765, https://doi.org/10.5194/gmd-12-2727-2019, 2019.

Thornhill, G., Collins, W., Olivié, D., Skeie, R. B., Archibald, A., Bauer, S., Checa-Garcia, R., Fiedler, S., Folberth, G., Gjermundsen, A., Horowitz, L., Lamarque, J.-F., Michou, M., Mulcahy, J., Nabat, P., Naik, V., O'Connor, F. M., Paulot, F., Schulz, M., Scott, C. E., Séférian, R., Smith, C., Takemura, T., Tilmes, S., Tsigaridis, K., and Weber, J.: Climate-driven chemistry and aerosol feedbacks in CMIP6 Earth system models, Atmos. Chem. Phys., 21, 1105–1126, https://doi.org/10.5194/acp-21-1105-2021, 2021a.

Thornhill, G. D., Collins, W. J., Kramer, R. J., Olivié, D., Skeie, R. B., O'Connor, F. M., Abraham, N. L., Checa-Garcia, R., Bauer, S. E., Deushi, M., Emmons, L. K., Forster, P. M., Horowitz, L. W., Johnson, B., Keeble, J., Lamarque, J.-F., Michou, M., Mills, M. J., Mulcahy, J. P., Myhre, G., Nabat, P., Naik, V., Oshima, N., Schulz, M., Smith, C. J., Takemura, T., Tilmes, S., Wu, T., Zeng, G., and Zhang, J.: Effective radiative forcing from emissions of reactive gases and aerosols – a multi-model comparison, Atmos. Chem. Phys., 21, 853–874, https://doi.org/10.5194/acp-21-853-2021, 2021b.

Turnock, S. T., Allen, R. J., Andrews, M., Bauer, S. E., Deushi, M., Emmons, L., Good, P., Horowitz, L., John, J. G., Michou, M., Nabat, P., Naik, V., Neubauer, D., O'Connor, F. M., Olivié, D., Oshima, N., Schulz, M., Sellar, A., Shim, S., Takemura, T., Tilmes, S., Tsigaridis, K., Wu, T., and Zhang, J.: Historical and future changes in air pollutants from CMIP6 models, Atmos. Chem. Phys., 20, 14547–14579, https://doi.org/10.5194/acp-20-14547-2020, 2020.

Turnock, S. T., Allen, R., Archibald, A. T., Dalvi, M., Folberth, G., Griffiths, P. T., Keeble, J., Robertson, E., and O'Connor, F. M.: The Future Climate and Air Quality Response From Different Near-Term Climate Forcer, Climate, and Land-Use Scenarios Using UKESM1, Earths Future, 10, e2022EF002687, https://doi.org/10.1029/2022EF002687, 2022.

Turnock, S. T., Reddington, C. L., West, J. J., and O'Connor, F. M.: The Air Pollution Human Health Burden in Different Future Scenarios That Involve the Mitigation of Near-Term Climate Forcers, Climate and Land-Use, 7, e2023GH000812, https://doi.org/10.1029/2023GH000812, 2023.

van Noije, T., Bergman, T., Le Sager, P., O'Donnell, D., Makkonen, R., Gonçalves-Ageitos, M., Döscher, R., Fladrich, U., von Hardenberg, J., Keskinen, J.-P., Korhonen, H., Laakso, A., Myriokefalitakis, S., Ollinaho, P., Pérez García-Pando, C., Reerink, T., Schrödner, R., Wyser, K., and Yang, S.: EC-Earth3-AerChem: a global climate model with interactive aerosols and atmospheric chemistry participating in CMIP6, Geosci. Model Dev., 14, 5637–5668, https://doi.org/10.5194/gmd-14-5637-2021, 2021.

Voldoire, A.: CMIP6 simulations of the CNRM-CERFACS based on CNRM-CM6-1 model for CMIP experiment historical, Earth System Grid Federation [data set], https://doi.org/10.22033/ESGF/CMIP6.4066, 2018.

Voldoire, A., Saint-Martin, D., Sénési, S., Decharme, B., Alias, A., Chevallier, M., Colin, J., Guérémy, J.-F., Michou, M., Moine, M.-P., Nabat, P., Roehrig, R., Salas y Mélia, D., Séférian, R., Valcke, S., Beau, I., Belamari, S., Berthet, S., Cassou, C., Cattiaux, J., Deshayes, J., Douville, H., Ethé, C., Franchistéguy, L., Geoffroy, O., Lévy, C., Madec, G., Meurdesoif, Y., Msadek, R., Ribes, A., Sanchez-Gomez, E., Terray, L., and Waldman, R.: Evaluation of CMIP6 DECK Experiments With CNRM-CM6-1, J. Adv. Model. Earth Sy., 11, 2177–2213, https://doi.org/10.1029/2019MS001683, 2019.

Volodin, E., Mortikov, E., Gritsun, A., Lykossov, V., Galin, V., Diansky, N., Gusev, A., Kostrykin, S., Iakovlev, N., Shestakova, A., and Emelina, S.: INM INM-CM4-8 model output prepared for CMIP6 CMIP historical, Earth System Grid Federation [data set], https://doi.org/10.22033/ESGF/CMIP6.5069, 2019a.

Volodin, E., Mortikov, E., Gritsun, A., Lykossov, V., Galin, V., Diansky, N., Gusev, A., Kostrykin, S., Iakovlev, N., Shestakova, A., and Emelina, S.: INM INM-CM5-0 model output prepared for CMIP6 CMIP historical, Earth System Grid Federation [data set], https://doi.org/10.22033/ESGF/CMIP6.5070, 2019b.

Volodin, E. M. and Kostrykin, S. V.: The aerosol module in the INM RAS climate model, Russ. Meteorol. Hydro.+, 41, 519–528, https://doi.org/10.3103/S106837391608001X, 2016.

Volodin, E. M., Dianskii, N. A., and Gusev, A. V.: Simulating present-day climate with the INMCM4.0 coupled model of the atmospheric and oceanic general circulations, Izv. Atmos. Ocean. Phy.+, 46, 414–431, https://doi.org/10.1134/S000143381004002X, 2010.

Volodin, E. M., Mortikov, E. V., Kostrykin, S. V., Galin, V. Y., Lykossov, V. N., Gritsun, A. S., Diansky, N. A., Gusev, A. V.,

and Iakovlev, N. G.: Simulation of the present-day climate with the climate model INMCM5, Clim. Dynam., 49, 3715–3734, https://doi.org/10.1007/s00382-017-3539-7, 2017.

Watson-Parris, D., Williams, A., Deaconu, L., and Stier, P.: Model calibration using ESEm v1.1.0 – an open, scalable Earth system emulator, Geosci. Model Dev., 14, 7659–7672, https://doi.org/10.5194/gmd-14-7659-2021, 2021.

Watson-Parris, D., Rao, Y., Olivié, D., Seland, Ø., Nowack, P., Camps-Valls, G., Stier, P., Bouabid, S., Dewey, M., Fons, E., Gonzalez, J., Harder, P., Jeggle, K., Lenhardt, J., Manshausen, P., Novitasari, M., Ricard, L., and Roesch, C.: ClimateBench v1.0: A Benchmark for Data-Driven Climate Projections, J. Adv. Model. Earth Sy., 14, e2021MS002954, https://doi.org/10.1029/2021MS002954, 2022.

Wieners, K.-H., Giorgetta, M., Jungclaus, J., Reick, C., Esch, M., Bittner, M., Legutke, S., Schupfner, M., Wachsmann, F., Gayler, V., Haak, H., de Vrese, P., Raddatz, T., Mauritsen, T., von Storch, J.-S., Behrens, J., Brovkin, V., Claussen, M., Crueger, T., Fast, I., Fiedler, S., Hagemann, S., Hohenegger, C., Jahns, T., Kloster, S., Kinne, S., Lasslop, G., Kornblueh, L., Marotzke, J., Matei, D., Meraner, K., Mikolajewicz, U., Modali, K., Müller, W., Nabel, J., Notz, D., Peters-von Gehlen, K., Pincus, R., Pohlmann, H., Pongratz, J., Rast, S., Schmidt, H., Schnur, R., Schulzweida, U., Six, K., Stevens, B., Voigt, A., and Roeckner, E.: MPI-M MPI-ESM1.2-LR model output prepared for CMIP6 CMIP historical, Earth System Grid Federation [data set], https://doi.org/10.22033/ESGF/CMIP6.6595, 2019.

Wilcox, L.: Opinion: The Role of AerChemMIP in Advancing Climate and Air Quality Research, OSF [data set], https://doi.org/10.17605/OSF.IO/8FWJ3, 2024.

Wilcox, L. J., Highwood, E. J., and Dunstone, N. J.: The influence of anthropogenic aerosol on multi-decadal variations of historical global climate, Environ. Res. Lett., 8, 024033, https://doi.org/10.1088/1748-9326/8/2/024033, 2013.

Wilcox, L. J., Liu, Z., Samset, B. H., Hawkins, E., Lund, M. T., Nordling, K., Undorf, S., Bollasina, M., Ekman, A. M. L., Krishnan, S., Merikanto, J., and Turner, A. G.: Accelerated increases in global and Asian summer monsoon precipitation from future aerosol reductions, Atmos. Chem. Phys., 20, 11955–11977, https://doi.org/10.5194/acp-20-11955-2020, 2020.

Wilcox, L. J., Allen, R. J., Samset, B. H., Bollasina, M. A., Griffiths, P. T., Keeble, J., Lund, M. T., Makkonen, R., Merikanto, J., O'Donnell, D., Paynter, D. J., Persad, G. G., Rumbold, S. T., Takemura, T., Tsigaridis, K., Undorf, S., and Westervelt, D. M.: The Regional Aerosol Model Intercomparison Project (RAMIP), Geosci. Model Dev., 16, 4451–4479, https://doi.org/10.5194/gmd-16-4451-2023, 2023.

Wu, T., Chu, M., Dong, M., Fang, Y., Jie, W., Li, J., Li, W., Liu, Q., Shi, X., Xin, X., Yan, J., Zhang, F., Zhang, J., Zhang, L., and Zhang, Y.: BCC BCC-CSM2MR model output prepared for CMIP6 CMIP historical, Earth System Grid Federation [data set], https://doi.org/10.22033/ESGF/CMIP6.2948, 2018.

Wu, T., Lu, Y., Fang, Y., Xin, X., Li, L., Li, W., Jie, W., Zhang, J., Liu, Y., Zhang, L., Zhang, F., Zhang, Y., Wu, F., Li, J., Chu, M., Wang, Z., Shi, X., Liu, X., Wei, M., Huang, A., Zhang, Y., and Liu, X.: The Beijing Climate Center Climate System Model (BCC-CSM): the main progress from CMIP5 to CMIP6, Geosci. Model Dev., 12, 1573–1600, https://doi.org/10.5194/gmd-12-1573-2019, 2019.

Wu, T., Zhang, F., Zhang, J., Jie, W., Zhang, Y., Wu, F., Li, L., Yan, J., Liu, X., Lu, X., Tan, H., Zhang, L., Wang, J., and Hu, A.: Beijing Climate Center Earth System Model version 1 (BCC-ESM1): model description and evaluation of aerosol simulations, Geosci. Model Dev., 13, 977–1005, https://doi.org/10.5194/gmd-13-977-2020, 2020.

Yu, Y.: CAS FGOALS-f3-L model output prepared for CMIP6 CMIP historical, Earth System Grid Federation [data set], https://doi.org/10.22033/ESGF/CMIP6.3355, 2019.

Yukimoto, S., Kawai, H., Koshiro, T., Oshima, N., Yoshida, K., Urakawa, S., Tsujino, H., Deushi, M., Tanaka, T., Hosaka, M., Yabu, S., Yoshimura, H., Shindo, E., Mizuta, R., Obata, A., Adachi, Y., and Ishii, M.: The Meteorological Research Institute Earth System Model Version 2.0, MRI-ESM2.0: Description and Basic Evaluation of the Physical Component, J. Meteorol. Soc. Jpn. Ser. II, 97, 931–965, 2019a.

Yukimoto, S., Koshiro, T., Kawai, H., Oshima, N., Yoshida, K., Urakawa, S., Tsujino, H., Deushi, M., Tanaka, T., Hosaka, M., Yoshimura, H., Shindo, E., Mizuta, R., Ishii, M., Obata, A., and Adachi, Y.: MRI MRI-ESM2.0 model output prepared for CMIP6 CMIP historical, Earth System Grid Federation [data set], https://doi.org/10.22033/ESGF/CMIP6.6842, 2019b.

Zanis, P., Akritidis, D., Georgoulias, A. K., Allen, R. J., Bauer, S. E., Boucher, O., Cole, J., Johnson, B., Deushi, M., Michou, M., Mulcahy, J., Nabat, P., Olivié, D., Oshima, N., Sima, A., Schulz, M., Takemura, T., and Tsigaridis, K.: Fast responses on pre-industrial climate from present-day aerosols in a CMIP6 multi-model study, Atmos. Chem. Phys., 20, 8381–8404, https://doi.org/10.5194/acp-20-8381-2020, 2020.

Zanis, P., Akritidis, D., Turnock, S., Naik, V., Szopa, S., Georgoulias, A. K., Bauer, S. E., Deushi, M., Horowitz, L. W., Keeble, J., Sager, P. L., O'Connor, F. M., Oshima, N., Tsigaridis, K., and Noije, T. V.: Climate change penalty and benefit on surface ozone: a global perspective based on CMIP6 earth system models, Environ. Res. Lett., 17, 024014, https://doi.org/10.1088/1748-9326/ac4a34, 2022.

Zeng, G., Morgenstern, O., Williams, J. H. T., O'Connor, F. M., Griffiths, P. T., Keeble, J., Deushi, M., Horowitz, L. W., Naik, V., Emmons, L. K., Abraham, N. L., Archibald, A. T., Bauer, S. E., Hassler, B., Michou, M., Mills, M. J., Murray, L. T., Oshima, N., Sentman, L. T., Tilmes, S., Tsigaridis, K., and Young, P. J.: Attribution of Stratospheric and Tropospheric Ozone Changes Between 1850 and 2014 in CMIP6 Models, J. Geophys. Res.-Atmos., 127, e2022JD036452, https://doi.org/10.1029/2022JD036452, 2022.

Zhang, H., Zhang, M., Jin, J., Fei, K., Ji, D., Wu, C., Zhu, J., He, J., Chai, Z., Xie, J., Dong, X., Zhang, D., Bi, X., Cao, H., Chen, H., Chen, K., Chen, X., Gao, X., Hao, H., Jiang, J., Kong, X., Li, S., Li, Y., Lin, P., Lin, Z., Liu, H., Liu, X., Shi, Y., Song, M., Wang, H., Wang, T., Wang, X., Wang, Z., Wei, Y., Wu, B., Xie, Z., Xu, Y., Yu, Y., Yuan, L., Zeng, Q., Zeng, X., Zhao, S., Zhou, G., and Zhu, J.: Description and Climate Simulation Performance of CAS-ESM Version 2, J. Adv. Model. Earth Sy., 12, e2020MS002210, https://doi.org/10.1029/2020MS002210, 2020.

Zhang, J., Wu, T., Shi, X., Zhang, F., Li, J., Chu, M., Liu, Q., Yan, J., Ma, Q., and Wei, M.: BCC BCC-ESM1 model output prepared for CMIP6 CMIP historical, Earth System Grid Federation [data set], https://doi.org/10.22033/ESGF/CMIP6.2949, 2018.

Zhang, J., Furtado, K., Turnock, S. T., Mulcahy, J. P., Wilcox, L. J., Booth, B. B., Sexton, D., Wu, T., Zhang, F., and Liu, Q.: The role of anthropogenic aerosols in the anomalous cooling from 1960 to 1990 in the CMIP6 Earth system models, Atmos. Chem. Phys., 21, 18609–18627, https://doi.org/10.5194/acp-21-18609-2021, 2021a.

Zhang, Y., Ciais, P., Boucher, O., Maignan, F., Bastos, A., Goll, D., Lurton, T., Viovy, N., Bellouin, N., and Li, L.: Disentangling the Impacts of Anthropogenic Aerosols on Terrestrial Carbon Cycle During 1850–2014, Earths Future, 9, e2021EF002035, https://doi.org/10.1029/2021EF002035, 2021b.

Zhao, A., Ryder, C. L., and Wilcox, L. J.: How well do the CMIP6 models simulate dust aerosols?, Atmos. Chem. Phys., 22, 2095–2119, https://doi.org/10.5194/acp-22-2095-2022, 2022.

Ziehn, T., Chamberlain, M., Lenton, A., Law, R., Bodman, R., Dix, M., Wang, Y., Dobrohotoff, P., Srbinovsky, J., Stevens, L., Vohralik, P., Mackallah, C., Sullivan, A., O'Farrell, S., and Druken, K.: CSIRO ACCESS-ESM1.5 model output prepared for CMIP6 CMIP historical, Earth System Grid Federation [data set], https://doi.org/10.22033/ESGF/CMIP6.4272, 2019.

Ziehn, T., Chamberlain, M. A., Law, R. M., Lenton, A., Bodman, R. W., Dix, M., Stevens, L., Wang, Y.-P., and Srbinovsky, J.: The Australian Earth System Model: ACCESS-ESM1.5, Journal of Southern Hemisphere Earth Systems Science, 70, 193–214, https://doi.org/10.1071/ES19035, 2020.